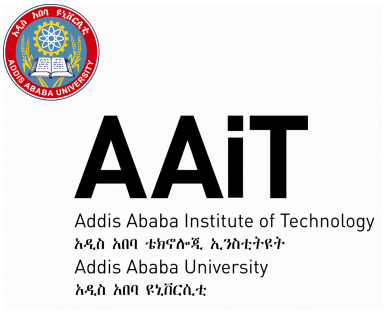

ADDIS ABABA UNIVERSITY

ADDIS ABABA INSTITUTE OF TECHNOLOGY

SCHOOL OF ELECTRICAL AND COMPUTER ENGINEERING

MSC. THESIS ON

Performance Analysis of Pilot-based Channel Estimation Techniques in Massive MIMO Systems

Author:
Abdulsemed MOHAMMED

Adviser:
Dr. -Ing. Dereje HAILEMARIAM

A thesis submitted in partial fulfillment of the requirements for the degree of Masters of Science in Communication Engineering

June 15, 2020

ADDIS ABABA UNIVERSITY
SCHOOL OF GRADUATE STUDIES
ADDIS ABABA INSTITUTE OF TECHNOLOGY
SCHOOL OF ELECTRICAL AND COMPUTER ENGINEERING

Performance Analysis of Pilot Based Channel Estimation Techniques in Massive MIMO Systems.

Abdulsemed MOHAMMED

APPROVED BY BOARD OF EXAMINERS

Chairman of School of Graduate Committee	Signature
Advisor	Signature
Examiner (internal)	Signature
Examiner (external)	Signature

Declaration of Authorship

I, Abdulsemed MOHAMMED, declare that this thesis titled, "Performance Analysis of Pilot-based Channel Estimation Techniques in Massive MIMO Systems" and the work presented in it are my own. I confirm that:

- This work was done wholly or mainly while in candidature for a Masters degree at Addis Ababa University.
- I have acknowledged all main sources of help.

Signed:

Date:

Abstract

The need for an internet connection is growing globally. So, day-by-day people need much higher data rate connection to meet their need but every physical resource in communication like frequency band, transmit signal strength are finite. Within the given limited resource, higher data speed is accomplished by a new technology called massive Multiple Input Multiple Output (massive MIMO) system. Massive MIMO fulfills the high data rate requirement through antenna diversity gain.

Received signal in massive MIMO system is usually distorted by different channel effects (noise, interference, fading). In order to recover the transmitted signal correctly, channel effect must be estimated and repaired at the receiver accordingly. This is done by using different channel estimation techniques. But which one of the channel estimators should be used for a specific situation is another problem. This thesis will analyze the performance of different pilot based channel estimation techniques specifically the least square (LS) and minimum mean square error channel (MMSE) estimation methods for massive MIMO systems and based on the analysis results different discussions and conclusions are made. Furthermore, comparison among their characteristics is simulated in MATLAB and useful conclusions are given. To achieve this goal different scientific articles and MATLAB simulation results will be used.

When the performance of the channel estimators was tested using the maximum ratio combining (MRC) detection algorithms, the result showed that the MMSE estimator performed better. Different comparison techniques were also run and they showed that the MMSE estimator was affected more than the LS estimator by the increase in the number of users while the increase in the number of antennas has almost the same effect on both estimators. The paper also gave possible future works in massive MIMO systems that continue from this work.

Keywords:- *pilot-based channel estimation, channel estimation, MIMO, massive MIMO, LS, MMSE, detection algorithms, MRC*

Acknowledgements

Firstly, I would like to thank God for giving me the knowledge and strength to finalize this thesis study.

I would like to express my sincere gratitude to my adviser Dr. –Ing. Dereje Hailemariam for his continuous support, patience, motivation and immense knowledge. His guidance helped me in all the time of research and writing of this thesis. I could not have imagined having a better adviser for this thesis study.

I would like to thank my family for supporting and carrying me through their prayer and providing the necessary help throughout this thesis study. Last but not least, I thank my friends and my board of examiners for their encouragement and support in providing me necessary needs and comments.

Contents

List of Figures

List of Tables

List of Abbreviations

1G	**1**st **G**eneration
2G	**2**nd **G**eneration
3G	**3**rd **G**eneration
4G	**4**th **G**eneration
5G	**5**th **G**eneration
aka	**a**lso **k**nown **a**s
AWGN	**A**dditive **W**hite **G**iassian **N**oise
BS	**B**ase **S**tation
CSI	**C**hannel **S**tate **I**nformation
DL	**D**own **L**ink
FDD	**F**requency **D**ivision **D**uplex
gNB	next **g**eneration **N**ode **B**
IEEE	**I**nstitute of **E**lectrical and **E**lectronics **E**ngineers
IMT	**I**nternational **M**obile **T**elecommunications
IoT	**I**nternet **o**f **T**hings
ISI	**I**nter **S**ymbol **I**nterference
LAN	**L**ocal **A**rea **N**etwork
LoS	**L**ine **o**f **S**ight
LS	**L**east **S**quare
LTE	**L**ong **T**erm **E**volution
MAP	**M**aximum **A** **P**osteriori
MATLAB	**MAT**rix **LAB**oratry
MIMO	**M**ultiple **I**nput **M**ultiple **O**utput
MISO	**M**ultiple **I**nput **S**ingle **O**utput
ML	**M**aximum **L**ikelihood
MMSE	**M**inimum **M**ean **S**quare **E**rror
MRC	**M**aximal **R**atio **C**ombining
MSE	**M**ean **S**quare **E**rror
MU	**M**ulti **U**ser
MWC	**M**obile **W**orld **C**onference
NB	**N**ode **B**
NLoS	**N**one **L**ine **o**f **S**ight
NR	**N**ew **R**adio
OFDM	**O**rthogonal **F**requency **D**ivision **M**ultiplexing
PA	**P**ower **A**mplifier
PC	**P**ersonal **C**omputer
PRB	**P**hyscal **R**esource **B**lock
QAM	**Q**adrature **A**mplitude **M**odulation
RF	**R**adio **F**requency

SE	**S**pectral **E**fficiency
SIMO	**S**ingle **I**nput **M**ultiple **O**utput
SINR	**S**ignal to **I**nterference and **N**oise **R**atio
SISO	**S**ingle **I**nput **S**ingle **O**utput
SU	**S**ingle **U**ser
TDD	**T**ime **D**ivision **D**uplex
UE	**U**ser **E**quipment
UL	**U**p **L**ink
UMa	**U**rban **Ma**crocell
UMi	**U**rban **Mi**crocell
WLAN	**W**ireless **L**ocal **A**rea **N**etwork
ZF	**Z**ero **F**orcing

Chapter 1

Introduction

In this chapter seven sections are included. Section 1.1 gives background on massive multiple-input multiple-output (massive MIMO) systems. Then the next section answers the question "why this thesis is done?". Different literatures are reviewed in Section 1.3. Section 1.4 provides the objectives of the thesis. Two kinds of objectives are discussed here, the general objective and the specific objectives. The methodologies that will be followed to achieve the objectives will be discussed in Section 1.5. The sixth section is the organization of the thesis. In the last section, contribution of this thesis with respect to this field will be presented.

1.1 Background

Massive MIMO is a form of MU-MIMO (Multi-user Multiple input multiple output) systems where the number of BS (base station) antennas and the numbers of users are large. In Massive MIMO, hundreds or thousands of BS antennas simultaneously serve tens or hundreds of users in the same frequency resource [1]. The increase in the number of antennas is the key to the increase in the capacity of the Massive MIMO systems. This feature makes the 5G network requirements possible.

Figures 1.1 and 1.2 are illustrations of the downlink and uplink transmission in a MU-MIMO system, where the BS is equipped with M antennas and serves K user terminals simultaneously. In this downlink and uplink transmission, beam-forming is applied to serve the users. Beam-forming will be discussed in Section 2.4. Uplink (or reverse link) transmission is the scenario where the K users transmit signals to the BS. A part of the coherence interval is used for the uplink data transmission. In the uplink, all K users transmit their data to the BS in the same time-frequency resource. The BS then uses the channel estimates together with the combining techniques to detect signals transmitted from all users.

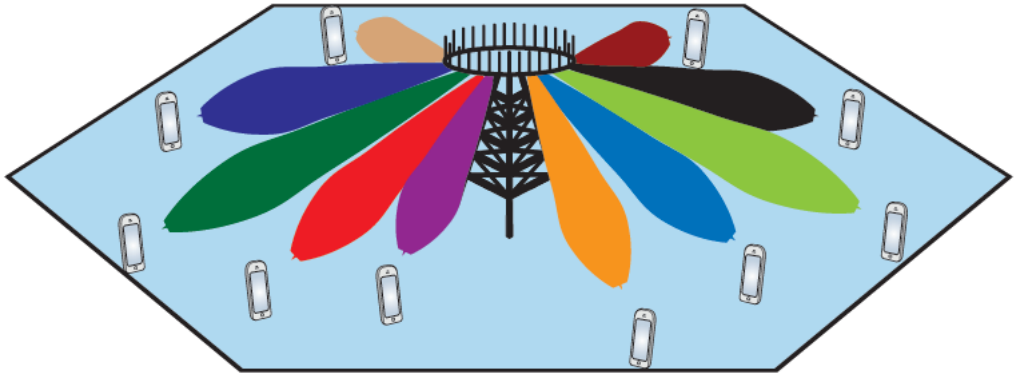

FIGURE 1.1: Illustration of downlink transmission in a MU-MIMO system, where the BS is equipped with M antennas and serves K user terminals simultaneously [1].

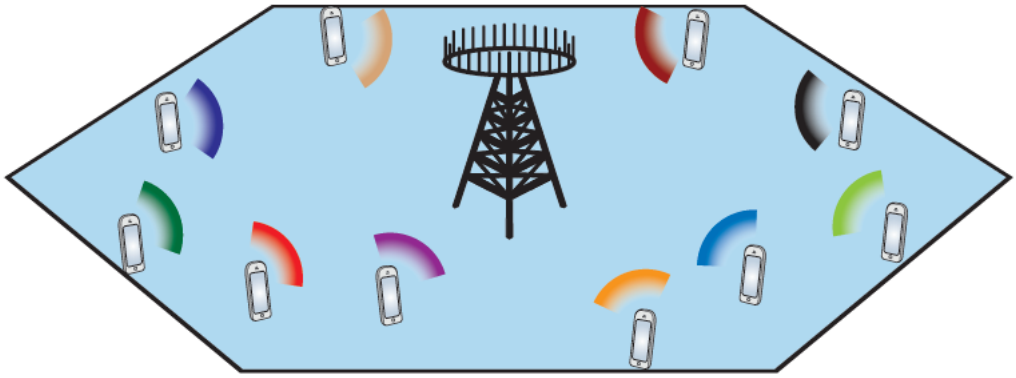

FIGURE 1.2: Illustration of uplink transmission in a MU-MIMO system, where the BS is equipped with M antennas and serves K user terminals simultaneously [1].

Downlink (or forward link) is the scenario where the BS transmits signals to all K users. In the downlink, the BS transmits signals to all K users in the same time-frequency resource. More specifically, the BS uses its channel estimates in combination with the symbols intended for the K users to create M precoded signals which are then fed to M antennas [1].

A very critical thing in massive MIMO is that for massive MIMO systems to work in optimal conditions channel estimation is required. The BS needs CSI (channel sate information) to detect the signals transmitted from the users in the uplink, and to precode the signals in the downlink. This CSI is obtained through the uplink training. Each user is assigned an orthogonal pilot sequence, and sends this pilot sequence to the BS. The BS knows the pilots sequences transmitted from all users, and then estimates the channels based on the received pilot signals. Furthermore, each user may need partial knowledge

of CSI to coherently detect the signals transmitted from the BS. This information can be acquired through downlink training algorithm. Since the BS uses linear precoding techniques to beamform the signals to the users, the user needs only the effective channel gain (which is a scalar constant) to detect its desired signals. Therefore, the BS can spend a short time to beamform pilots in the downlink for CSI acquisition at the users [1].

There are different channel estimation techniques. They can be broadly divided in to three categories. These are pilot based, blind, and semi-blind channel estimation techniques. We will have a deep discussion on these channel estimation techniques in Chapter 4.

Channel estimation is usually performed with the aid of pilot symbols [2]. Therefore, pilot-based channel estimation techniques will be discussed more in this thesis. Chapter 4 Section 4.3 will be devoted to discussing the pilot based channel estimation techniques. The other channel estimation techniques will also be given an introduction.

1.2 Motivation

Data traffic (both forms of mobile and fixed networks) has grown exponentially due to the dramatic growth of smart phones, tablets, laptops, and many other wireless data consuming devices. The paper [3] states that in the near future, we expect an explosive increase in connected devices, including phones, tablets, wearable devices, sensors, internet of things (IoT), connected vehicles and so on.

As shown in Figure 1.3, around 21.2 billion connected devices are expected by 2020, of which 11.3 billion will be phones, tablets, laptops and PCs (Non-IoT). This shows that the growing trend and a prediction of the number of connected devices from 2015 to 2020. Much higher data rates than today's 4G systems are required due to, e.g., high quality video streaming, cloud computing and IoT. We can also that by the end of 2025 the number will grow to 34.2 billion active device connected world wide [4]. This is a very large number and it will continue to grow.

As shown in Figure 1.4, in 2014, video accounted for around 45% of mobile data traffic. By 2020, it is expected that 60% of all mobile data traffic will be from video. This shows that by 2020 the amount of mobile data traffic due to video streaming is predicted to be 13 times more than that in 2014 [3]. SO, as the need for video streaming grows the need for high data rate internet connection grows.

Massive MIMO has the potential to meet these future requirements. So, because data demand is always increasing, we need to think of a way to increase the the capacity of cellular networks in a way that has not been seen before because the data traffic is increasing in a way that has not been seen before. In order to do this we need to understand the

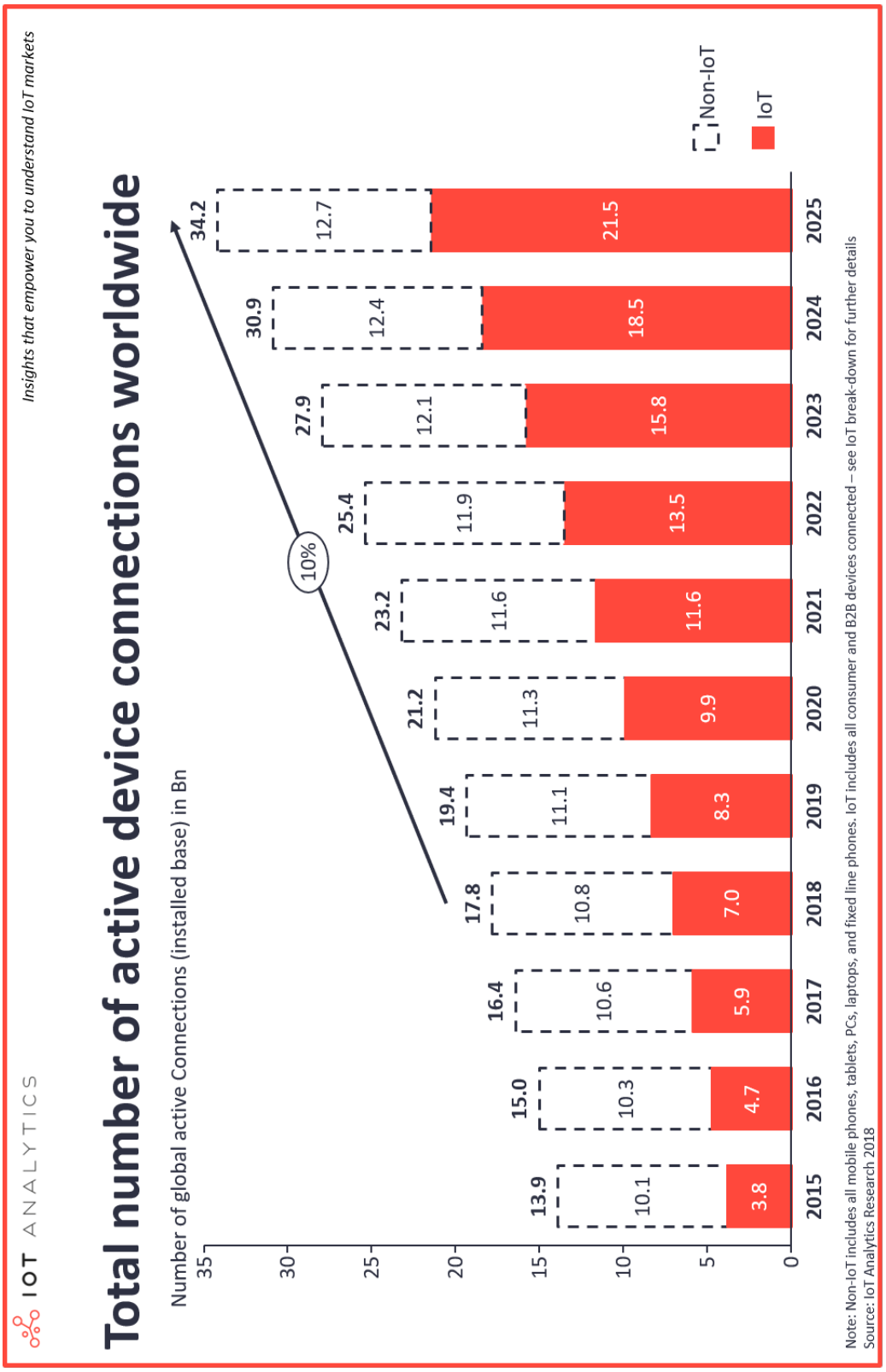

FIGURE 1.3: Number of connected devices [4].

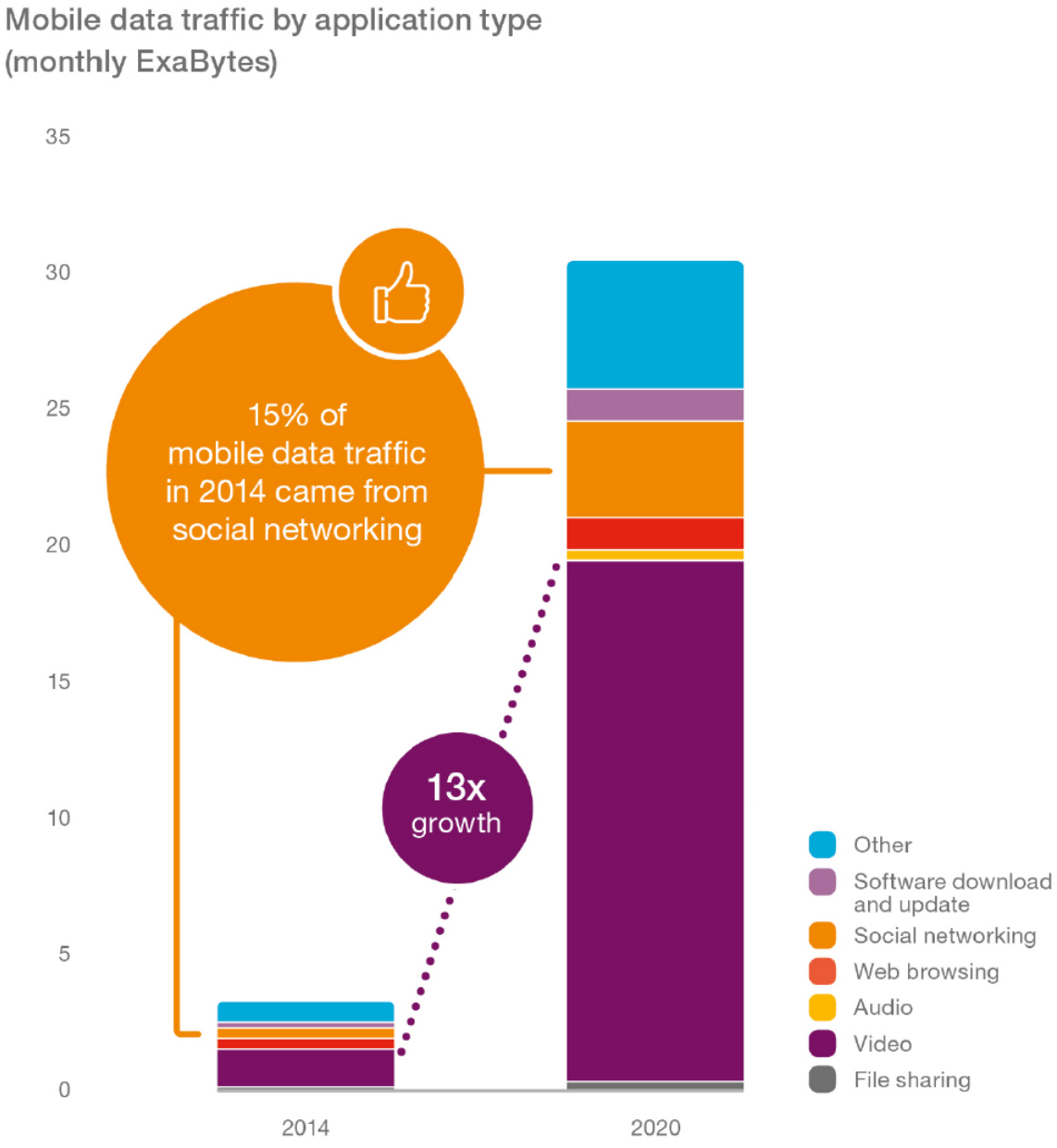

FIGURE 1.4: Growth in mobile data traffic [3].

way that the capacity of a cellular network can be increased. The main parameter that measures the capacity of a network is the throughput. The expression for throughput is given as:-

$$\begin{aligned} Throughput\ (bit/s/km^2) = Cell\ Density\ [Cell/km^2] \times Bandwidth\ (Hz) \\ \times Spectral\ efficiency\ (bits/s/Hz/cell) \end{aligned} \tag{1.1}$$

[1]

As we can see from Equation 1.1, if we want to increase the throughput of a given communication system, we can increase the bandwidth, the cell density and/or the spectral efficiency (SE). The method of increasing the cell density and the bandwidth has been used to much till now. We need a different way of increasing the throughput. A well-known way to increase the throughput is by increasing the spectral efficiency of the cellular network. One way to increase the spectral efficiency is by increasing the number of antennas in the BS and/or UE (user equipment).

When the number of antennas increases, it is as if the Shannon capacity is multiplied by the minimum number of antennas of the BS or the UE. This increases the SE by several factors. This is because the Shannon capacity limit is for single antenna to single antenna communication. Here, we are forming several single antenna to single antenna communication for all users which greatly increases the capacity of the network highly even to an extent of several tens times the conventional single antenna to single antenna communication. When the number of antennas becomes extensively large the system are called massive MIMO systems. Massive MIMO systems are also efficient in energy usage. But, the use of multiple antennas at the transceivers requires the estimation of the channel characteristics that the system is working on.

1.3 Literature Review

Since the focus of this thesis is on channel estimation methods in massive MIMO systems, in this section, we will review few important papers that are written in the topic related to channel estimation in Massive MIMO systems. Many papers have been written on different channel estimation techniques. For this thesis I have reviewed many papers some of these are:-

The first paper [5] assumes cellular time-division duplexing systems with a large number of antennas at each base station. The paper wanted to challenge the idea that blind channel estimation is always better than the other two channel estimation techniques. The objective of the paper was to compare and contrast between pilot based, blind, and

semi-blind channel estimation techniques. The paper concluded that semi-blind channel estimation techniques are the best for the current technologies. It also stated that blind channel estimations have unsatisfactory results for typical massive MIMO systems. One of the short coming of the paper was that the paper only considers MAP estimator to compare these channel estimation techniques and does not consider the performance difference of different algorithms within a given channel estimation techniques.

The second paper [6] is written by one of the pioneers of this field. This paper discusses massive MIMO systems under pilot contamination and favorable propagation conditions. The objective of the paper was to analyze in massive MIMO systems terms of SE and energy efficiency and Effects of pilot contamination in massive MIMO systems. The paper does not use other comparisons methods to compare between the channel estimation techniques. It does not also estimate the effect of the increase in the number of users on the estimation algorithms.

[7] is the third paper and it is written by the same author as the second paper. The objective of the paper is to study Massive MIMO with Spatially Correlated Rician Fading Channels using LS and MMSE channel estimation algorithms. The SE is used as a comparison method between the channel estimation techniques. This paper as the previous paper does not use other comparisons methods to compare between the channel estimation techniques. It does not also estimate the effect of the increase in the number of users on the estimation algorithms. This paper does not incorporate the recommended antenna spacing between the antennas.

The paper [8] is one of the significant papers written in this field. This paper addresses on how channel estimation techniques are done. The objective of the paper is on how to reduce pilot contamination. The paper concluded that covariance-aided channel estimation methods are good methods in order to decrease the pilot contamination. It also stated that blind and semi-blind channel estimation have a good estimate but are complex. This paper compares between the estimators based on SE and mean square error (MSE). It does not consider other comparison merits. This paper does not compare different channel estimation algorithms with in the pilot based channel estimation category.

[1] is another important paper written in Massive MIMO. It starts from the problem of studying massive MIMO systems deeply. Its objective is to study communication theory behind the Massive MIMO technology, and provides implementation related design guidelines. The paper concluded that Massive MIMO can theoretically provide ten-fold or even 50-fold improvements in SE over IMT-Advanced (International Mobile Telecommunications-Advanced). It does not consider comparison between different channel estimation techniques.

The paper [9] states that it is crucial to define techniques for channel estimation that together with pilot contamination mitigation allow best system performance and at same time low complexity. This paper concluded that a channel estimation technique with Zadoff-Chu sequences was introduced in order to replace channel estimation based on matrix inversions, such as the MMSE estimator. The paper uses BER (bit error rate) and MSE to compare between different channel estimation techniques. The paper does not consider other merits of comparison.

1.4 Research Objectives

1.4.1 General Objective

The general objectives of this thesis is to analyze the performance of the LS and MMSE pilot-based channel estimation techniques when the number of users and the number of antennas vary.

1.4.2 Specific Objectives

The specific objectives of this paper are:-

1. Study massive MIMO systems.
2. Study the LS and MMSE channel estimation techniques for massive MIMO systems.
3. Study the mathematics of LS and MMSE channel estimation techniques when implemented to a massive MIMO cellular system.
4. Create simulations results from MATLAB to provide the analysis for LS and MMSE channel estimation techniques.
5. Study the effect of increasing the number users on LS and MMSE.
6. Study the effect of increasing the number antennas on LS and MMSE.
7. This paper will also try to come up with a different comparison parameter (the value of $\mathbf{H}$) for LS and MMSE channel estimation techniques.

1.5 Methodology

To come up with a comparison between the LS and MMSE estimators, books, journals, scholarly articles, research papers and simulation results will be reviewed and documented for the accomplishment of the goal. Different simulation results from MATLAB will also be used for analysis and discussion.

Algorithms from different scientific articles will be used in order to compare these techniques. These algorithms will be used in order to run simulation in MATLAB simulation tool for the comparison. Algorithm's for channel estimation techniques and for detection will be used in order to run our cellular system.

To compare between different channel estimation technique journals and articles on written this topic, research papers on written on this topic and simulation software are used. After this comparison, we will use the MATLAB simulation software tool and research papers on this topic to come up with discussion and recommendations on the channel estimation techniques.

1.6 Organization of the Thesis

The rest of this thesis is organized as follows.

Chapter 2 studies massive MIMO systems deeply. Section 2.1 discuss MIMO sytems generally. Then in Section 2.2 the steps in advancing from MIMO to massive MIMO are discussed. Section 2.3 studies massive MIMO systems. Then the sections following this section will discuss the operation, properties and advantageous of massive MIMO. Beamforming in massve MIMO and limiting factors in massive MIMO are also studied in their respected sections.

Chapter 3 is devoted for the discussion of the system model for massive MIMO systems. The system model, channel model and mathematical model for the system will be discussed. In Section 3.1 the system model for massive MIMO is developed. Based on the system model, the next chapter will discuss simulation results and discussions for the LS and MMSE channel estimation techniques.

Chapter 4 studies channel estimation methods in Massive MIMO systems. Section 4.2 discusses channel estimation techniques. Then Section 4.3 studies about pilot based channel estimation techniques specially the LS and MMSE algorithms. Then the detection algorithms are studied in Section 4.4.

Chapter 5 is devoted for the discussion of the simulation results and discussion of these channel estimators. All these will be discussed in Section 5.2. Here in this chapter different simulation results will be presented and explained.

Finally, Chapter 6 is for the conclusion and future work. Section 6.1 is for discussing the conclusion of the paper. Section 6.2 gives indications for possible future works related to this work. This is what the organization of the paper looks like.

1.7 Contributions of the Thesis

A lot of papers have been written on this topic, the topic of pilot based channel estimation in massive MIMO systems. One may ask "What would be the contribution of this particular thesis?" Well, There will be contribution from this paper. Some of the contributions of this paper would be:-

- The thesis will compare between different channel estimation techniques in a way that is different from other scientific papers (using SE and **H**).
- The thesis will predict the effect of the number of users and the number of antennas in the LS and MMSE channel estimators. It will also predict which of these estimators is affected more than the other by these two system parameters(the number of users and the number of antennas).

Chapter 2

Massive MIMO Systems

2.1 MIMO Systems

Technologies are always advancing. The first communication was point-to-point communication which is called single input single out put communication system (SISO). And then it was advanced to SIMO (single input multiple output) and MISO (multiple input single output) communication systems and then to MIMO systems. Figure 2.1 shows the basics of SISO, SIMO, MISO and MIMO systems.

MIMO technology is a wireless technology that uses multiple transmitters and receivers to transfer more data at the same time. MIMO technology takes advantage of a radio-wave phenomenon called multipath where transmitted information bounces off walls, ceilings, and other objects, reaching the receiving antenna multiple times via different angles and at slightly different times. The MIMO channel technology targets to increase the capacity in the wireless communication network. After the invention of MIMO, it gained the popularity in the field. It was implemented in the commercial wireless products and networks such as broadband wireless access systems, wireless local area networks (WLAN), 3G networks, 4G networks. Figure 2.2 shows a line of sight (LoS) antenna setup of a MIMO system where each h's represent path (channel) characteristics.

The capacity of MIMO systems is several times that of SISO systems. This can be shown as an example in a system where the communication channel is 20MHz. If we assume some value of SNR for the the speed of the connection to be 8 Mbps. Now if we use 2x2 MIMO system, by using Shannon's equation we can show that the capacity of the new system would be 16 Mbps. By the same argument if use 4x4 MIMO system, the capacity of the new system would be 32 Mbps. The capacity of the system was doubled by doubling the antennas on both sides of the communication system. This is a very promising technology for communication systems. That is why it is popular in the technology industry. This is also the reason behind why the current communication system are looking forward for massive MIMO systems. Figure 2.3 shows a comparison between SIMO/MISO systems

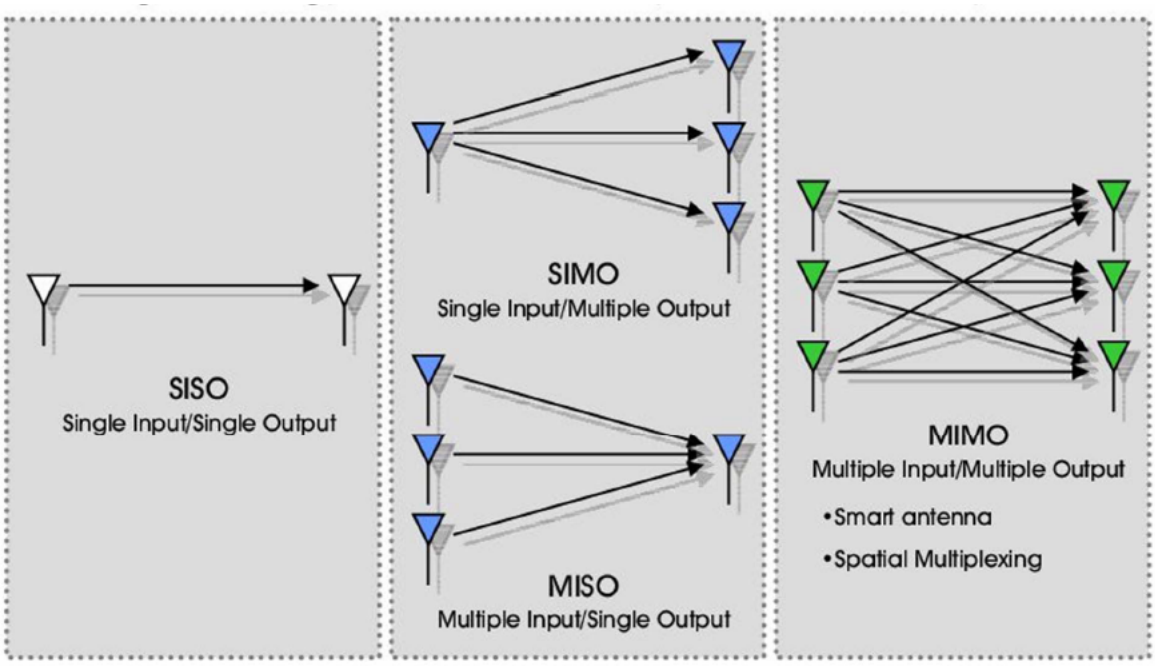

FIGURE 2.1: Basics of SISO, SIMO, MISO and MIMO systems [10].

and MIMO systems. It is clear from the figure that MIMO systems have very high capacity because of the increase in the number of antennas.

As a result of the use of multiple antennas, MIMO wireless technology is able to considerably increase the capacity of a given channel. By increasing the number of receive and transmit antennas it is possible to linearly increase the throughput of the channel with every pair of antennas added to the system. This makes MIMO wireless technology one of the most important wireless techniques to be employed in recent years. As spectral bandwidth is becoming an ever more valuable commodity for radio communications systems, techniques are needed to use the available bandwidth more effectively. MIMO wireless technology is one of these techniques.

2.2 Advancements from MIMO to Massive MIMO

The paper [11] states that today's MIMO antennas typically use two transmit and two receive antenna elements, which double the capacity of a basic antenna. But now in these days, 4 to 8 antenna elements are used. Developed by Nokia's Bell Labs, Massive MIMO goes further, using many antenna elements to simultaneous transmit and receive streams of signals controlled by advanced software to create a much higher network capacity [11]. The capacity gains from MIMO systems was very high to such an extent that many scientists started to study the effect of increasing the number of antennas even beyond the common MIMO systems. This led to massive MIMO technology. The main reason for

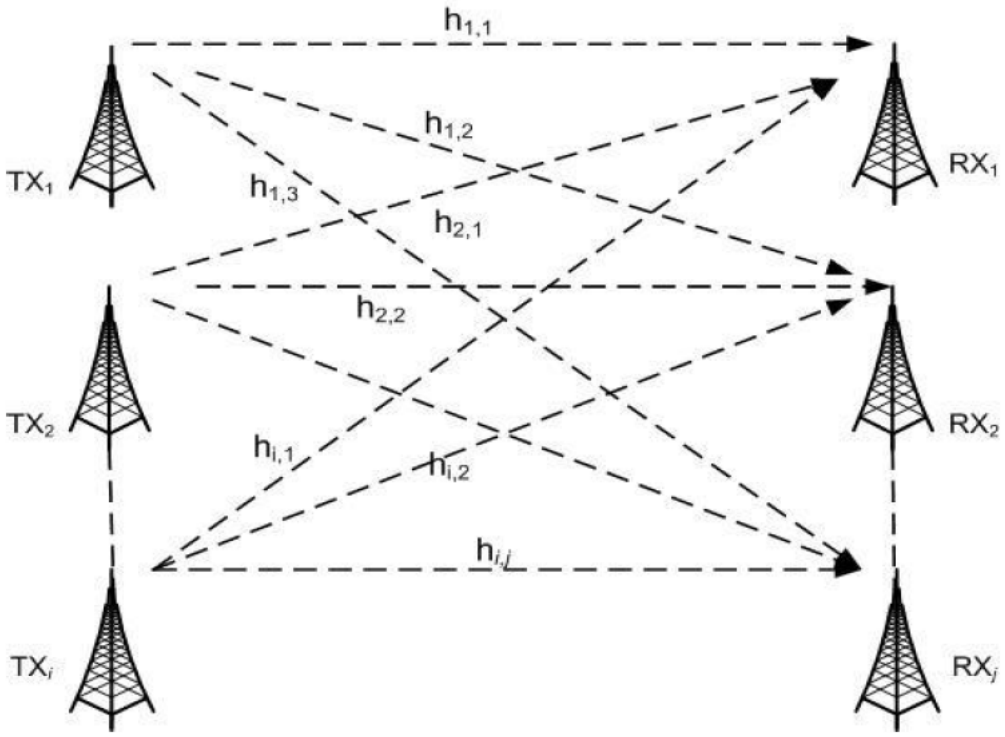

FIGURE 2.2: Line of sight (LoS) antenna setup of a MIMO system [10].

increasing the capacity of our communication systems is the high data rate required by users. This need is even increasing from time to time.

The main changes that were applied when advancing from MIMO to massive MIMO

- The antennas that were used in MIMO systems were 2,4,8, ... while the antennas that are used in massive MIMO systems are hundreds of antennas or even thousands of antennas [1].
- Massive MIMO systems are characterized by [1],

$$Number_{(BTS\ antennas)} >> Number_{(users)}$$

- Other outstanding characteristics of massive MIMO systems come from the above properties of the massive MIMO systems.

Currently the cellular technologies are cell centric and this is not good if we are heading for a very high speed connection. so, we need to move from cell centric cellular networks to user centric networks using the technology called beamforming (Beamforming will be discussed in Section 2.4.) Massive MIMO with beam forming improves the end user experience by significantly increasing network capacity and coverage while also reducing

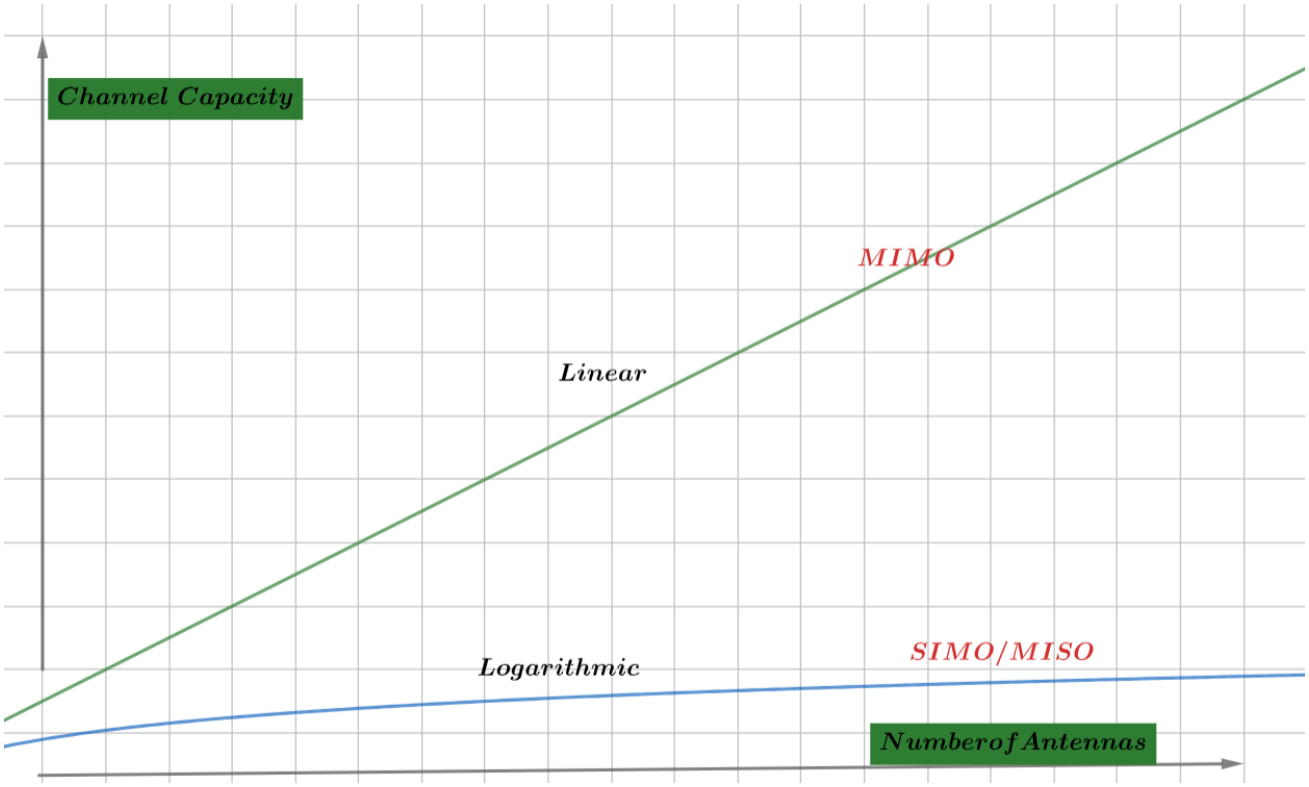

FIGURE 2.3: Comparing SIMO/MISO systems with MIMO systems.

interference. This is done by increasing the effectiveness of the transmission. Sending out radio waves as highly focused beams delivers a stronger radio signal, with a higher data throughput for greater distances. This is also an ideal solution to increase capacity in congested areas – especially when adding another frequency band isn't really an option. The Massive MIMO antenna array with a large number of steerable ports enables beam forming, which means that radio signals and information are sent directly to the device instead of broadcasting across the entire cell. This has the added benefit of also reducing radio interference across the cell, resulting in a more enjoyable user experience [12]. See Figure 2.4 for detail.

2.3 Massive MIMO Systems

Massive MIMO is a promising technology for future huge capacity connection needs. Massive MIMO is currently the most compelling wireless physical layer technology, and a key component of 5G systems [13]. In this thesis, we will develop the system model for massive MIMO communication systems. We will also run different simulations to test the performance of different channel estimation techniques. pilot contamination will not be considered in this thesis. Massive MIMO is a huge system that includes many infrastructures and equipment's. One of the main part of massive MIMO is the antenna.

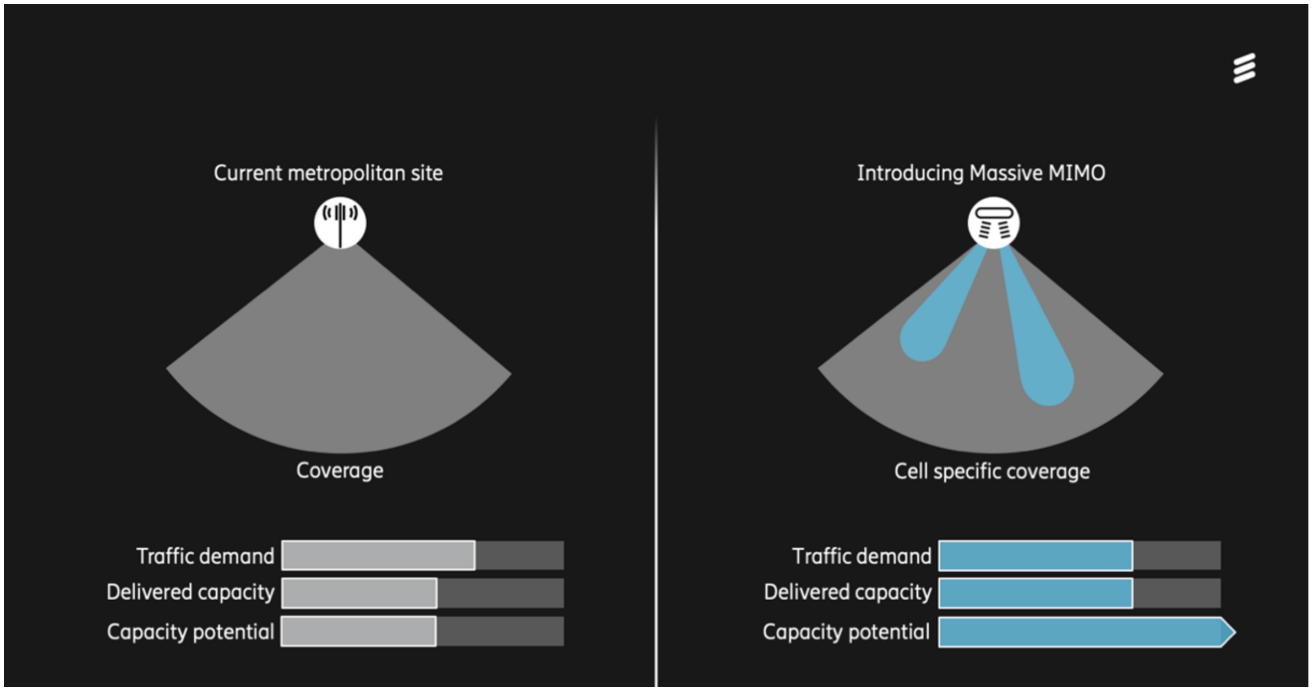

FIGURE 2.4: Cell Centric and User Centric Cellular Networks [12].

since there is large number of antennas, the antennas need to be configured in some way for the best results. Figure 2.6 shows possible antenna configuration for massive MIMO.

Figure 2.5 shows typical massive MIMO systems. Where the figure shows a massive MIMO systems that use antenna arrays with a few hundred antennas, simultaneously serving many tens of terminals in the same time-frequency resource. The basic premise behind massive MIMO is to reap all the benefits of conventional MIMO, but on a much greater scale. Overall, massive MIMO is an enabler for the development of future broadband (fixed and mobile) networks which will be energy-efficient, secure, and robust, and will use the spectrum efficiently. As such, it is an enabler for the future digital society infrastructure that will connect the Internet of people, Internet of things, with clouds and other network infrastructure. With Massive MIMO, operators now have a powerful new tool to boost capacity using their existing spectrum [11]. This makes the massive MIMO an attractive technology for the telecommunication industries. As demand for mobile broadband services explodes, operators need to maximize the efficiency of their valuable spectrum resources to increase network capacity. Massive MIMO techniques and products hold the to achieving this.

Massive MIMO relies on spatial multiplexing that in turn relies on the base station having good enough channel knowledge, both on the uplink and the downlink. On the uplink, this is easy to accomplish by having the terminals send pilots, based on which the base station estimates the channel responses to each of the terminals. The downlink is more difficult. In conventional MIMO systems, like the LTE (long term evolution) standard,

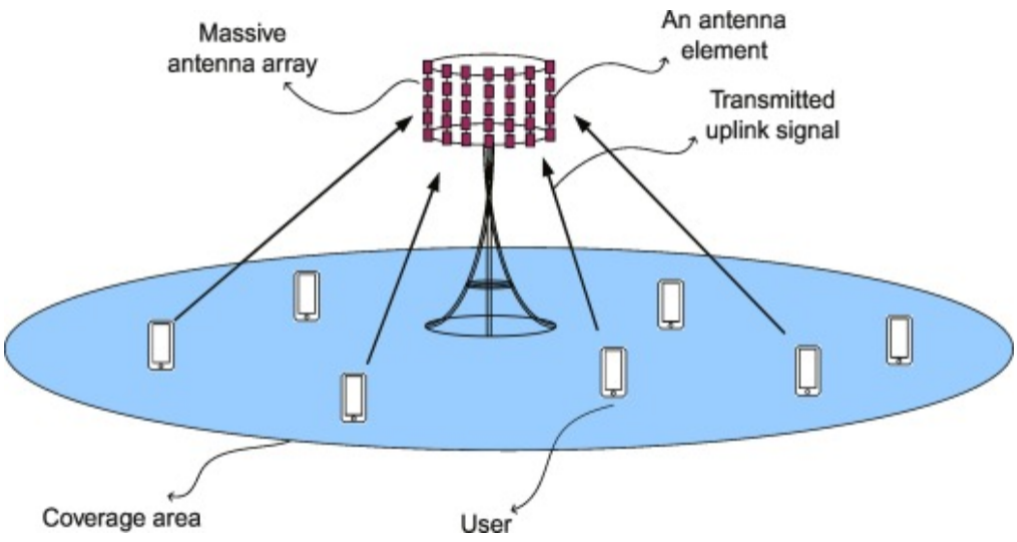

FIGURE 2.5: Particular massive MIMO system in the uplink transmission [14].

the base station sends out pilot waveforms based on which the terminals estimate the channel responses, quantize the so-obtained estimates and feed them back to the base station. This will not be feasible in massive MIMO systems, at least not when operating in a high-mobility environment, for two reasons. First, optimal downlink pilots should be mutually orthogonal between the antennas. This means that the amount of time frequency resources needed for downlink pilots scales as the number of antennas, so a massive MIMO system would require up to a hundred times more such resources than a conventional system. Second, the number of channel responses that each terminal must estimate is also proportional to the number of base station antennas. Hence, the uplink resources needed to inform the base station about the channel responses would be up to a hundred times larger than in conventional systems [15]. Generally, the solution is to operate in TDD mode, and rely on reciprocity between the uplink and downlink channels—although FDD operation may be possible in certain cases [15].

2.3.1 Massive MIMO and 5G

While standard MIMO principles are already in use across multiple Wi-Fi and 4G standards, Massive MIMO will really come into play once 5G arrives. Indeed, it's widely expected that Massive MIMO will be a key enabler and foundational component of 5G [16]. And indeed as we have seen it in these days that the massive MIMO is the main component of the 5G network. One of the key roles of any 5G network will be to handle the huge increase in data usage that's around the corner. Cisco estimates that by 2020 -

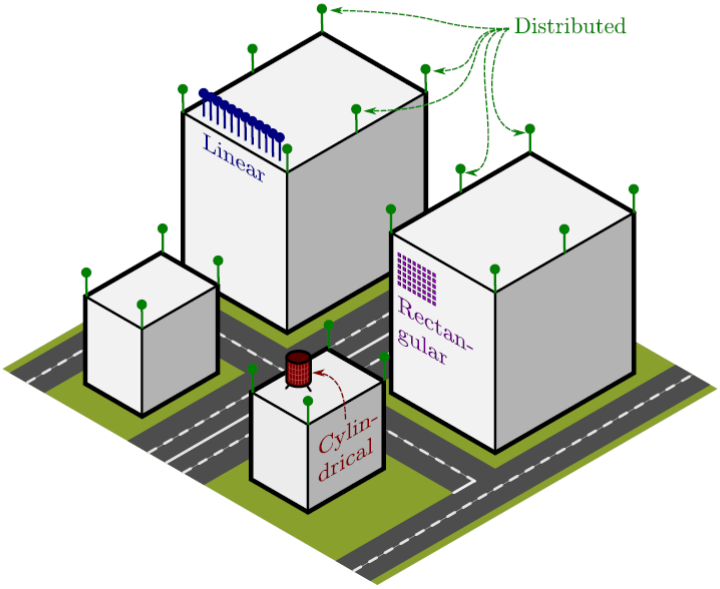

FIGURE 2.6: Some possible antenna configurations and deployment scenarios for a massive MIMO base station [15].

when 5G is set to roll out to a mainstream audience - there will be 5.5 billion mobile users around the world, each consuming 20 GB of data per month. That's not even factoring in the huge impact the Internet of Things is predicted to have on our mobile networks [16]. Massive MIMO's ability to serve multiple users - and multiple devices - simultaneously within a condensed area while maintaining fast data rates and consistent performance makes it the perfect technology to address the needs of the forthcoming 5G era.

In general, 5G will use higher radio spectrums than 2G/3G/4G, including centimeter waves and millimeter waves such as 3.5 GHz and 28 GHz. Its radio propagation loss is much bigger than previous sub-1GHz and around 2 GHz. Also, 5G radio propagation can be strongly affected by the surrounding environment, such as building shadowing, reflection from walls, human bodies and rain attenuation. This sensitivity would make massive MIMO's coverage enhancement ability stand out [17]. As we have mentioned, both beamforming and MU-MIMO can increase single-user throughput and total network capacity per basestation. Massive MIMO becomes far more practical at higher frequencies, such as those planned for many 5G deployments [17].

At the debate session on "5G Deployments in High-Frequency Bands are Uneconomic" on February 26 at the Mobile World Conference (MWC) 2019, Mr. Yang Chaobin, president of Huawei's 5G product line, elaborated on the idea that Massive MIMO is the key to simplified 5G networks. Drawing on rigorous theoretical analysis and extensive testing

results, he responded positively to the much debated topic on the economy of 5G network construction. Deployed on the same sites with LTE in 1:1 mode, Mr. Yang emphasized, 5G with 3.5 GHz Massive MIMO delivers better coverage and greater capacity than LTE. In addition, operators will see significantly lower cost per bit and lower overall deployment costs [18]. Generally, massive MIMO looks very promising for the future of 5G. In the long run, it's very likely that service providers would find massive MIMO the only path to achieve IMT-2020 [17].

2.3.2 Channel Estimation

There are two massive MIMO systems based on the method of sharing the available spectrum in massive MIMO systems. TDD and FDD are two topologies by which critical resources time and frequency are shared among mobile subscribers or terminals. LTE uses both of these flavors to provide facility for the mobile subscribers or UEs to utilize the scarse resource efficiently based on the need.

2.3.3 Channel Estimation in TDD Systems

Originaly, Massive MIMO concept assumes TDD and exploits reciprocity for the acquisition of CSI at the BS. UEs send pilots on the uplink (UL); all UE-to-BS channels are estimated, and each antenna has its own RF electronics. The concept has, since its introduction a decade ago matured significantly: rigorous information-theoretic analyses are available, field-trials have demonstrated its performance in high-mobility scenarios, and circuit prototypes have shown the true practicality of implementations [19].

In a TDD system, the uplink and downlink transmissions use the same frequency spectrum, but different time slots. The uplink and downlink channels are reciprocal [14]. As we can see from Figure 2.7, same carrier frequency F_c is used at different time instants t_1 and t_2 for uplink and downlink transmission purpose. Thus, the CSI can be obtained by using following scheme (see Figure 2.8):

- For the uplink transmission: the BS needs CSI to detect the signals transmitted from the K users. This CSI is estimated at the BS. More precisely, the K users send K orthogonal pilot sequences to the BS on the uplink. Then the BS estimates the channels based on the received pilot signals. This process requires a minimum of K channel uses [14].
- For the downlink: the BS needs CSI to precode the transmitted signals, while each user needs the effective channel gain to detect the desired signals. Due to the channel reciprocity, the channel estimated at the BS in the uplink can be used to precode the transmit symbols. To obtain the knowledge of the effective channel gain, the BS

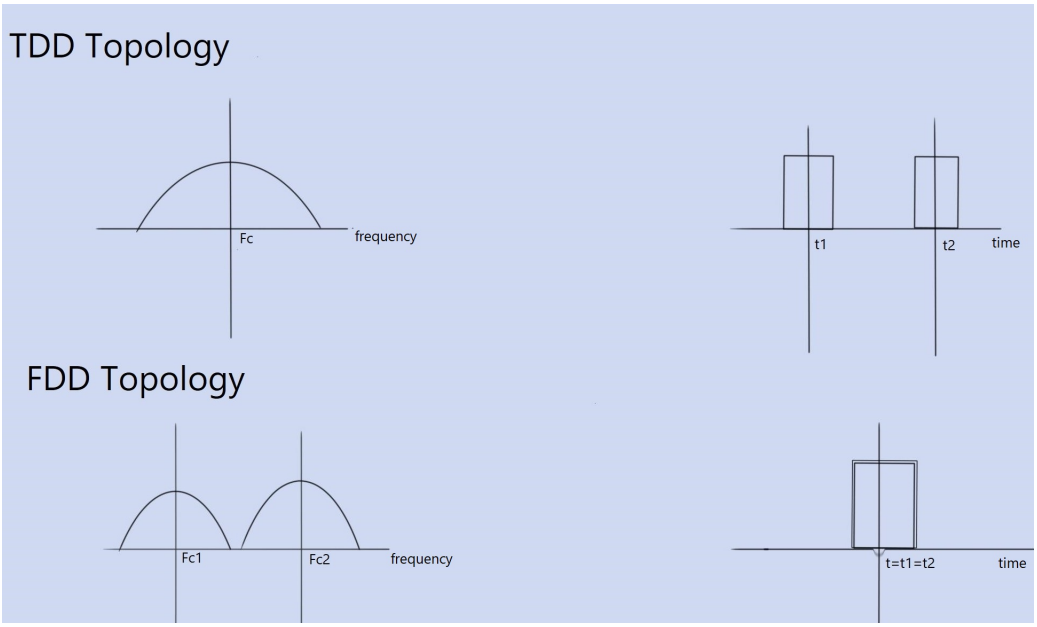

FIGURE 2.7: TDD and FDD topologies.

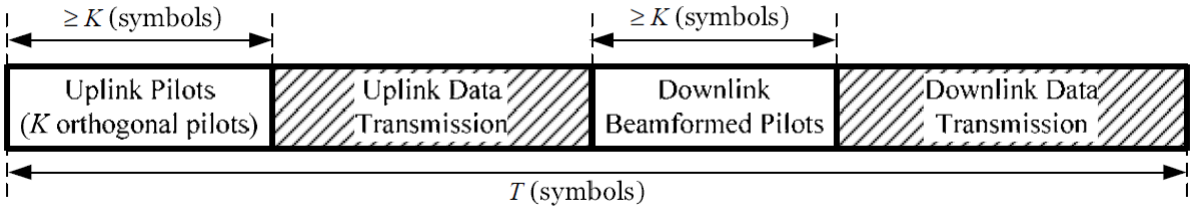

FIGURE 2.8: Slot structure and channel estimation in TDD systems [14].

can beamform pilots, and each user can estimate the effective channel gains based on the received pilot signals. This requires at least K channel uses [14].

As shown in the Figure 2.9, both uplink and downlink has been allocated same frequency $f_1 = f_2$ and but both uses different time slots for mapping their information data. Hence the subframes of the entire radio frame is divided and used for both the uplink and downlink direction. In total, the training process requires a minimum of $2K$ channel uses. We assume that the channel stays constant over T symbols. Thus, it is required that $2K < T$ [14]. An illustration of channel estimation in TDD systems is shown in Figure 2.8.

2.3.4 Channel Estimation in FDD Systems

In an FDD system, the uplink and downlink transmissions use different frequency spectrum, and hence, the uplink and downlink channels are not reciprocal [14]. The channel knowledge at the BS and users can be obtained by using following training scheme:

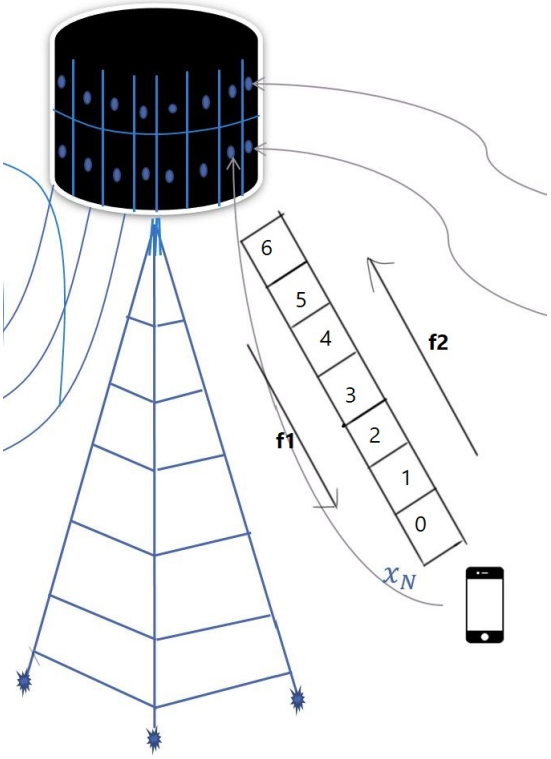

FIGURE 2.9: TDD scenario.

As we can see from Figure 2.7, two different carrier frequencies F_{c1} and F_{c2} are used for uplink and downlink respectively at the same time t_1. Downlink is related to upper part of the spectrum while uplink is related to lower part of the spectrum with guard band (i.e. duplex gap) between these parts.

As shown in the Figure 2.10, f_1 and f_2 are one pair of frequencies allocated separately for both the uplink and downlink direction. Hence f_1 is allocated for downlink band and f_2 is allocated from uplink frequency band. The entire radio frame is used simultaneously over downlink and uplink directions.

- For the downlink transmission: the BS needs CSI to precode the symbols before transmitting to the K users. The M BS antennas transmit M orthogonal pilot sequences to K users. Each user will estimate the channel based on the received pilots. Then it feeds back its channel estimates (M channel estimates) to the BS through the uplink. This process requires at least M channel uses for the downlink and M channel uses for the uplink [14].
- For the uplink transmission: the BS needs CSI to decode the signals transmitted from the K users. One simple way is that the K users transmit K orthogonal pilot

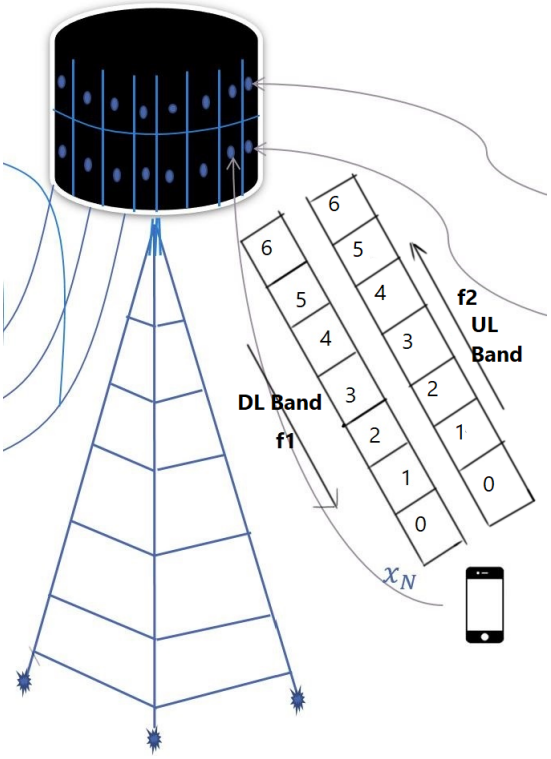

FIGURE 2.10: FDD scenario.

sequences to the BS. Then, the BS will estimate the channels based on the received pilot signals. This process requires at least K channel uses for the uplink [14].

Therefore, the entire channel estimation process requires at least $M + K$ channel uses in the uplink and M channel uses in the downlink. Assume that the lengths of the coherence intervals for the uplink and the downlink are the same and are equal to T. Then we have the constraints: $M < T$ and $M + K < T$. As a result $M + K < T$ is the constraint for FDD systems. An illustration of channel estimation in FDD systems is shown in Figure 2.11 [14].

System constraint between TDD and FDD can be performed in order to choose the best system because system constraint is one parameter for comparison. The paper [14] shows a good comparison between the two systems based on system constraint. With FDD, the channel estimation overhead depends on the number of BS antennas, M. By contrast, with TDD, the channel estimation overhead is independent of M. In Massive MIMO, M is large, and hence, TDD operation is preferable. For example, assume that the coherence interval is $T = 200$ symbols (corresponding to a coherence bandwidth of $200kHz$ and a coherence time of $1ms$). Then, in FDD systems, the number of BS antennas and the number of users are constrained by $M + K < 200$, while in TDD systems, the constraint

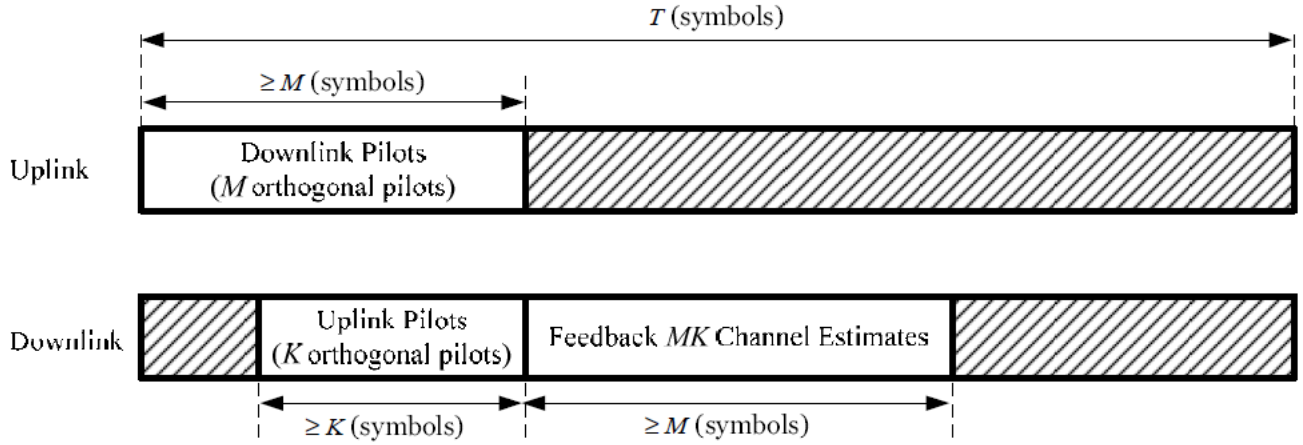

FIGURE 2.11: Slot structure and channel estimation in FDD systems [14].

on M and K is $2K < 200$. Figure 2.12 shows the regions of feasible (M, K) in FDD and TDD systems. We can see that the FDD region is much smaller than the TDD region. With TDD, adding more antennas does not affect the resources needed for the channel estimation.

It is not that much difficult to switch between TDD and FDD systems because Now a days, many chip-set manufacturers such as Ericsson, Altair semiconductor, Qualcomm support both TDD and FDD versions of LTE on a single chip and this flexibility can be exploited by telecommunication operators based on traffic and other requirements.

2.4 Beamforming and Massive MIMO

Massive MIMO offers two major innovations: beamforming and MU-MIMO (multi-user MIMO) [17]. So, in this section we will give an introduction to beamforming in massive MIMO. Massive MIMO systems exploit the use of large antenna arrays at wireless base stations to simultaneously serve a large number of autonomous terminals through spatial multiplexing. The multiplexing takes the form of beamforming, also known as multiuser precoding, effectively creating transmitted signals that add up constructively on the spots where the terminals are located and destructively almost every where else. Base stations consisting of large numbers of antennas that simultaneously communicate with multiple spatially separated user terminals over the same frequency resource and exploit multipath propagation are one option to achieve this efficiency saving. This technology is often referred to as massive MIMO (multiple-input, multiple-output). You may have heard massive MIMO described as beamforming with a large number of antennas. But this leads us to the question "what is beamforming?"

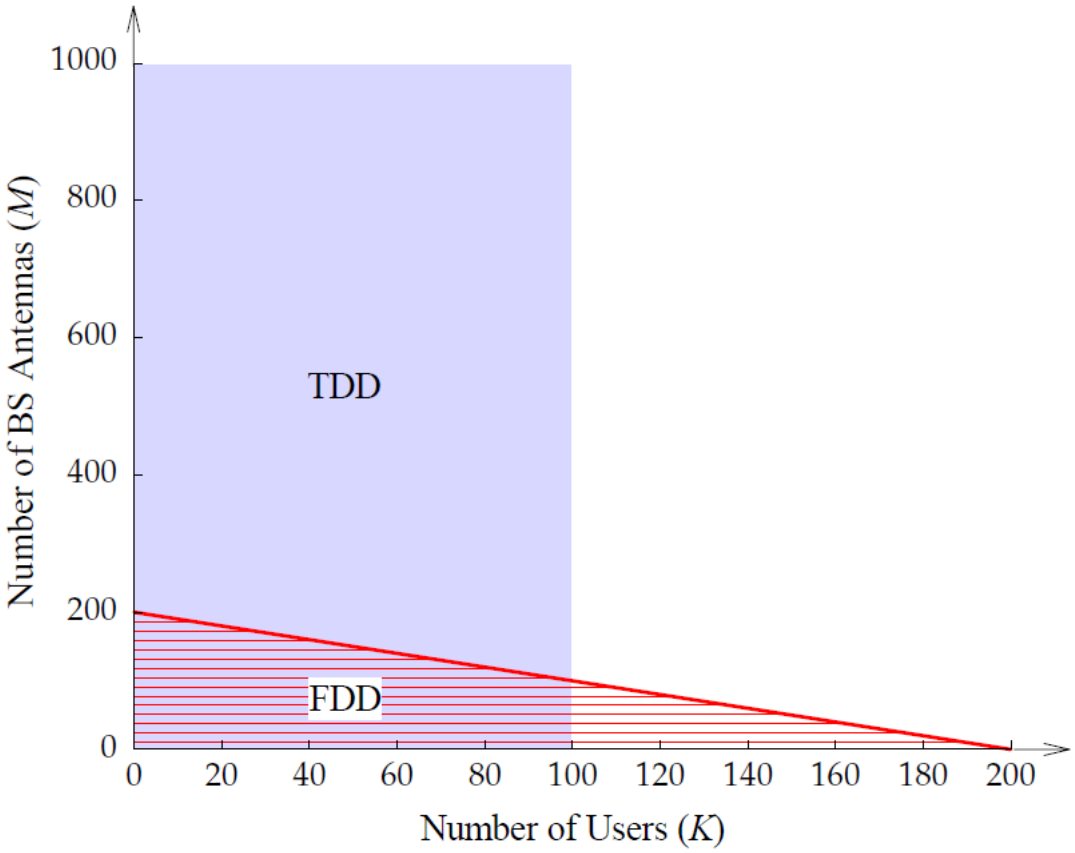

FIGURE 2.12: The regions of possible (M, K) in TDD and FDD systems, for a coherence interval of 200 symbols [14].

Beamforming is a word that means different things to different people. Beamforming is the ability to adapt the radiation pattern of the antenna array to a particular scenario. In the cellular communications space, many people think of beamforming as steering a lobe of power in a particular direction toward a user, as shown in Figure 2.13. Relative amplitude and phase shifts are applied to each antenna element to allow for the output signals from the antenna array to coherently add together for a particular transmit/receive angle and destructively cancel each other out for other signals. The spatial environment that the array and user are in is not generally considered. This is indeed beamforming, but is just one specific implementation of it [20].

While an individual antenna has a fixed radiation pattern, antenna arrays are capable of changing their radiation patterns over time and frequency, for both transmission and reception. This is traditionally illustrated as the formation of spatial beams in one (or a few) distinct angular directions, but antenna arrays are also capable of many other types of spatial filtering. For example, the signal processing that controls the array can be used to focus a signal at an arbitrary point in space which, in a rich multi-path propagation

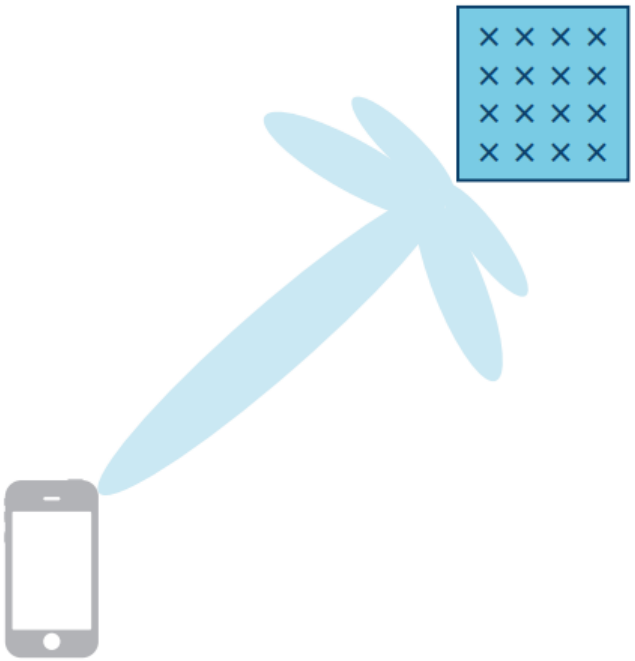

FIGURE 2.13: Traditional Beamforming [21].

environment, corresponds to emitting a superposition of many angular beams so that the radiated pattern has no dominant directivity. In addition, the array can be used to sense the propagation environment, for example, to detect anomalies or moving objects [22]. Figure 2.14 shows beamforming from an antenna array can be used to (a) focus the radiated signal in one angular direction or (b) focus the signal at one particular point in space, in which case the radiated signal might have no dominant directivity. The radiation patterns in this figure were computed using eight antenna uniform linear arrays.

The terms beamforming and massive MIMO are sometimes used interchangeably. One way to put it is that beamforming is used in massive MIMO, or beamforming is a subset of massive MIMO. In general, beamforming uses multiple antennas to control the direction of a wave-front by appropriately weighting the magnitude and phase of individual antenna signals in an array of multiple antennas. That is, the same signal is sent from multiple antennas that have sufficient space between them (at least $\frac{1}{2}$ wavelength). In any given location, the receiver will thus receive multiple copies of the same signal. Depending on the location of the receiver, the signals may be in opposite phases, destructively averaging each other out, or constructively sum up if the different copies are in the same phase, or anything in between [23]. Achieving a certain directivity or beamforming requires an antenna array where the RF signal at each antenna element is amplitude and phase weighted. There are three possible ways to apply amplitude and phase shifts [21]. Different types of beamforming used for massive MIMO systems are discussed below.

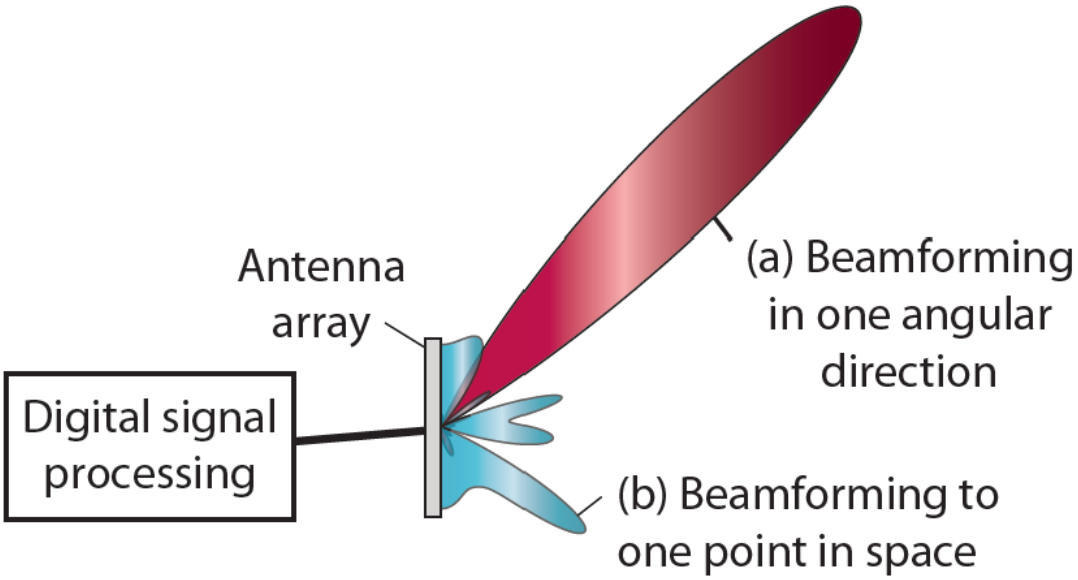

FIGURE 2.14: Beamforming from an antenna array [21].

- **Digital Beamforming (aka. Baseband beamforming, aka precoding):** the signal is pre-coded (amplitude and phase modifications) in baseband processing before RF transmission. Multiple beams (one per each user) can be formed simultaneously from the same set of antenna elements. In the context of LTE/5G, MU-MIMO equals to digital beamforming. Multiple TRX chains, one per each simultaneous MU-MIMO user, are needed in the base station. Digital beamforming (MU-MIMO) is used in LTE Advanced Pro (transmission modes 7,8, and 9) and in 5G NR. Digital beamforming improves the cell capacity as the same PRBs (frequency/time resources) can be used to transmit data simultaneously for multiple users [23].

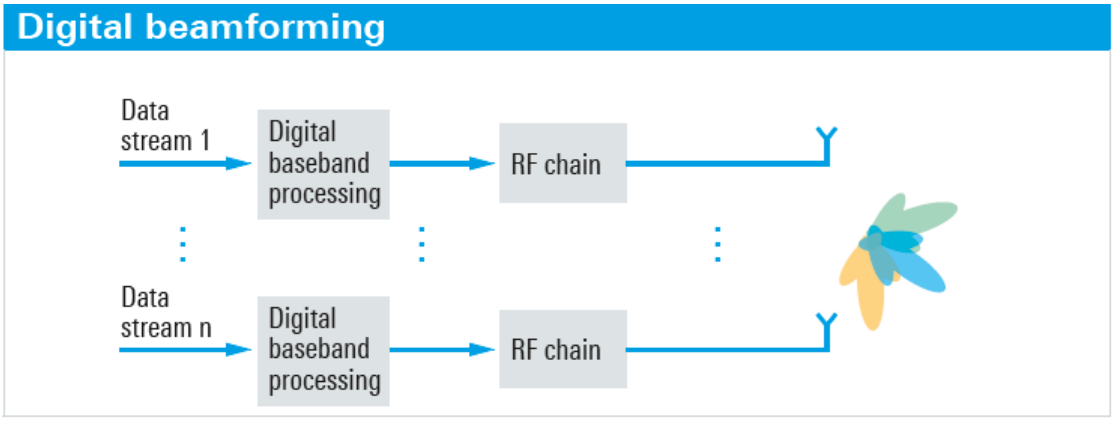

FIGURE 2.15: Digital Beamforming [21].

- **Analog Beamforming:** the signal phases of individual antenna signals are adjusted in RF domain. Analog beamforming impacts the radiation pattern and gain of the antenna array, thus improves coverage. Unlike in digital beamforming, only one beam per set of antenna elements can be formed. The antenna gain boost provided by the analog beamforming overcomes partly the impact of high pathloss in mmWave. Therefore analog beamforming is considered mandatory for the mmWave frequency range 5G [23].

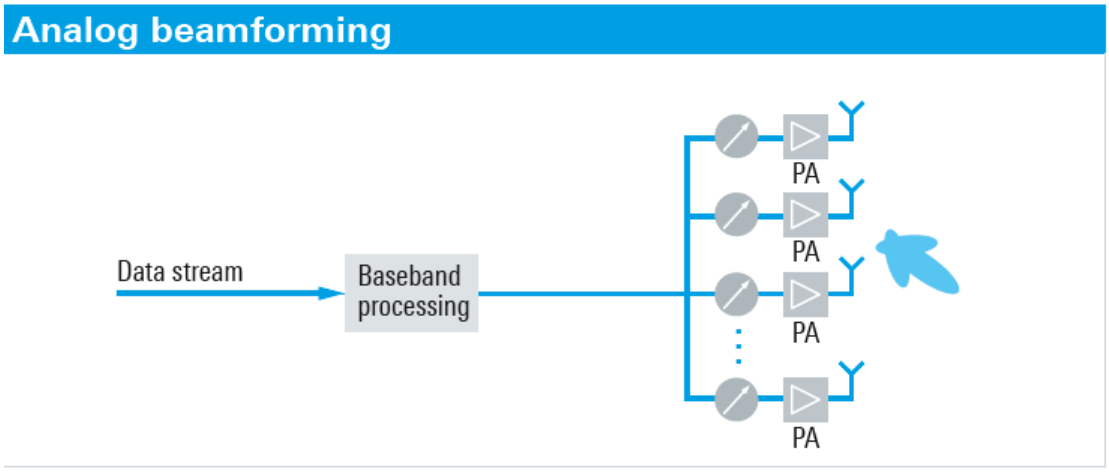

FIGURE 2.16: Analogue Beamforming [21].

- **Hybrid Beamforming:** hybrid beamforming combines the analog beamforming and digital beamforming. It is expected that mm-wave gNB (5G base station) implementations will use some form of hybrid beamforming. One approach is to use analog beamforming for coarse beamforming, and inside the analog beam use a digital beamforming scheme as appropriate, either MU-MIMO or SU-MIMO [23].

2.5 Properties and Advantageous of Massive MIMO

Massive MIMO is a form of MU-MIMO systems where the number of BS antennas and the numbers of users are large. In Massive MIMO, hundreds or thousands of BS antennas simultaneously serve tens or hundreds of users in the same frequency resource. Some main points of Massive MIMO are:

- TDD operation: as discussed in Section 2.3.2, with FDD, the channel estimation overhead depends on the number of BS antennas, M. By contrast, with TDD, the channel estimation overhead is independent of M. In Massive MIMO, M is large, and hence, TDD operation is preferable. Figure 2.18 shows Transmission protocol of TDD Massive MIMO.

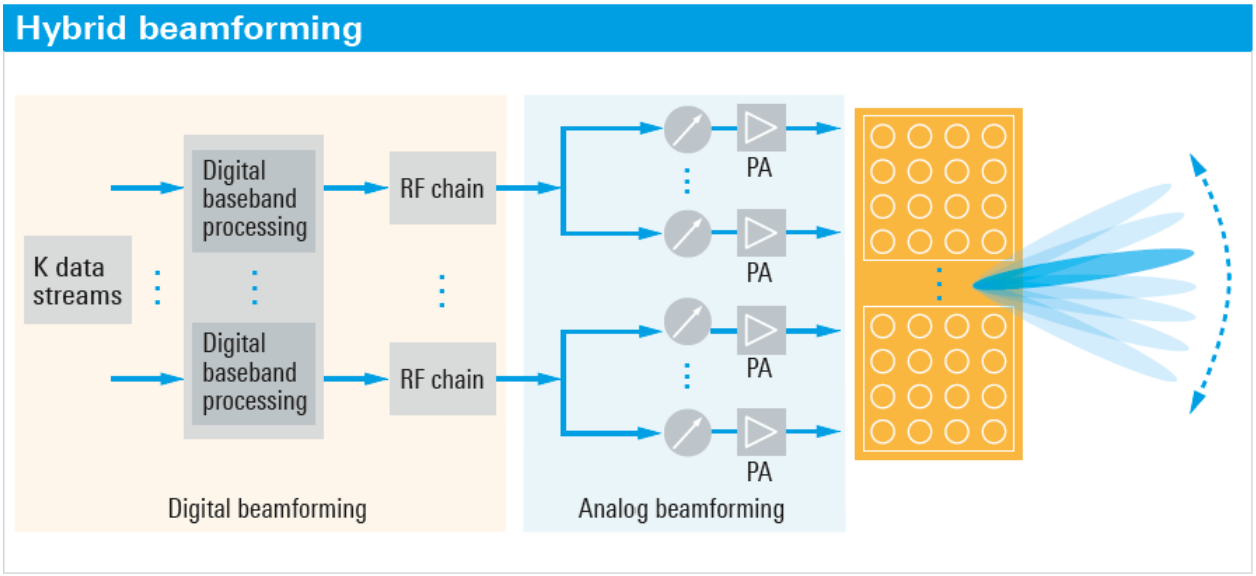

FIGURE 2.17: Hybrid Beamforming [21].

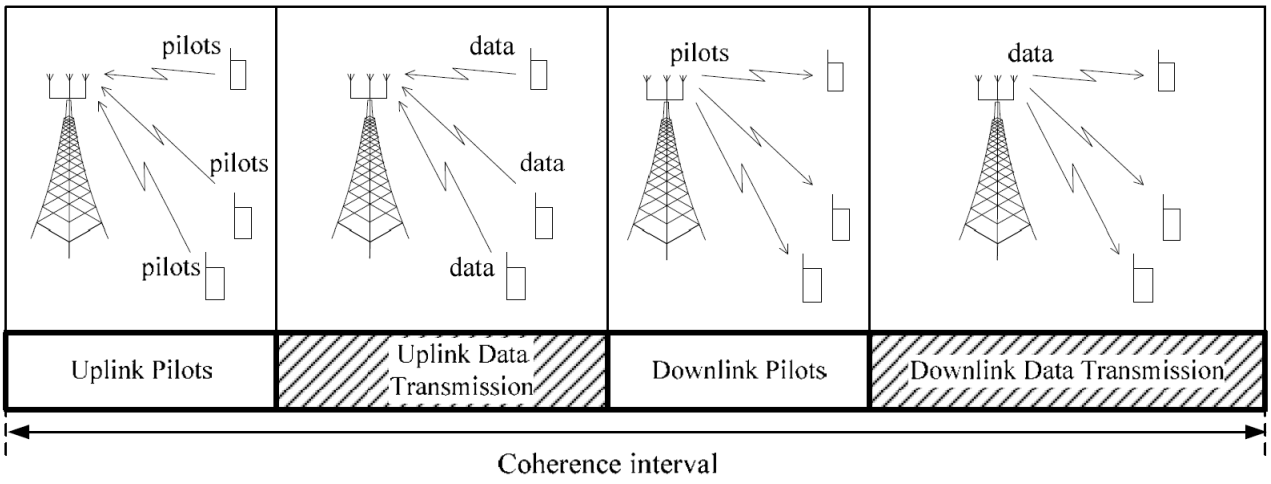

FIGURE 2.18: Transmission protocol of TDD Massive MIMO [14].

- Linear processing: since the number of BS antennas and the number of users are large, the signal processing at the terminal ends must deal with large dimensional matrices/vectors. Thus, simple signal processing is preferable. In Massive MIMO, linear processing (linear combing schemes in the uplink and linear precoding schemes in the downlink) is nearly optimal [14].
- Favorable propagation: favorable propagation means that the channel matrix between the BS antenna array and the users is well-conditioned. In Massive MIMO, under some conditions, the favorable propagation property holds due to the law of large numbers [14].
- A massive BS antenna array does not have to be physically large. For example

consider a cylindrical array with 128 antennas, comprising four circles of 16 dual-polarized antenna elements. At $2.6GHz$, the distance between adjacent antennas is about $6cm$, which is half a wavelength, and hence, this array occupies only a physical size of $28cm * 29cm$ [14].

- Massive MIMO is scalable: in Massive MIMO, the BS learns the channels via uplink training, under TDD operation. The time required for channel estimation is independent of the number of BS antennas. Therefore, the number of BS antennas can be made as large as desired with no increase in the channel estimation overhead. Furthermore, the signal processing at each user is very simple and does not depend on other users' existence, i.e., no multiplexing or de-multiplexing signal processing is performed at the users. Adding or dropping some users from service does not affect other users' activities [14].
- All the complexity is at the BS [14].

Massive MIMO system have many advantageous that makes them preferable over previous technologies. One of these advantageous is that it can increase the capacity 10 times or more and simultaneously improve the radiated energy-efficiency in the order of 100 times [15]. The capacity increase results from the large number of antennas used in massive MIMO. the energy-efficiency comes from the capacity of massive in beamforming. The fundamental principle that makes the dramatic increase in energy efficiency possible is that with large number of antennas, energy can be focused with extreme sharpness into small regions in space. By appropriately shaping the signals sent out by the antennas, the base station can make sure that all wave fronts collectively emitted by all antennas add up constructively at the locations of the intended terminals, but destructively (randomly) almost everywhere else. Interference between terminals can be suppressed even further by using different combining techniques and algorithms.

The second advantage is that it can be built with inexpensive, low-power components [15]. Massive MIMO technology is the best choice both with regard to theory, systems and implementation. With massive MIMO, expensive non-linear equipment's used in conventional systems are replaced by low-cost linear equipment's. Several expensive and bulky items, such as large coaxial cables, can be eliminated altogether. The typical coaxial cables used for tower-mounted base stations today are more than four centimeters in diameter! Massive MIMO reduces the constraints on accuracy and linearity of each individual amplifier and RF chain. All what matters is their combined action. In a way, massive MIMO relies on the law of large numbers to make sure that noise, fading and hardware imperfections average out when signals from a large number of antennas are combined in the air together. The same property that makes massive MIMO resilient against fading also makes the technology extremely robust to failure of one or a few of

the antenna units. A massive MIMO system has a large surplus of degrees of freedom. For example, with 200 antennas serving 20 terminals, 180 degrees of freedom are unused. These degrees of freedom can be used for hardware-friendly signal shaping. In particular, each antenna can transmit signals with very small peak-to-average ratio or even constant envelope at a very modest penalty in terms of increased total radiated power [15].

The third advantage is that it enables a significant reduction of latency on the air interface [15]. The performance of wireless communications systems is normally limited by fading. The fading can render the received signal strength very small at some times. This happens when the signal sent from a base station travels through multiple paths before it reaches the terminal, and the waves resulting from these multiple paths interfere destructively. It is this fading that makes it hard to build low-latency wireless links. If the terminal is trapped in a fading dip, it has to wait until the propagation channel has sufficiently changed until any data can be received. MassiveMIMO relies on the law of large numbers and beamforming in order to avoid fading dips, so that fading no longer limits latency [15].

Massive MIMO simplifies the multiple-access layer [15]. By the law of large numbers, the channel hardens so that frequency-domain scheduling no longer pays off. With OFDM, each subcarrier in a massive MIMO system will have substantially the same channel gain. Each terminal can be given the whole bandwidth, which renders most of the physical-layer control signaling redundant.

The other advantage of Massive MIMO is increasing the robustness both to unintended man-made interference and to intentional jamming [15]. Intentional jamming of civilian wireless systems is a growing concern and a serious cybersecurity threat that seems to be little known to the public. Simple jammers can be bought off the Internet for a few 100, and equipment that used to be military-grade can be put together using off-the-shelf software radio-based platforms for a few 1000 [15].

2.6 Pilot Contamination: The Limiting Factors of Massive MIMO

Ideally every terminal in a Massive MIMO system is assigned an orthogonal uplink pilot sequence. However the maximum number of orthogonal pilot sequences that can exist is upper bounded by the duration of the coherence interval divided by the channel delay-spread. In [14], for a typical operating scenario, the maximum number of orthogonal pilot sequences in a one millisecond coherence interval is estimated to be about 200. It is easy to exhaust the available supply of orthogonal pilot sequences in a multi-cellular system.

The effect of re-using pilots from one cell to another, and the associated negative consequences, is termed "pilot contamination". More specifically, when the service-array correlates its received pilot signal with the pilot sequence associated with a particular terminal it actually obtains a channel estimate that is contaminated by a linear combination of channels to the other terminals that share the same pilot sequence. Downlink beamforming based on the contaminated channel estimate results in interference that is directed to those terminals that share the same pilot sequence. Similar interference is associated with uplink transmissions of data. This directed interference grows with the number of service-antennas at the same rate as the desired signal [14]. Even partially correlated pilot sequences result in directed interference. Pilot contamination as a basic phenomenon is not really specific to massive MIMO, but its effect on massive MIMO appears to be much more profound than in classical MIMO [14].

Chapter 3

System Model for Massive MIMO

Here in this chapter, the system model for massive MIMO will be developed. In the process of developing the model for massive MIMO systems, we will also chose models for our channel and we will also see the mathematical model for our system. Then, simulation results for the modeled system will be produced in Chapter 5.

3.1 System Model for Massive MIMO

The system we will be assuming is a single cell massive MIMO system. The channel between the UE and BS is rician (i.e. the presence of LoS component is assumed). Figure 3.1 shows one particular such system. The general system model for our single cell system is shown in Figure 3.2. The figure shows the transmission of data starting from the UE to the BS. The figure also shows the process of the channel estimation in the BS.

Figure 3.3 shows the process in the UE. The two main processes that undertake in the UE are:

- Pilot generation and
- Transmitter processing.

We consider a Massive MIMO system with a single cell where each cell consists of one base station (BS) with M antennas that serves K single-antenna user equipment (UEs). The system operates in TDD mode where the channel responses remain constant over a coherence block of τ_c samples. Also, we assume that the channel realizations are independent between any pair of coherence blocks.

A coherence block consists of a number of subcarriers and time samples over which the channel response can be approximated as constant and flat-fading. If the coherence bandwidth is Bc and the coherence time is Tc, then each coherence block contains $\tau_c = B_c * T_c$ complex-valued samples [6].

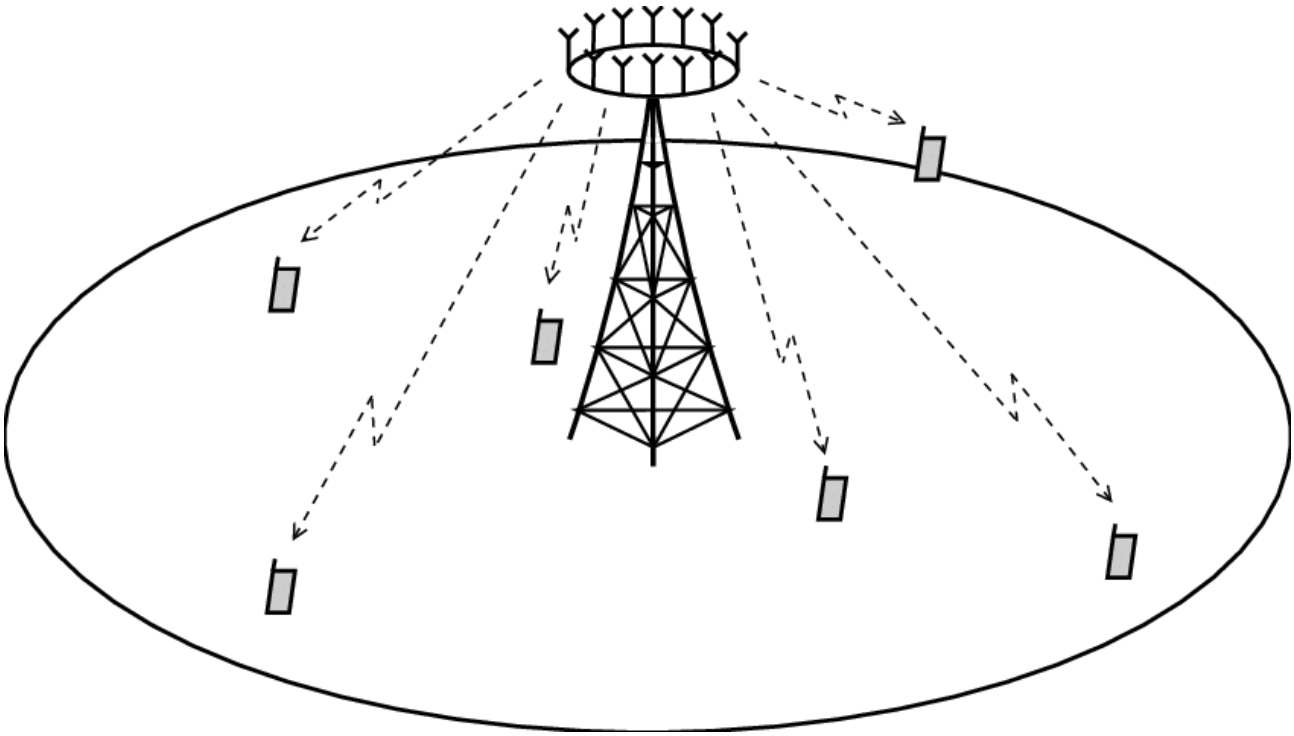

FIGURE 3.1: Single cell with circular base station array and line-of-sight to all terminals [14].

The random channel responses in one coherence block are statistically identical to the ones in any other coherence block, irrespective of whether they are separated in time and/or frequency. Hence, the channel fading is described by a stationary random process. The performance analysis is therefore carried out by studying a single statistically representative coherence block. We assume that the channel realizations are independent between any pair of blocks, which is known as a block fading assumption.

Each coherence block is operated in TDD mode. Figures 3.4 and 3.5 illustrate how the τ_c samples are located in the time and frequency plane. The samples are used for three different things:

- τ_p UL pilot signals;
- τ_u UL data signals;
- τ_d DL data signals.

As we can see, we need $\tau_p + \tau_u + \tau_d = \tau_c$. The fraction of UL and DL data can be selected based on the network traffic characteristics, while the number of pilots per coherence block is a design parameter. Many user applications (e.g., video streaming and web browsing) mainly generate DL traffic, which can be dealt with by selecting $\tau_d > \tau_u$. The size of a coherence block is determined by different parameters. Some of the parameters are the propagation environment, UE mobility, and carrier frequency. Each UE has an

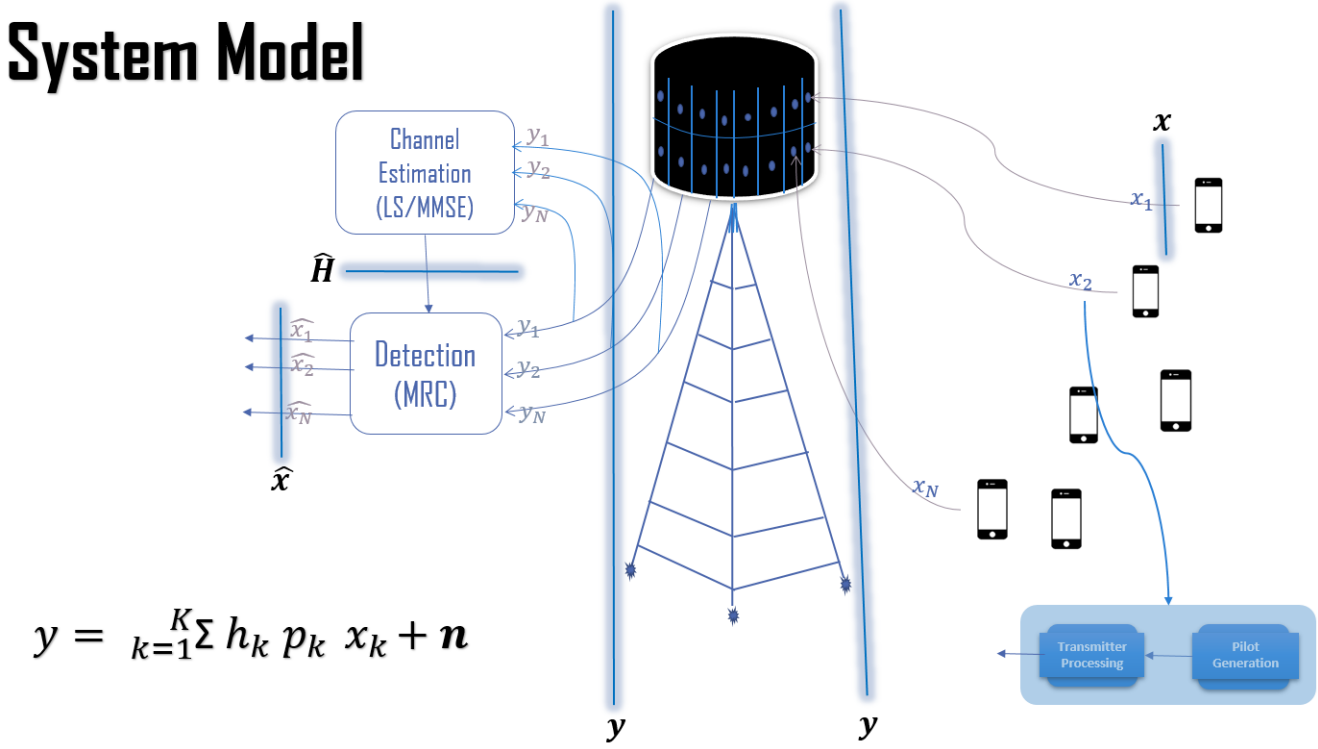

FIGURE 3.2: The Overall System Model for a single system.

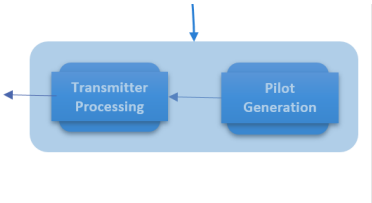

FIGURE 3.3: The process in the UE.

individual coherence bandwidth and coherence time, but it is hard to dynamically adapt the network to these values since the same protocol should apply to all UEs. A practical solution is to dimension the coherence block for the worst-case propagation scenario that the network should support. If a UE has a much larger coherence time/bandwidth, then it does not have to send pilots in every block.

The samples are used for three different tasks: τ_p samples for uplink (UL) pilot signals, τ_u samples for UL data transmission and τ_d samples for downlink (DL) data transmission where $\tau_c = \tau_p + \tau_u + \tau_d$. Both UL and DL channels are estimated by uplink pilot signals by exploiting channel reciprocity in the TDD protocol. We will specify the length of coherence block for our system in Chapter 5.

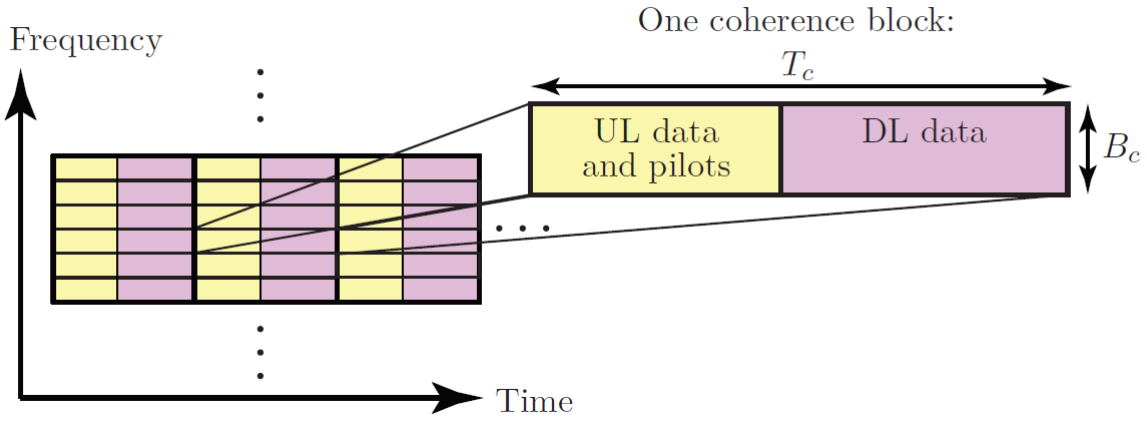

FIGURE 3.4: The TDD multi-carrier modulation scheme of a canonical Massive MIMO network. The time-frequency plane is divided into coherence blocks in which each channel is time-invariant and frequency-flat [6].

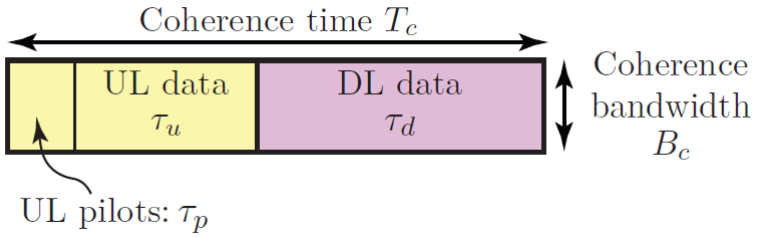

FIGURE 3.5: Each coherence block contains $\tau_c = [B_c] * [T_c]$ complex-valued samples. The samples are used for UL pilots, UL data, and DL data [6].

3.2 Channel Model

Generally the channel is the medium between the UE and the BS. There are different channel models present that are already studied. To be able to design and build a wireless communication system it is essential to have some understanding of different kinds of channel models and their properties. Channel models are used when modeling networks in order to see how the system design works in different situations and under certain circumstances. One example is fading which describes the varying attenuation which a signal experience in different propagation environments. Some of these models are:-

1. **Perfect Channel**
2. **Additive White Gaussian Noise (AWGN)**
3. **Rayleigh fading**
4. **Rician fading**

Each of these channel models will be discussed in the following sections;

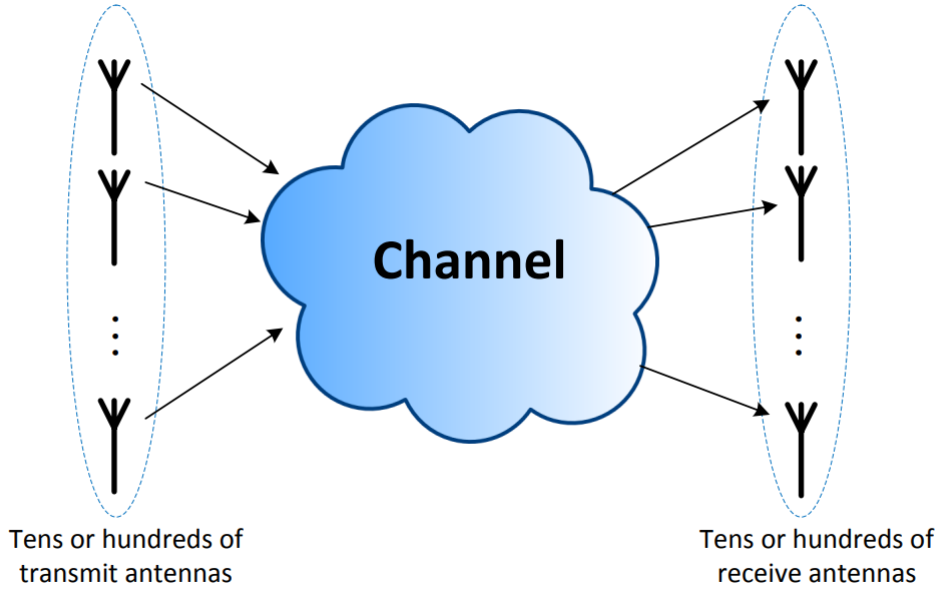

FIGURE 3.6: A diagram of massive MIMO systems with the channel [24].

3.2.1 Perfect Channel

The perfect channel is a type of channel where all noises, interference's and fading effects of the environment are ignored. Here, it is assumed that the channel can be perfectly estimated and measured. Most prior studies assume perfect channel reciprocity by constraining that the time delay from the UL channel estimation to the DL transmission is less than the coherence time of the channel.

Such an assumption ignores two key facts:

1. UL and DL radio-frequency (RF) chains are separate circuits with random impacts on the transmitted and received signals.
2. The interference profile at the BS and UE sides may be significantly different.

The former phenomenon is known as RF mismatch. RF mismatches can cause random deviations of the estimated values of the UL channel from the actual values of the DL channel within the coherent time of the channel. Such deviations are known as reciprocity [25].

3.2.2 Additive White Gaussian Noise

The Additive White Gaussian Noise (AWGN) is often used as a channel model in which the only impairment to communication is a linear addition of wideband or white noise

with a constant spectral density (expressed as watts per hertz of bandwidth) and a Gaussian distribution of amplitude. The model does not account for fading, frequency selectivity, interference, nonlinearity or dispersion. However, it produces simple and tractable mathematical models which are useful for gaining insight into the underlying behavior of a system before these other phenomena are considered.

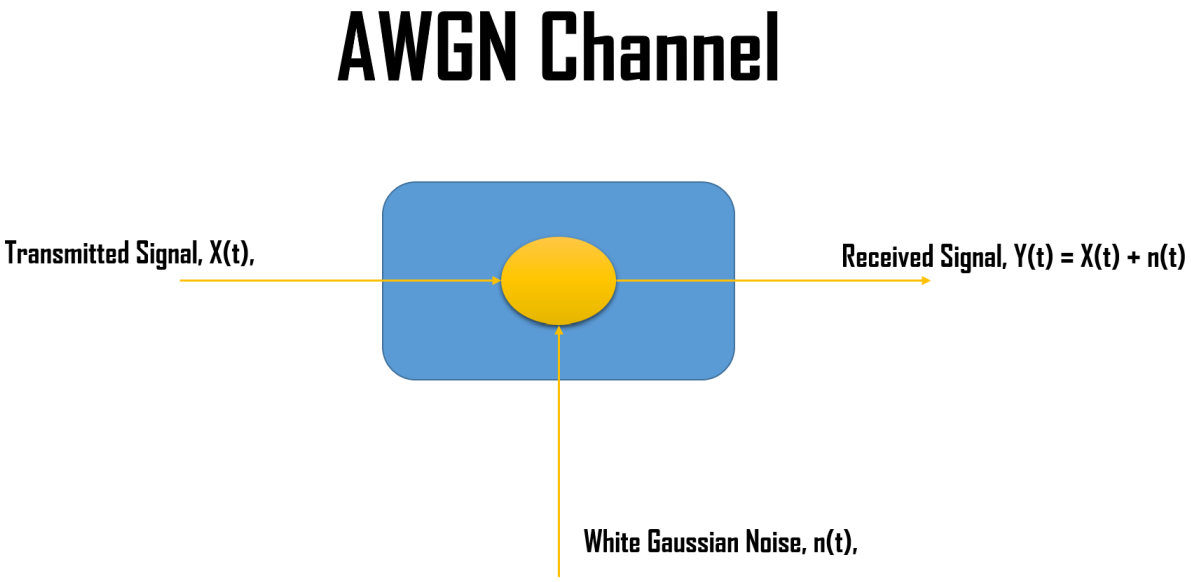

FIGURE 3.7: Block diagram of AWGN channel model.

AWGN is a statistical model which gives the distribution of noise, which naturally occurs in a communication system. There are several sources to AWGN, e.g. thermal noise in the receiver circuits and external noise sources picked up by the antenna. It is additive because it is added to the received signal. It is white because the power of the noise is independent of the frequency and therefore the same for the whole spectrum. It is Gaussian because its distribution is Gaussian [26].

3.2.3 Rayleigh Fading

The Rayleigh fading models assume that the magnitude of a signal that has passed through such a transmission medium (also called a communication channel) will vary randomly, or fade, according to a Rayleigh distribution — the radial component of the sum of two uncorrelated Gaussian random variables.

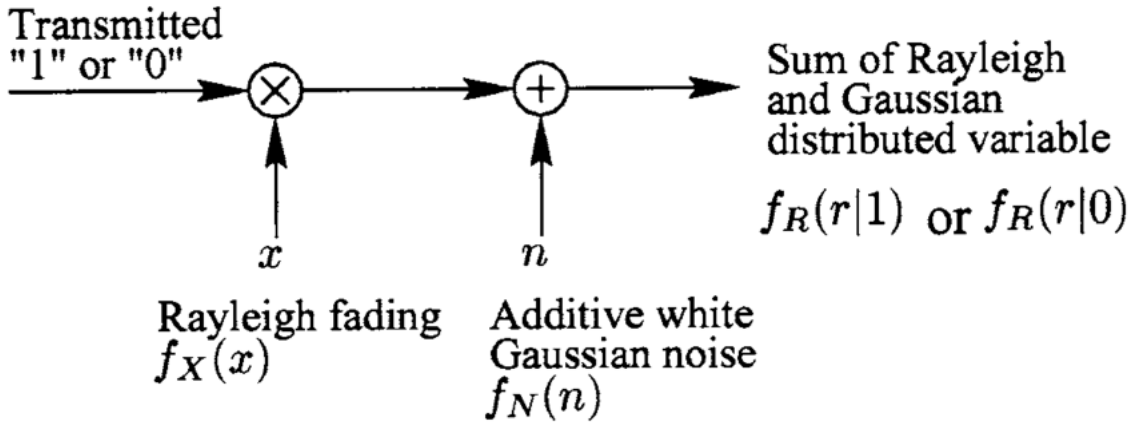

FIGURE 3.8: Block diagram of rayleigh channel model [27].

Rayleigh fading is a statistical model for a small-scale fading channel when there is no line of sight (LOS) component, which is typical in urban areas. A Rayleigh distribution describes the amplitude variations of two uncorrelated orthogonal Gaussian random variables [26].

Figure 3.8 shows a possible signal representation of a communication medium involving a rayleigh fading channel where both the rayleigh fading and AWG noise are considered in the system.

Where:

- $f_X(x)$ represents the distribution of the rayleigh fading
- $f_N(n)$ represents the distribution of the noise in the channel and
- $f_R(r|1)$ and $f_R(r|0)$ represent the effect of both the rayleigh fading and AWGN.

3.2.4 Rician Fading

The Rician fading channel block implements a baseband simulation of a Rician fading propagation channel. This block is useful for modeling mobile wireless communication systems when the transmitted signal can travel to the receiver along a dominant line-of-sight or direct path. If the signal can travel along a line-of-sight path and also along other fading paths, then you can use this block in parallel with the Multipath Rayleigh Fading Channel block.

The Rician fading channel is a statistical model for a small-scale fading channel when there is line of sight (LOS) component in addition to the non LOS. As discussed in the previous sections, from the above channel models we will choose Rician channel model. This choice is better from Rayleigh model which was usually chosen for cellular networks because in massive MIMO systems the cell radius is small compared to other cellular

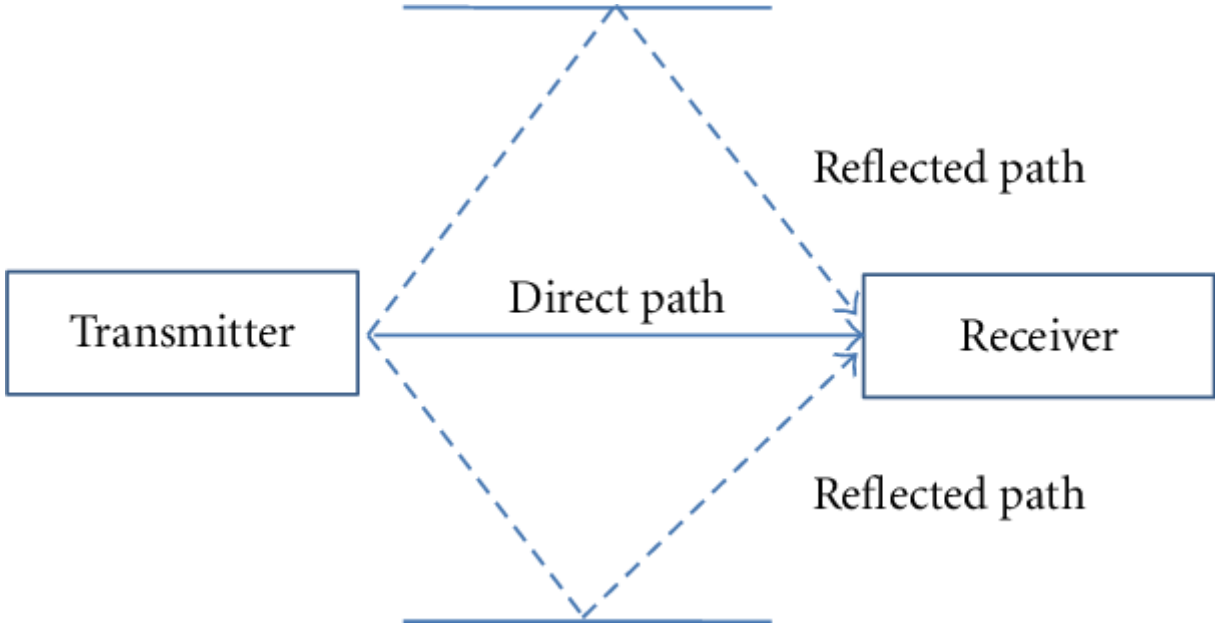

FIGURE 3.9: Block diagram of rician channel model [28].

networks. So, the assumption of the presence of line of sight between the BS and the UE is reasonable which leads to choice of Rician channel model.

Now, we will define mathematical symbols and parameters that will be used for discussing the channel model for massive MIMO. The channel response between UE k in cell l and the BS in cell j is denoted by h^j_{lk}. Each element of h^l_{lk} corresponds to the propagation channel from the UE to one of the $BS's M_j$ antennas. The superscript of h^l_{jk} indicates the BS index and the subscript identifies the index of the cell and the UE. The channel responses are the same in the UL and DL of a coherence block. In this paper, we consider spatially correlated Rician fading channels. Each channel vector $h^l_{lk}, \forall l, l\epsilon 1, ..., L \; and \; \forall \; k \; \epsilon \; 1, ..., K$, is modeled as a realization of the circularly symmetric complex Gaussian distribution.

3.3 Mathematical Model for the UL Transmission

Having defined Massive MIMO systems and the channel, we will now define the UL system models that are used in this thesis. The received baseband signal $\mathbf{y_l} \; \epsilon \; \mathbb{C}^M$ at the l_th BS for each uplink symbol for a multicellular massive MIMO network is modeled as:-

$$\mathbf{y_l} = \sum_{l=1}^{L} \sum_{i=1}^{K} \mathbf{h}^l{}_{i,k} \sqrt{p_{i,k}} x_{i,k} + \mathbf{n_l} \tag{3.1}$$

Where

- $x_{l,i}$ is the normalized transmission symbol (with $\mathbb{E}\{\mid x_{l,i} \mid^2\} = 1$) and

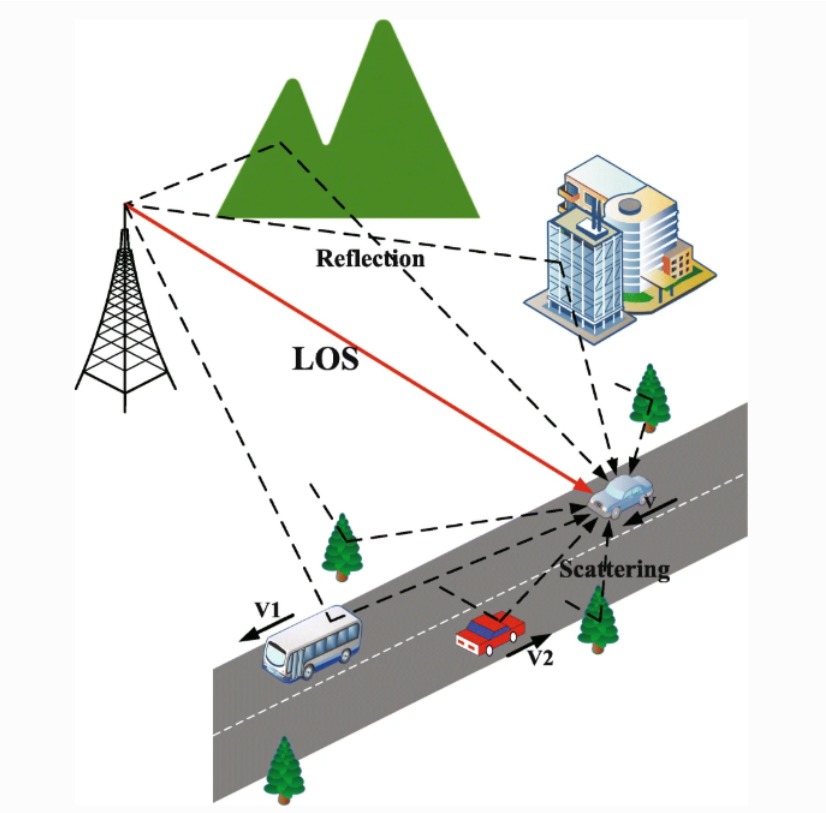

FIGURE 3.10: Communication scenario for rician channel model [29].

- $p_{l,i}$ is the transmit power of user i in cell l.

In the receiver side,the receiver hardware at the BS is contaminated by additive white noise, as modeled by the vector $n_l \ \epsilon \ \mathbb{C}^M$ which is zero-mean circularly symmetric complex Gaussian distributed with variance σ^2_{UL} ; that is, $\mathbf{n_l} \ \sim \ \mathbb{C} \ \mathcal{N}(\mathbf{0}, \sigma^2_{UL}\mathbf{I_M})$. The channels $\mathbf{h}^l_{l,k}$ need to be estimated at BS l to perform good detection and this is done in the uplink by letting each user transmit a sequence of τ_p pilot symbols; see Figures 3.4 and 3.5.

After defining the baseband signal for the uplink symbol, let us define the uplink received signal $\mathbf{y}^{\mathbf{pilot}}_{\mathbf{l}}$ at the l_th BS during pilot transmission (for multi-cellular system):

$$\mathbf{y}^{\mathbf{pilot}}_{\mathbf{l}} = \sum_{l=1}^{L}\sum_{k=1}^{K} \mathbf{h}^l{}_{l,k}\sqrt{p_{l,k}}\phi_{l,k} + \mathbf{n_l} \tag{3.2}$$

Having defined the general uplink system in terms of equations, we will now define the the uplink systems for a single cell system. For the uplink symbol, the received baseband signal, $\mathbf{y} \ \epsilon \ \mathbb{C}^M$, in case of single cell system at the available BS is modeled as:-

$$\mathbf{y} = \sum_{k=1}^{K} \mathbf{h}_k\sqrt{p_k}x_k + \mathbf{n} \tag{3.3}$$

Now let us define the uplink received signal $\mathbf{y^{pilot}}$ at the available BS during pilot transmission as:

$$\mathbf{y^{pilot}} = \sum_{k=1}^{K} \mathbf{h}_k \sqrt{p_k} \phi_k + \mathbf{n} \tag{3.4}$$

Equation 3.4 defines the mathematical model for the uplink pilot transmission. It contains the channel parameter ,$\mathbf{h}_k$, the transmitter power ,p_k, the pilot generated ,ϕ_k, and the noise, $\mathbf{n}$. We will use this equation in the coming chapters to produce full mathematical expression for the channel estimation and the simulations.

Chapter 4

Channel Estimation Techniques in Massive MIMO Systems

4.1 System Model for Massive MIMO

As discussed in Chapter 3, this thesis assumes a cellular network where a base station is equipped with M antennas and K users in that particular cell. The thesis also assumes Rician fading channel. The channel estimation is done only in the uplink.

4.2 Channel Estimation Techniques

In this thesis, as mentioned in Chapter 2, channel estimation techniques in massive MIMO systems are discussed. We have also discussed that FDD based channel estimation requires orthogonal pilots which are equal in number with the number of antennas while TDD based channel estimation requires orthogonal pilots which are equal in number with the number of users which much smaller than the numbers of antennas. So, TDD based channel estimation is used for our massive MIMO system.

In TDD channel estimation technique, there are 3 kinds of channel estimation. These are pilot based (non-blind) channel estimation techniques, blind channel estimation techniques, and semi-blind channel estimation techniques. We will discuss all these three techniques in the following subsections. The classification of different channel estimation techniques is shown in Figure 4.1. These are training based, blind channel estimation or semi-blind channel estimation.

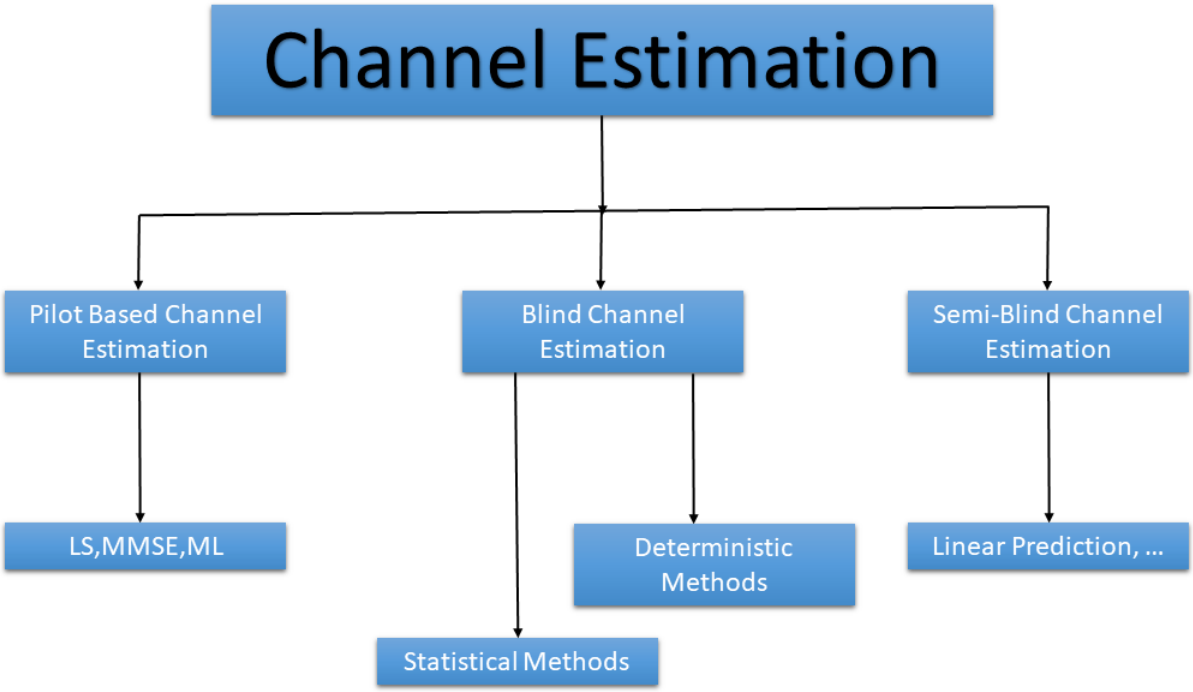

FIGURE 4.1: The classification of different channel estimation techniques.

4.2.1 Pilot-based (non-blind) Channel Estimation Techniques

In pilot-based estimation, the channel estimation can be performed by either inserting pilot tones into all of the sub-carriers of OFDM (orthogonal frequency division multiplexing) symbols with a specific period or inserting pilot tones into each OFDM symbol. Pilots are known to both transmitters and receivers. The receiver can utilize the known pilot bits and the corresponding received samples. Based on known pilot bits the channel can be estimated [30]. There are three kinds of channel estimation arrangements for pilot based channel estimation. These will be discussed in Section 4.3.

4.2.2 Blind Channel Estimation Techniques

Blind channel estimation techniques do not use pilots for channel estimation rather they use the data streams for estimating the channel. The blind channel estimation algorithm is proposed for orthogonal space-time-coded systems [31]. Blind method uses a combination linear prediction and noise subspace method [32].

The blind channel estimation is carried out by evaluating the statistical information of the

channel and particular properties of the transmitted signals. This blind channel estimation has no overhead loss and it is only suitable for slowly time varying channels. But in training based channel estimation, training symbols or pilot tones that are known to the receiver, are multiplexed along with the data stream for channel estimation [33].

4.2.3 Semi-Blind Channel Estimation Techniques

The Semi-blind channel estimation algorithms, exploit the second-order stationary statistics, correlative coding, and other properties, normally have better spectral efficiency With a small number of training symbols. These methods have been proposed to estimate the channel ambiguity matrix in MIMO-OFDM systems [34].

The Semi-blind channel estimation algorithm is a hybrid combination of blind channel estimation and training based channel estimation which utilizes pilot carriers and other natural constraints to perform channel estimation [33]. A semi-blind MIMO-OFDM channel estimation is based on blind channel and pilot based channel estimation. For example A semi-blind MIMO-OFDM channel estimation can be done based on blind channel estimation and least squares pilot based algorithm [32].

4.3 Pilot-based Channel Estimation Techniques

A Massive MIMO system is developed based on a conventional MIMO system but where the BS is equipped with a very large number of antennas [35]. Massive numbers of antennas at each BS provide Massive MIMO with several advantages. It should be noted that these benefits rely on the BS obtaining good estimates of the CSI of each user [8]. The deterministic pilot sequence of UE k in the given cell is denoted by

$$\phi_k \, \epsilon \, \mathbb{C}^{\tau_p} \; and \;\; \| \, \phi_k \, \|^2 = \tau_p.$$

Then the received pilot signal would be, as discussed in Chapter 3:-

$$\mathbf{y^{pilot}} = \sum_{k=1}^{K} \mathbf{h}_k \sqrt{p_k} \phi_k + \mathbf{n} \tag{4.1}$$

Where $n \; \epsilon \; \mathbb{C}^M$ which is zero-mean circularly symmetric complex Gaussian distributed with variance σ^2_{UL} ; that is, $\mathbf{n} \; \sim \; \mathbb{C} \, \mathcal{N}(\mathbf{0}, \sigma^2_{UL} \mathbf{I_M})$.

Now, the task of the channel estimation is to estimate the channel vector, h_k, from the pre-known pilot vectors, ϕ_k. This is what is called pilot based channel estimation. Based

on the techniques used, pilot based channel estimation can follow different algorithms. In this paper, two of the most popular channel estimation techniques are discussed. The two algorithms that will be discussed are the least square (LS) and mean minimum square error (MMSE) algorithms.

The pilot based channel estimation methods are based on the pilot symbols which are transmitted along with the information signal. The pilot sequence or symbols are inserted into fixed positions of the transmitted signals so as to keep track of the varying radio channel statistics. The receiver has perfect knowledge of the pilot sequence and also the fixed pilot positions so that it can estimate the channel depending on the received pilot sequence.

Depending on the arrangement of pilots, three different types of pilot structures are considered: block type, comb type, and lattice type. These three types are explained as:-

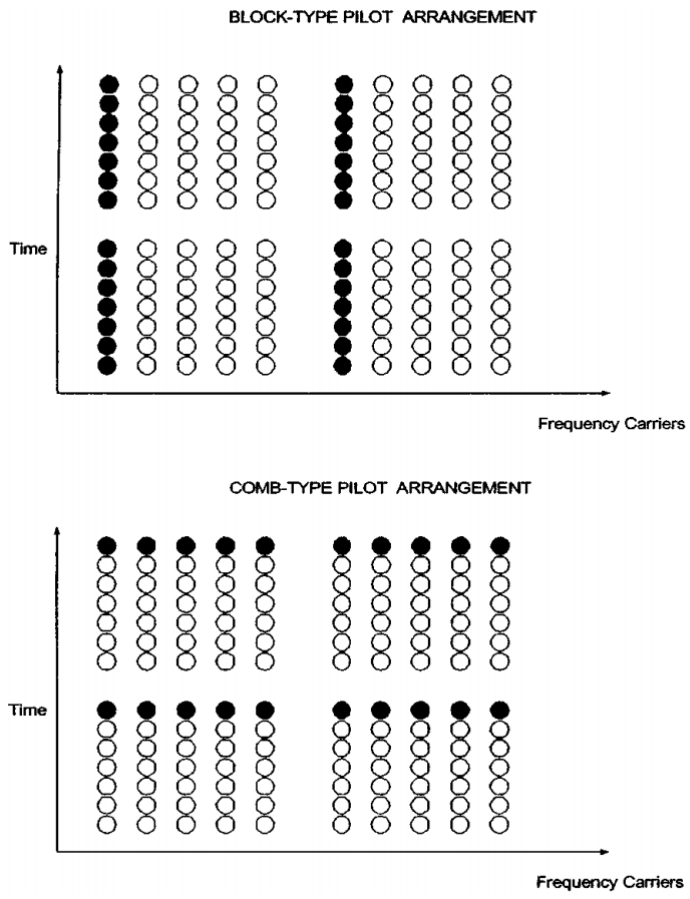

FIGURE 4.2: Pilot Arrangement [31].

1. **Block-type pilot channel estimation:** is performed by inserting pilot tones into all

subcarriers of OFDM symbols with a specific period in time. The pilot symbols, because covering all frequencies, could be effective against the selective frequency fading, but more sensitive for the impact of fast fading channel. Therefore, the block-type pilot is developed under the assumption of slow fading channel. In case of same number of pilots, the performance is decided by channel change rate, known as coherent time [36]. Figure 4.3 shows the arrangement of Comb-type pilot channel estimation.

Block type pilot channel estimation, has been developed under the assumption of slow fading channel. The estimation of the channel for this block-type pilot arrangement can be based on Least Square (LS) or Minimum Mean-Square (MMSE). Figure 4.2 shows Pilot arrangement for training based channel estimation [31]. pilot tones are inserted into all frequency bins within the periodic intervals of OFDM blocks. This estimation is suitable for slow fading channels.

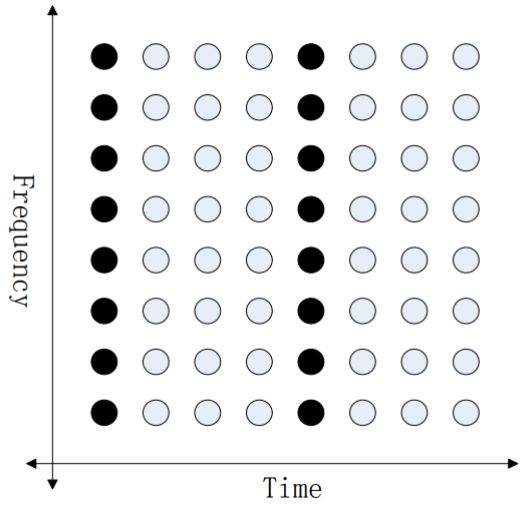

FIGURE 4.3: Block-type pilot channel estimation arrangement. The black dots represent the pilot while the white dots represent the actual data [36].

2. **Comb-type pilot channel estimation:** is performed by inserting pilot tones into certain subcarriers of each OFDM symbol, where the interpolation is needed to estimate the conditions of date subcarriers. Compared with the block-type pilot, because pilot symbols are inserted into subcarriers with same interval, comb-type pilot channel estimation is introduced to satisfy the need for equalizing when the channel changes even from one OFDM block to the subsequent one. In case of same number of pilots, the performance is decided by channel multipath time delay, known as coherent bandwidth [36]. Figure 4.4 shows the arrangement of Comb-type pilot channel estimation [33].

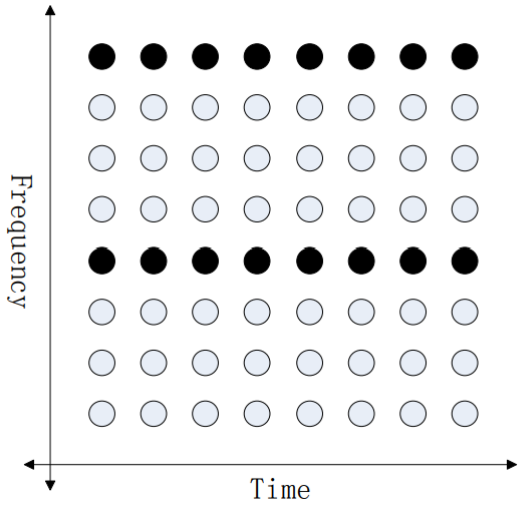

FIGURE 4.4: comb-type pilot channel estimation arrangement. The black dots represent the pilot while the white dots represent the actual data [36].

The comb-type pilot channel estimation algorithms estimate the channel at pilot frequencies and interpolate the channel. The estimation of the channel is based on LS and MMSE results show that MMSE performs much better than LS [37]. The blind channel estimation algorithm is proposed for orthogonal space-time-coded systems [31]. pilot tones are inserted into each OFDM symbol with a specific period of frequency bins. This type of channel estimation is very much suitable where the changes even in one OFDM block [33].

3. **Lattice-type pilot channel estimation:** is an arrangement of pilots where pilots are inserted along both the time and the frequency axes for channel estimation. A frequency-domain interpolation along the frequency axis and a time domain interpolation along the time axis are performed using the pilots to estimate the channel. In order to keep track of the frequency-selective and the time varying channel characteristics, the pilot subcarrier spacing must be less than the coherence bandwidth and the pilot symbol period must be less than the coherence time [38].

4.3.1 The Least Square Algorithm

The LS channel estimation is a simple estimation technique with very low complexity. It does not require any prior knowledge of the channel statistics. It is widely used because of its simplicity. However, it suffers from a high mean square error [40].

LS estimation method does not use any prior knowledge about the channel, basing the estimates entirely on the received matrices . This makes this method robust to lack of knowledge about the CSI [7]. We will next describe the LS estimation of the CSI.

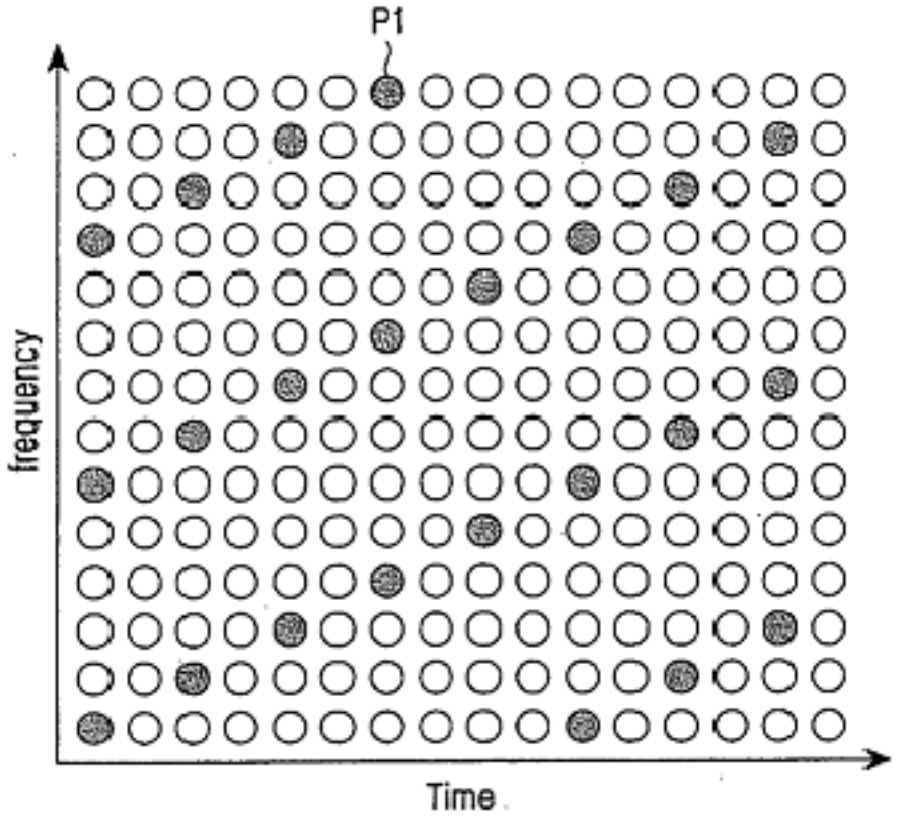

FIGURE 4.5: Lattice type pilot channel estimation arrangement. The black dots represent the pilot while the white dots represent the actual data [39].

Ideally, the channel used to be assumed perfectly known (i.e. there is no noise and channel imperfectness). This situation is called Perfect channel state information because the channel state can is perfectly known. In this case, the equation for the system can be written as (in vector form), For the analysis purpose, we will use $\mathbf{X}$ to represent both the data and the pilots sent from the user equipment to the BS:-

$$\mathbf{Y} = \mathbf{H} * \mathbf{X} \tag{4.2}$$

From this, we can calculate the channel estimation as:-

$$\mathbf{H} = \mathbf{Y} * \mathbf{X^{-1}} \tag{4.3}$$

Here $\mathbf{N}$ is assumed to be 0. But, in reality because of Channel imperfectness $\mathbb{N} \neq 0$. So, the equation for the system can be written as (in vector form):-

$$\hat{\mathbf{Y}} = \hat{\mathbf{H}} * \mathbf{X} \tag{4.4}$$

In LS algorithm, only first order statistics considered. second order and beyond channel statistics are ignored in this algorithm. From this, we can calculate the LS channel estimation as:-

The job of the any estimator is to to estimate an unknown parameter H from an observed variable $\hat{\mathbf{Y}}$. i.e. to find the value of

$$\mathbb{E}\{\mathbf{h}/\hat{\mathbf{Y}}\} \tag{4.5}$$

In order to do this job, the LS channel estimator is designed to minimize $(\mathbf{Y} - \hat{\mathbf{Y}})$.

$$\hat{\mathbf{Y}} = \hat{\mathbf{H}} * \mathbf{X} \tag{4.6}$$

In Ls algorithm, Only first order statistics considered. second order and beyond channel statistics are ignored in this algorithm. From this, we can calculate the LS channel estimation as:-

As mentioned in the above statement, the task of LS is to minimize $(\mathbf{Y} - \hat{\mathbf{Y}})$, In the equation $(\mathbf{Y} - \hat{\mathbf{Y}})$, Substitute for $\mathbf{Y}$ and $\hat{\mathbf{Y}}$ by the values $\mathbf{Y} = \mathbf{H} * \mathbf{X}$ and $\hat{\mathbf{Y}} = \mathbf{H} * \hat{\mathbf{X}}$, and trying to minimize it, we get the following expression.

$$Minimize : \parallel \mathbf{Y} - \hat{\mathbf{Y}} \parallel^2 \tag{4.7}$$

$$\parallel \frac{d(\mathbf{Y} - \hat{\mathbf{Y}})}{d\hat{H}} \parallel^2 = 0 \tag{4.8}$$

$$\frac{d\parallel ((\mathbf{H} * \mathbf{X}) - (\hat{\mathbf{H}} * \mathbf{X})) \parallel^2}{d\hat{H}} = 0 \tag{4.9}$$

similarly, the above equation can be represented as:-

$$\frac{d\parallel ((\hat{\mathbf{H}} * \mathbf{X}) - \mathbf{Y}) \parallel^2}{d\hat{H}} = 0 \tag{4.10}$$

$$\frac{d((\hat{\mathbf{H}} * \mathbf{X}) - \mathbf{Y})((\hat{\mathbf{H}} * \mathbf{X}) - \mathbf{Y})^H}{d\hat{H}} = 0 \tag{4.11}$$

$$\frac{d}{d\hat{H}}((\hat{\mathbf{H}}\mathbf{X}) - \mathbf{Y})((\hat{\mathbf{H}}\mathbf{X}) - \mathbf{Y})^H = 0 \tag{4.12}$$

Using the above property, we manipulate Equation 4.11 to get the following equation,

$$\frac{d}{d\hat{H}}[(\hat{\mathbf{H}}\mathbf{X})^H(\hat{\mathbf{H}}\mathbf{X}) - \mathbf{Y}^H\hat{\mathbf{H}}\mathbf{X} - (\hat{\mathbf{H}}\mathbf{X})^H\mathbf{Y} + \mathbf{Y}^H\mathbf{Y}] = 0 \tag{4.13}$$

By using the properties of matrix and the properties of derivatives, the above equation becomes:-

$$\frac{d}{d\hat{H}}[(\mathbf{X}^H\hat{\mathbf{H}}^H)(\hat{\mathbf{H}}\mathbf{X}) - (\mathbf{Y}^H\hat{\mathbf{H}}\mathbf{X}) - (\mathbf{X}^H\hat{\mathbf{H}}^H\mathbf{Y}) + (\mathbf{Y}^H\mathbf{Y})] = 0 \tag{4.14}$$

After evaluating the above equation by solving the derivative, setting all second order and higher statistics to zero and lastly solving for $\hat{\mathbf{H}}$ we get the following expression:-

$$2\mathbf{X}^H\mathbf{X}\mathbf{H} - 2\mathbf{X}^HY = 0 \tag{4.15}$$

$$\mathbf{X}^H\mathbf{X}\hat{\mathbf{H}} = \mathbf{X}^H\mathbf{Y} \tag{4.16}$$

lastly, solving for $\hat{\mathbf{H}}$ we get he following expression for $\hat{\mathbf{H}}$ which is the equation for an LS algorithm.

$$\hat{\mathbf{H}} = (X^H * X)^{-1}(X^H * Y) \tag{4.17}$$

Which in the same way can be implemented as follows (it is just the assumption assumed when we start our derivation of the equation. the difference comes from the assumption whether you assume $\hat{\mathbf{Y}} = \mathbf{H} * \hat{\mathbf{X}}$ or $\hat{\mathbf{Y}} = \hat{\mathbf{H}} * \mathbf{X}$) :-

$$\hat{\mathbf{H}} = \hat{X}^{-1} * (Y) \tag{4.18}$$

Now, substituting $\hat{X}^{-1}$ by the pilot vector and substituting the other vectors by their values, we can get the following expression for LS algorithm:-

$$\hat{h}_k = \frac{1}{\sqrt{\phi_k} * \tau_p} * y^{pilot} \tag{4.19}$$

4.3.2 The Minimum Mean Square Error Algorithm

The MMSE channel estimation is an estimation technique with very high computational complexity. It requires prior knowledge of the second order channel statistics [40].

MMSE channel estimation is a more accurate version of the LS channel estimation. The MMSE channel estimator minimizes the MSE between the true channel, **H**, and the MMSE estimated channel, $\hat{H}_{MMSE}$, by finding a good linear estimate in terms of M and the value of LS estimate, $\hat{H}_{LS}$ [9].

The high complexity of MMSE estimator is due to the inversion matrix. Every time data changes, inversion is needed. The complexity of this estimator can be reduced by averaging the transmitted data [41].

As we have seen it in the LS estimator algorithm calculation, the job of the any estimator is to to estimate an unknown parameter H from an observed variable $\hat{Y}$. i.e. to find the value of

$$\mathbb{E}\{\mathbf{H}/\hat{\mathbf{Y}}\}$$

In order to do this job, the MMSE channel estimator is designed to minimize the mean square error (MSE) of the estimation [41]. The MSE is expressed by its correlation matrix. The correlation matrix of the error of the the given channel estimations given by [42].

$$\mathbf{R_{ee}} = [\mathbf{H} - \hat{\mathbf{H}}] \times [\mathbf{H} - \hat{\mathbf{H}}]^H \tag{4.20}$$

As mentioned above, the task of MMSE is to minimize MSE of the LS estimator. i.e.

$$MSE = [\mathbf{H} - \hat{\mathbf{H}}] * [\mathbf{H} - \hat{\mathbf{H}}]^H \tag{4.21}$$

$$MMSE = Min[Argument[MSE]] \tag{4.22}$$

$$MMSE = Min \parallel [\mathbf{H} - \hat{\mathbf{H}}] \times [\mathbf{H} - \hat{\mathbf{H}}]^H] \parallel \tag{4.23}$$

$$MMSE => Solve\frac{d}{d\hat{H}} \parallel [[\mathbf{H} - \hat{\mathbf{H}}] \times [\mathbf{H} - \hat{\mathbf{H}}]^H] \parallel = 0 \tag{4.24}$$

$$H_{MMSE} => Solve\frac{d}{d\hat{H}} \parallel \mathbf{H}\mathbf{H}^H - \mathbf{H}\hat{\mathbf{H}}_H - \mathbf{H}^H\mathbf{H}^H + \hat{\mathbf{H}}^H\hat{\mathbf{H}} \parallel = 0 \tag{4.25}$$

$$H_{MMSE} => Solve\frac{d}{d\hat{H}} \parallel \mathbf{H}\mathbf{H}^H - \mathbf{H}\hat{\mathbf{H}}^H - \hat{\mathbf{H}}\mathbf{H}^H + \hat{\mathbf{H}}^H\hat{\mathbf{H}} \parallel = 0 \tag{4.26}$$

$$H_{MMSE} => Solve \frac{d}{d\hat{H}} \parallel \mathbf{H}\mathbf{H}^H - \mathbf{H}\hat{\mathbf{H}}_H - \mathbf{H}^H\mathbf{H}^H + \hat{\mathbf{H}}^H\hat{\mathbf{H}} \parallel = 0 \tag{4.27}$$

To solve the above equation, we will differentiate the above equation with respect to $\hat{H}$, set the resulting equation to zero and after all this solve for $\hat{H}$. After solving the above equation for $\hat{H}$ we will get the following result, bear in mind that $\hat{H}$ here is the H_{MMSE};

$$H_{MMSE} = [R_{hy}] \times [R_{YY}^{-1}] * [R_{yh}] \tag{4.28}$$

Substituting the values for R_{hy} and R_{YY}, we get the following result.

$$H_{MMSE} = \sigma_h^2 X^H [\sigma_h^2 X X^H + \sigma^2 I_{M*M}]^{-1} * [R_{yh}] \tag{4.29}$$

$$H_{MMSE} = \sigma_h^2 X^H [\sigma_h^2 X^H X + \sigma^2 I_{M*M}]^{-1} X^H * [R_{yh}] \tag{4.30}$$

Equation 4.30 is for rayleigh channel. In order to modify it for Rician channel, we will just add LOS component, $\bar{h}$. So, by doing this we get the expression for the Rician channel:-

$$H_{MMSE} = \bar{h} + \sigma_h^2 I_{M*M} [\sigma_n^2 (X^H X)^{-1} + \sigma_h^2 I_{M*M}]^{-1} X^H * [R_{yh}] \tag{4.31}$$

Where $\bar{h}$ is the LOS component, and is given as:-

$$\bar{h} = R_{hh} \tag{4.32}$$

Going back to the original equation, we can write the above equation as:-

$$H_{MMSE} = \bar{h} + [R_{hy}] * [R_{YY}^{-1}] * [R_{yh}] \tag{4.33}$$

$$H_{MMSE} = R_{hh} + [R_{hy}] * [R_{YY}^{-1}] * [R_{yh}] \tag{4.34}$$

Where:

- $R_{hy} = E[h * y^H] = \sigma_h^2 X^H$,
- $R_{yh} = E[h * y^H] = \sigma_h^2 X$,
- $R_{YY} = E[y * y^H] = \sigma_h^2 X X^H + \sigma^2 I_{M \times M}$,

- $R_h = E[h \times h * H] = \sigma_h^2 I$,

The above equation be more simplified by substituting $R_{hy}, R_{yh}, R_{YY}, R_h$, by doing so we will achieve the following equation:-

$$H_{MMSE} = \sigma_h^2 I + \sigma_h^2 I_{M*M}[\sigma_n^2 (X^H X)^{-1} + \sigma_h^2 I_{M*M}]^{-1} X^H * \sigma_h^2 X \tag{4.35}$$

Collecting like terms and rearranging the above equation we get a more simplified expression, given as:-

$$H_{MMSE} = \sigma^2 \sigma_h^2 [\sigma_h^2 X^H X + \sigma^2 I_{M*M}]^{-1} \tag{4.36}$$

$$H_{MMSE} = \Big[\frac{X^H X}{\sigma^2}\sigma_h^2 + \frac{I_{M*M}}{\sigma_h^2}\Big]^{-1} \tag{4.37}$$

Now, substituting $\hat{X}^{-1}$ by the pilot vector and substituting the other vectors by their values, we can get the following expression for MMSE algorithm [7]:-

$$H_{MMSE} = \bar{h} + \sqrt{p_k}\mathbf{R}_k \Psi_k (y_k^{pilot} - \hat{y}_k^{pilot}) \tag{4.38}$$

Where:

- $\bar{h}$ is the LOS component.
- $\mathbf{R}_k$ is the covariance matrix describing the spatial correlation of the NLoS components.
- $\Psi_k = \tau_p \, Cov\{y_k^{pilot}\}^{-1}$
- $\hat{\mathbf{y}}_{\mathbf{k}}^{\mathbf{pilot}} = \sum_{k=1}^{K} \hat{\mathbf{h}}_k \sqrt{p_k}$

Both the above estimators suffer from different drawbacks. The MMSE usually suffers from a high complexity than LS but the LS estimator suffers from MSE which is high compared to the LS estimator. The MMSE estimator requires to calculate an $N * N$ matrix which results in a high complexity when N becomes large value. Here keep in mind that both these estimators are derived under the assumption of known channel correlation and noise variance, σ_n^2 [43]. The situation differs when the channel correlation and the noise variance are not known which is the reality.

4.4 Detection Vector (Detection Algorithm)

In order to compare between different channel estimation techniques, one way is, to detect the signal using different detection algorithms and then compare the estimation techniques based on the SE of the detected signal. In order to do this, we will now consider different detection algorithms. As we can see from Figure 4.6, detection in the BS requires detection algorithms. After the data arrives at the BS, the data vector is multiplied by the detection vector.

There are different detection algorithms available for a system to pick from. The main parameter of choice are simplicity and accuracy of the algorithm. In this thesis, the Maximum Ratio Combining (MRC) algorithm is chosen as a detection algorithm for our massive MIMO system. There are different detection algorithms available for massive MIMO systems. Below is list of some detection algorithm:-

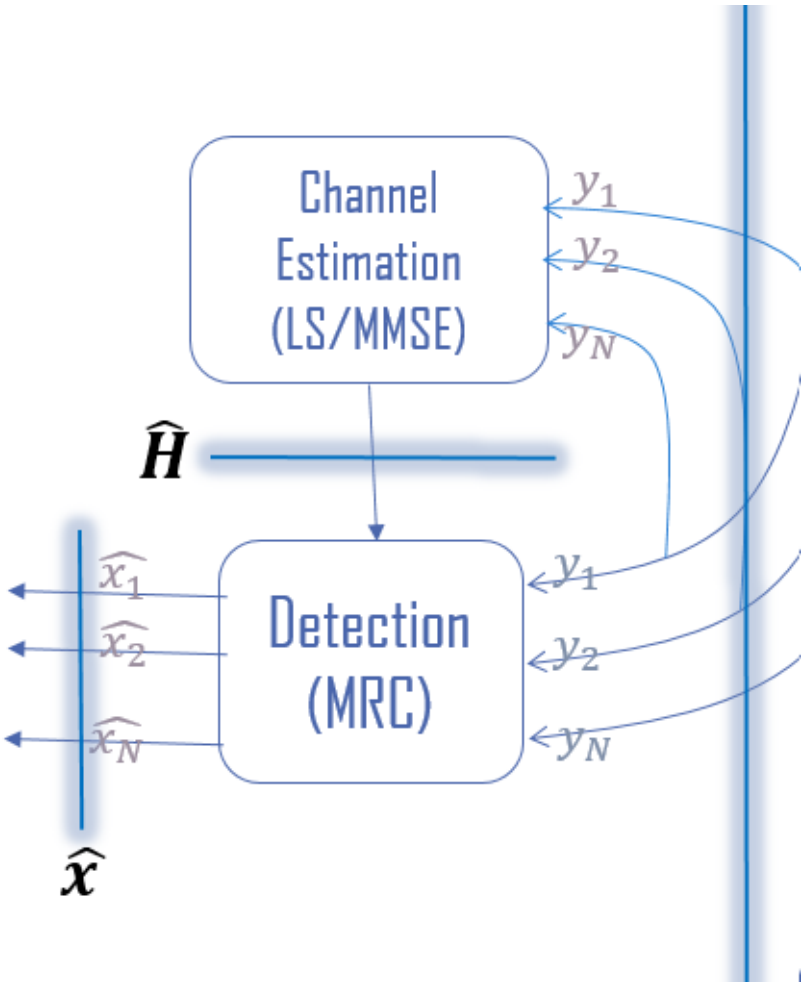

FIGURE 4.6: Detection Algorithm.

4.4.1 ALGORITHM 1: Maximum Likelihood

In a massive MIMO system, multiple element antenna arrays are deployed at both the transmitter and the receiver. The communications challenge lies in designing the sets of signals simultaneously sent by the transmit antennas and the algorithms for processing those observed by the receive antennas, so that the quality of the transmission (its data rate) are superior to those supported by traditional single antenna systems.

This is the optimal detector from the point of view of minimizing the probability of error. The ML receiver computes the most probable symbol X given the measurements Y . The maximum likelihood detector with some kind of noise at the receiver antennas [44].

4.4.2 ALGORITHM 2: Zero Forcing

Zero Forcing algorithm is a linear algorithm used in communication systems, which inverts the frequency response of the channel. The Zero-Forcing algorithm applies the inverse of the channel to the received signal, to restore the signal before the channel. The name Zero Forcing corresponds to bringing down the ISI to zero in a noise free case. This will be useful when ISI is significant compared to noise.

For a channel with frequency response $F(f)$ the zero forcing algorithm $C(f)$ is constructed such that $C(f) = 1/F(f)$. Thus the combination of channel and the detector gives a flat frequency response and linear phase $F(f) * C(f) = 1$. If the channel response for a particular channel is $H(s)$, then the input signal is multiplied by the reciprocal of this. This is intended to remove the effect of channel from the received signal, in particular the Inter-symbol Interference (ISI). This will be discussed in detail in the Section 4.5.

4.4.3 ALGORITHM 3: The MMSE Algorithm

A minimum mean square error (MMSE) estimator describes the approach which minimizes the mean square error (MSE), which is a common measure of estimator quality. The main feature of MMSE equalizer is that it does not usually eliminate ISI (inter symbol interference) completely but, minimizes the total power of the noise and ISI components in the output [45].

Traditional channel estimation algorithms such as minimum mean square error (MMSE) are widely used in massive multiple-input multiple-output (MIMO) systems. The problem is that the minimum mean square error (MMSE) detection method involved matrix inversion operation with excessive computational burden [46]. To overcome the matrix inversion problem, many different forms of the minimum mean square error (MMSE) were proposed by different papers.

A minimum mean square error (MMSE) Algorithm describes the approach which minimizes the mean square error (MSE). The main feature of MMSE Algorithm is that it does not usually eliminate ISI completely but, minimizes the total power of the noise and ISI components in the output [45].

4.4.4 ALGORITHM 4: The MRC Algorithm

Various techniques are known to combine the signals from multiple diversity branches. In Maximum Ratio combining each signal branch is multiplied by a weight factor that is proportional to the signal amplitude. That is, branches with strong signal are further amplified, while weak signals are attenuated.

In telecommunications, maximal-ratio combining is a method of diversity combining in which the signals from each channel are added together and the gain of each channel is made proportional to the RMS value of signal and inversely proportional to the mean square noise level in that channel. Different proportionality constants are used for each channel. It is also known as ratio-squared combining and pre detection combining. Maximal-ratio-combining is the optimum combiner for independent AWGN channels [47]. This detection algorithm will be discussed in detail in the Section 4.5. The mathematical model of this algorithm will also be discussed in detail.

4.5 The Maximum Ratio Combining Algorithms

For this particular thesis, the MRC detection algorithm is chosen. The reason for this choice is that the MRC combining is a detection where each signal branch is multiplied by a weight factor that is proportional to the signal amplitude. That is, branches with strong signal are further amplified, while weak signals are attenuated. In telecommunications, maximal-ratio combining is a method of diversity combining in which the signals from each channel are added together and the gain of each channel is made proportional to the RMS value of signal and inversely proportional to the mean square noise level in that channel [48]. Different proportionality constants are used for each channel. It is also known as ratio-squared combining and pre-detection combining.

The ZF and the MRC detection algorithms are applicable for pilot based channel estimation. As sated in [49], the ZF algorithm can be used for pilot based channel estimation techniques but the paper [48] states that the MRC detection has a better performance for MIMO systems. So, we have chosen the MRC as our detection algorithm for our thesis. Now let us discuss the MRC detection algorithm and and its mathematical derivation.

From the previous sections we have the expressions for LS and MMSE estimator. We will use these expressions for our detection. The expressions we founded in the previous sections are:

The expression for the MMSE estimator:

$$\hat{\mathbf{H}} = (X^H * X)^{-1}(X^H * Y) \tag{4.39}$$

The expression for the MMSE estimator in other forms as was achieved in the previous sections is:

$$H_{MMSE} = \bar{h} + [R_{hy}] * [R_{YY}^{-1}] * [Y] \tag{4.40}$$

The next step would be to use this algorithm for our system. Using the channel estimates derived in previous sections, in this section, we will analyze the performance of the single cell Massive MIMO network. During uplink payload data transmission, the BS in cell only utilizes its own received signal $\mathbf{y}$ and only targets to detect the signals sent by its own K users. Since we are considering single cell system, signals coming from users in other cells are ignored. The BS in the cell discriminates the signal transmitted by its k_{th} user from the interference by multiplying the received signal in Equation 3.3 with a detection vector $\mathbf{v_k}\ \epsilon\ \mathbb{C}^M$ as follows:

$$(\mathbf{v}_k^H)\mathbf{y} = \sum_{k=1}^{K}(\mathbf{v}_k^H)\mathbf{h}_k\sqrt{p_k}x_k + (\mathbf{v}_k^H)\mathbf{n} \tag{4.41}$$

$$(\mathbf{v}_k^H)\mathbf{y} = (\mathbf{v}_K^H)\mathbf{h}_K\sqrt{p_K}x_K + \sum_{k=1}^{K}(\mathbf{v}_k^H)\mathbf{h}_k\sqrt{p_k}x_k + (\mathbf{v}_k^H)\mathbf{n} \tag{4.42}$$

where x_k is the transmitted data symbol from user k in the defined cell. As seen from Equation 4.42, the processed received signal is the superposition of three parts: the desired signal, intra-cell interference, and residual noise. Since the detection vector v_k appears in all these terms, it can be used to amplify the desired signal, suppress the interference, and or suppress the noise. More precisely, by gathering the detection vectors at BS in matrix form as $\mathbf{V} = [v_l ... v_K]\mathbf{v_k}\ \epsilon\ \mathbb{C}^M$,

As we have seen in Section 4.4, there are four types of detection algorithms. From these four algorithms, two main schemes being considered in the Massive MIMO literature: maximum ratio (MR) and zero forcing (ZF). These are given by

$$\mathbf{V} = \begin{cases} \hat{H}, & \text{for MR.} \\ \hat{H}(\hat{H}^H\hat{H})^{-1}, & \text{for ZF.} \end{cases} \tag{4.43}$$

MRC detection exploits the M observations in $\mathbf{y}$ to maximize the ratio between the average signal gain in Equation 4.42. In contrast, the ZF detection matrix utilizes the M observations over the antennas to minimize the average intra-cell interference, while retaining the desired signals.

The purpose of the detection is to make the detected signal $\hat{x}_k$ at the given BS equal to the true signal x_k, at least up to a scaling factor. Due to noise and estimation errors, there is always a mismatch between the signals which is why the communication link has a limited capacity. If the true signal x_k originates from a discrete constellation set X (e.g., a quadrature amplitude modulation (QAM)), $\hat{x}_k$ is selected based on $(\mathbf{v}_k^H)\mathbf{y}$ by finding the minimum distance over all the candidates $x \epsilon \mathbb{C}^M$:

$$\hat{x}_k = min_{x\epsilon\mathbb{C}^M} \parallel (\mathbf{v}_k^H)\mathbf{y} - (\mathbf{v}_K^H)\hat{\mathbf{h}}_K\sqrt{p_K}x_K \parallel^2 \tag{4.44}$$

This expression can be utilized to compute bit error rates and similar uncoded performance metrics. Since modern communication systems apply channel coding over relatively long data blocks, to protect against errors, the ergodic channel capacity is a more appropriate performance metric in 5G networks.

It merits to note that the ergodic capacities of the individual communication links are hard to characterize exactly, particularly under imperfect channel knowledge, but tractable lower bounds are obtained by the following theorem [1].

Theorem 1. *In the uplink, a lower bound on the ergodic (shannon) capacity of an arbitrary user k in the given cell is:-*

$$SE_k = \gamma\left(1 - \frac{\tau_p}{\tau_c}\right)\log_2(1 + SINR_k^{UL}) \tag{4.45}$$

Where the general SE is the spectral efficiency and the signal-to-interference-and-noise ratio (SINR) is given as:-

$$SINR_k^{UL} = \frac{p_k \parallel \mathbb{E}\{\mathbf{v}_k^H\mathbf{h}_k\} \parallel^2}{\sum_{k=1}^K p_k\mathbb{E}\{\parallel \mathbf{v}_k^H)\mathbf{h}_k \parallel^2\} + \sum_{i=1}^K p_i \parallel \mathbb{E}\{\mathbf{v}_k^H)\mathbf{h}_i\} \parallel^2 + \sigma^2\mathbb{E}\{\parallel v_k \parallel^2\}} \tag{4.46}$$

Uplink spectral efficiency with LS estimator:

From Section 4.3.1, we have the expression for $\hat{h}_k = H_{LS}$ given as:-

$$\hat{h}_k = H_{LS} = \frac{1}{\sqrt{\phi_k} * \tau_p} * y^{pilot} \tag{4.47}$$

Now, by inserting Equation 4.47 to the Equations 4.57 and 4.46, we get the SE expression for the LS estimator. The SINR expression for the LS estimator was derived by the paper [7]. After adjusting the equation as per our system, we get the following expression of SINR for the LS estimator:-

$$SINR_k^{UL,LS} = \frac{p_k \parallel tr(\mathbf{R_k}) + \sum_{i=1}^{K} \frac{\sqrt{p_i}}{\sqrt{p_k}} \hat{\mathbf{h}}_i^H \hat{\mathbf{h}}_k \parallel^2}{\sum_{i=1}^{K} p_i \chi_i - p_k \parallel tr(\mathbf{R}_k) + \sum_{i=1}^{K} \frac{\sqrt{p_i}}{\sqrt{p_k}} \hat{\mathbf{h}}_i^H \hat{\mathbf{h}}_k \parallel^2 + \sigma_{UL}^2 (\frac{tr(\mathbf{\Psi}_k^{-1})}{p_k \tau_p} + \frac{\|\mathbf{y}_k^p\|^2}{p_k \tau_p^2})} \tag{4.48}$$

Where:

$$p_k \tau_p^2 \chi_i = p_k \tau_p^2 \mathbb{E}\{\parallel \mathbf{v}_k^H \mathbf{h}_i \parallel\} = \tau_p tr(\mathbf{R}_i {\mathbf{\Psi_k}}^{-1}) + 2\sqrt{p_i} \tau_p Re\{(\hat{\mathbf{y}}_k^p)^H \hat{\mathbf{h}}_i tr(\mathbf{R_i}) + (\hat{\mathbf{y}}_k^p)^H (\mathbf{R_i}) \hat{\mathbf{h}}_i\} \tag{4.49}$$

Then, after finding the expression for the SINR for our system, we can now easily find the expression for SE by using the Equation 4.57. We just need to replace the SINR variable in Equation 4.57 by the expression for it derived in Equation 4.48. We first re-write Equation 4.57 after modifying it for the LS estimator as:

$$SE_k^{UL,LS} = \gamma \left(1 - \frac{\tau_p}{\tau_c}\right) \log_2(1 + SINR_k^{UL,LS}) \tag{4.50}$$

Then, we replace the SINR variable in Equation 4.57 by the expression for it derived in Equation 4.48 and we get the SE expression of our massive MIMO system when using the LS estimator to be:

$$SE_k^{UL,LS} = \gamma \left(1 - \frac{\tau_p}{\tau_c}\right) \log_2 \left(1 + \frac{p_k \parallel tr(\mathbf{R_k}) + \sum_{i=1}^{K} \frac{\sqrt{p_i}}{\sqrt{p_k}} \hat{\mathbf{h}}_i^H \hat{\mathbf{h}}_k \parallel^2}{\sum_{i=1}^{K} p_i \chi_i - p_k \parallel tr(\mathbf{R}_k) + \sum_{i=1}^{K} \frac{\sqrt{p_i}}{\sqrt{p_k}} \hat{\mathbf{h}}_i^H \hat{\mathbf{h}}_k \parallel^2 + \sigma_{UL}^2 (\frac{tr(\mathbf{\Psi}_k^{-1})}{p_k \tau_p} + \frac{\|\mathbf{y}_k^p\|^2}{p_k \tau_p^2})}\right) \tag{4.51}$$

Uplink spectral efficiency with MMSE estimator:

From Section 4.3.2, we have the expression for $\hat{h}_k = H_{MMSE}$ given as:-

$$\hat{h}_k = H_{MMSE} = \bar{h} + \sqrt{p_k}\mathbf{R}_k\Psi_k(y_k^{pilot} - \hat{y}_k^{pilot}) \tag{4.52}$$

Now, by inserting Equation 4.52 to the Equation 4.57 and 4.46, we get the SE expression for the MMSE estimator. The SINR expression for the MMSE estimator was derived by the paper [7]. After adjusting the equation as per our system, we get the following expression of SINR for the MMSE estimator:-

$$SINR_k^{UL,MMSE} = \frac{p_k^2\tau_p tr(\mathbf{R_k}\mathbf{\Psi_k}\mathbf{R_k}) + p_k \parallel \hat{\mathbf{h}}_k \parallel^2}{\sum_{i=1}^{K} p_i\xi_i\mathbb{E}\{\mathbf{v}_i^H\xi_i + \sum_{k=1}^{K} p_k\Gamma_i - p_k\nu_i + \sigma_{UL}^2\}} \tag{4.53}$$

Where:

$$\nu_k = \frac{\parallel \hat{\mathbf{h}}_k \parallel^4}{p_k\tau_p tr(\mathbf{R_k}\mathbf{\Psi_k}\mathbf{R_k}) + p_k \parallel \hat{\mathbf{h}}_k \parallel^2\}} \tag{4.54}$$

$$\xi_k = \frac{p_k\tau_p tr(\mathbf{R_i}\mathbf{R_k}\mathbf{\Psi_k}\mathbf{R_k}) + p_k\tau_p\hat{\mathbf{h}}_i^H\mathbf{R_k}\mathbf{\Psi_k}\mathbf{R_k}\hat{\mathbf{h}}_i + \hat{\mathbf{h}}_k^H\mathbf{R_i}\hat{\mathbf{h}}_i + \parallel \hat{\mathbf{h}}_k^H\hat{\mathbf{h}}_i \parallel^2}{p_k\tau_p tr(\mathbf{R_k}\mathbf{\Psi_k}\mathbf{R_k}) + p_k \parallel \hat{\mathbf{h}}_k \parallel^2} \tag{4.55}$$

$$\Gamma_k = \frac{p_k p_i\tau_p^2 \parallel \tau_p tr(\mathbf{R_k}\mathbf{\Psi_k}\mathbf{R_k}) \parallel^2 + 2\sqrt{p_k p_i}\tau_p Re\{tr(\mathbf{R_k}\mathbf{\Psi_k}\mathbf{R_k})\hat{\mathbf{h}}_i^H\hat{\mathbf{h}}_k\}}{p_k\tau_p tr(\mathbf{R_k}\mathbf{\Psi_k}\mathbf{R_k}) + p_k \parallel \hat{\mathbf{h}}_k \parallel^2} \tag{4.56}$$

Then, after finding the expression for the SINR for our system, we can now easily the expression for SE by using the Equation 4.57. We just need to replace the SINR variable in Equation 4.57 by the expression for it derived in Equation 4.53. We first re-write Equation 4.57 after modifying it for the LS estimator as:

$$SE_k^{UL,MMSE} = \gamma\left(1 - \frac{\tau_p}{\tau_c}\right)\log_2(1 + SINR_k^{UL,MMSE}) \tag{4.57}$$

Then, we replace the SINR variable in Equation 4.57 by the expression for it derived in Equation 4.53 and we get the SE expression of our massive MIMO system when using the MMSE estimator to be:

$$SE_k^{UL,MMSE} = \gamma\left(1 - \frac{\tau_p}{\tau_c}\right)\log_2\left(1 + \frac{p_k^2\tau_p tr(\mathbf{R_k}\mathbf{\Psi_k}\mathbf{R_k}) + p_k \parallel \hat{\mathbf{h}}_k \parallel^2}{\sum_{i=1}^{K} p_i\xi_i\mathbb{E}\{\mathbf{v}_i^H\xi_i + \sum_{k=1}^{K} p_k\Gamma_i - p_k\nu_i + \sigma_{UL}^2\}}\right) \tag{4.58}$$

Finally, we have founded mathematical expressions for the SINR and SE of the LS and MMSE estimators that will enable us to compare between the different channel estimators. In the next chapter, we will use these expressions to produce different simulations results in order to compare between the different channel estimators.

Chapter 5

Simulation Results

5.1 The Simulation Software

Simulations are good way of comparing between different algorithms. In order to compare between different channel estimation, we will use the MATLAB simulation tool. [50] states that MATLAB (short for MATrix LABoratory) is a special-purpose computer program optimized to perform engineering and scientific calculations. It started life as a program designed to perform matrix mathematics, but over the years it has grown into a flexible computing system capable of solving essentially any technical problem.

5.2 Simulation Results and Discussions

Here, we will set up our environment before starting the simulations. For our system, we will assume normal walking speed of humans with no vehicular speed considered. The distribution of the users with in the cell is assumed to be random with in the cell. The BTS is located at the center of the cell. Since we are planning 5G system, it reasonable to assume urban environment because high data rate is usually for required urban duelers. There are different types of cells based on their size. We will assume our cell to be UMa (Urban Macro-cell) because the UMa have a coverage of less than $2000m$ as stated in [51] and our system have a coverage of $250m$. So, it is reasonable to chose UMa cell for our system.

Now, from the above assumed environment, we will calculate the length of coherence block for our system based on our choice of our environment. As stated in the previous chapters, our system consists of many coherence blocks. We will assume all coherence blocks are the same and we will do our system evaluation picking only one coherence block.

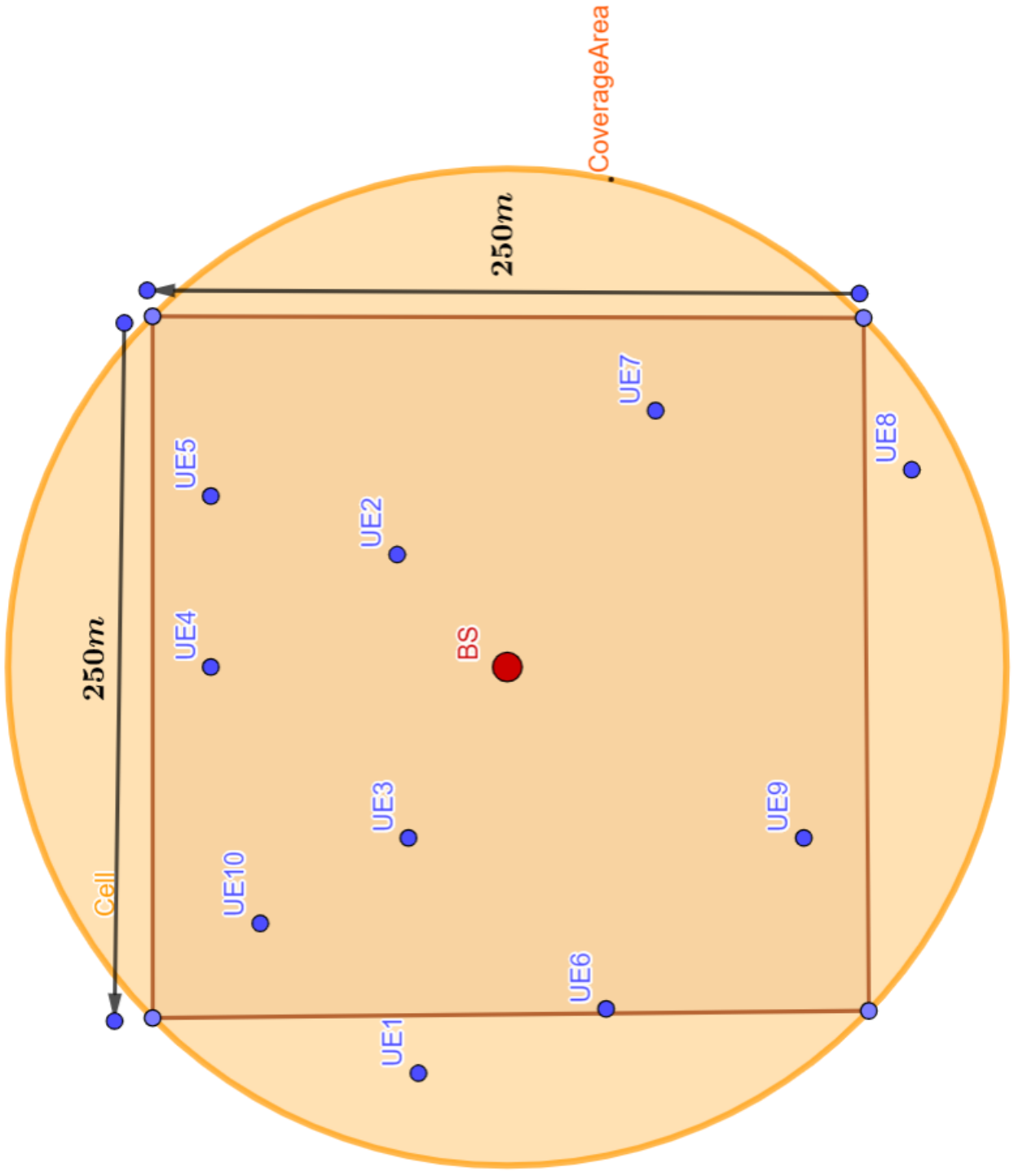

FIGURE 5.1: Single-cell setup with ten UEs per cell.

$$Length\ of\ the\ Coherence\ Block = T_c * B_c \tag{5.1}$$

Then, we will chose our operating frequency for our system. According to the recommendation of the [52], we will choose 50 GHz for our operation. Massive MIMO operates at a frequency starting from $5GHz$. Choosing higher frequencies is recommended by different papers including the paper [52] and choosing higher frequencies is advantageous for a couple of reasons. Some of the advantageous of choosing higher frequencies are:-

- The higher the frequency, the smaller the antenna array size.
- The higher the frequency, the higher the data rate it can serve.

One of the significant disadvantageous of using higher frequency for telecommunication is it can't travel long distance and this is not a problem in massive MIMO because cell size in massive MIMO is designed to be small. For example, our particular system has a cell size of $250m$.

Now, from the frequency chosen, we can then calculate the T_c and B_c. From this frequency value we first calculate the λ. Using the equation $C = \lambda * f$, We get the λ to be about $6.30mm$. From this λ value, we can now calculate the T_c using the equation,

$$T_c = \frac{\lambda}{8 * v} \tag{5.2}$$

Where v is the speed of the UE. In this thesis, normal walking speed of humans is used as the speed of the UE and this speed is usually assumed to be around 1.4 m/s (averaged) as it stated in the paper [53] and [54]. Now, using Equation 5.2 we can calculate the value of T_c. After the calculation, get the value of T_c to be about 0.60 ms.

According to the paper [55], the B_c can be calculated as;

$$B_c = \frac{1}{2\pi * D_s} \tag{5.3}$$

Where the D_s is the delay spread. Now, using the parmeters defined above (UMa cell and operating frequency of 50 GHz) we will choose D_s for our system from Table 5.1. We will choose the D_s for our system to be 240 ns according to the paper [56]. We chose this value because according the paper [56] the following delay spreed values are recommended for different system shown in Table 5.1. By inserting this value to Equation 5.3, we get the value of the B_c to be 665 KHz. And this is s reasonable result because the value of the B_c can range up to 1000 KHz and even more to several MHz values. Now, by inserting the value of both B_c and T_c in to Equation 5.1, we get the length of the coherence block

to be approximately 400 *samples*. So, We will consider communication over a $20MHz$ channel and we will assume the total receiver sensitivity to be $-94dB$. Each coherence block consists of $\tau_c = 400$ samples and the same $\tau_p = 10$ pilots are allocated randomly in the cell.

5.2.1 Steps Followed to Reach to Results

In this section we will show the steps followed to produce the simulation results. First we will produce the noise; Then we will produce the pilot signal,Y^{pilot}. Then the LS channel estimator and the MMSE channel estimator values are produced. After finding the estimation of the channel, we will use this estimation value for detection. Then SINR value for the system is produced based on the estimation value and the detection algorithm. Lastly, comparison between the LS channel estimator and MMSE channel estimator is done based on the SE and using other metrics.

5.2.2 The First Result

In this section, we will try to see the performance of our new defined system. We will try to compare our new system with other systems based on the SE and other parameters. We will also mention some recommendation for massive MIMO systems given by different papers.

In this simulation section, the SE expressions derived in the previous sections are validated and evaluated by simulating a Massive MIMO cellular network. We have a single cell setup where the cell covers a square of $250m \times 250m$. There are K = 10 UEs per cell and these are independently and randomly distributed in each cell, at distances larger than 35 m from the BS. Each UE is assigned to the BS that provides largest channel gain considering all the combinations of the UE and BS in the system. The location of each UE is used when computing the large-scale fading and nominal angle between the UE and BS.

Each BS is equipped with a Uniform Linear Array (ULA) antennas having 0.8 antenna spacing. Dipole antenna is used as an antenna element for our antenna array. In the papers used as a reference, most of them assume half wavelength spaced antennas. The 0.8 antenna spacing is selected and was mentioned as having better performance in the article [57] written by one of the most important companies in antenna manufacturing. For simplicity, the same transmit power is used in the uplink for all users in the system. As stated in [58], Increasing the coherence block means that the precoding/combining matrices are computed less frequently, which reduces the computational complexity and together with this advantage the performance of the system will increase.

Proposed Scaling Factor Delay Spread desired [ns])		Frequency [GHz]						
		2	6	15	28	39	60	70
Indoor office	Short-delay profile	20	16	16	16	16	16	16
	Normal-delay profile	39	30	24	20	18	16	16
	Long-delay profile	59	53	47	43	41	38	37
UMi Street-canyon	Short-delay profile	65	45	37	32	30	27	26
	Normal-delay profile	129	93	76	66	61	55	53
	Long-delay profile	634	316	307	301	297	293	291
UMa	Short-delay profile	93	93	85	80	78	75	74
	Normal-delay profile	363	363	302	266	249	228	221
	Long-delay profile	1148	1148	955	841	786	720	698
RMa & RMa O2I	Short-delay profile	32	32	N/A	N/A	N/A	N/A	N/A
	Normal-delay profile	37	37	N/A	N/A	N/A	N/A	N/A
	Long-delay profile	153	153	N/A	N/A	N/A	N/A	N/A
UMi / UMa O2I	Normal-delay profile	240						
	Long-delay profile	616						

TABLE 5.1: How to calculate absolute delay values [56].

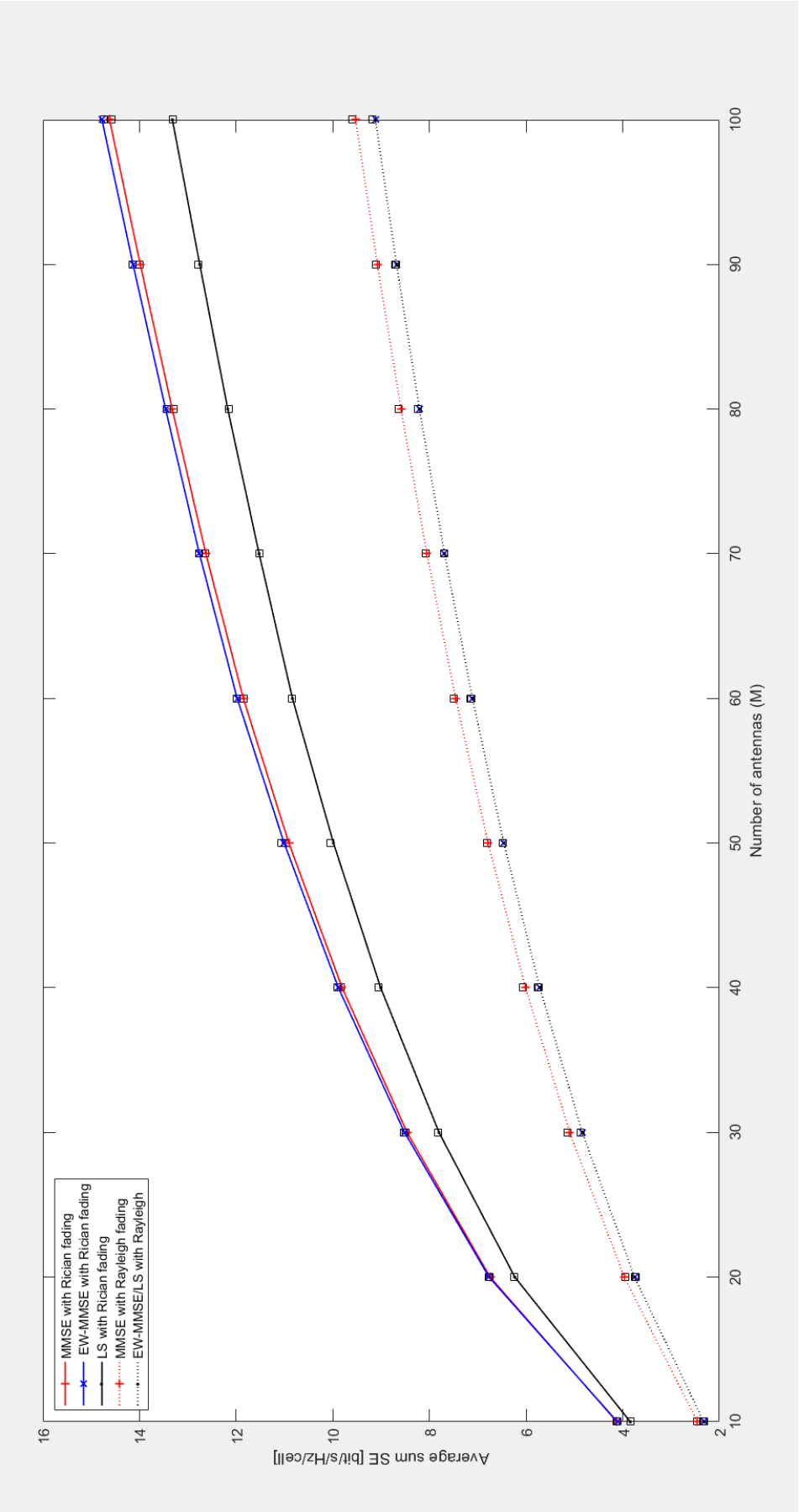

FIGURE 5.2: Average UL sum SE for K = 10 as a function of the number of BS antennas for different channel estimators as simulated by [58].

Figure 5.2 shows the sum UL SE averaged over different UE locations and shadow fading realizations, when using MRC detection based on either the MMSE or LS estimators. This is an original work from the paper [7].

Now, we will use our own specifically defined system and produce system performance evaluation results. We will use the values of standard deviation of shadow fading specified by the research paper [59]. Using the paper stated, the standard deviation of shadow fading in dB for NLOS channel I used was 6.7 dB, and for LOS channel was 3.9 dB.

Figure 5.3 shows the sum UL SE averaged over different UE locations and shadow fading realizations, when using MRC detection based on either the MMSE or LS estimators. This result is for our specifically defined system. The SE of the LS estimator at $M = 100$ is about 21.5 $bits/s/Hz/cell$ and the SE of the MMSE estimator at $M = 100$ is about 22.5 $bits/s/Hz/cell$.

When the system performance was compared between our system and other systems previously defined by other papers like [7], there was a performance difference between them. When our specifically defined system was run, we got a different performance of the system from the research paper that were used and as stated the SE of the massive MIMO system got improved a lot. The improvements were approximately about 7 $bits/s/Hz/cell$. As we have seen it from the results, When the recommendation for the antenna spacing was applied, values of standard deviation of shadow fading used and other system changes were applied better performance was achieved.

Now, within our system, we will compare between the LS and the MMSE channel estimators. When doing this, we got that the value of SE of MMSE estimator was larger than the value of SE of LS estimator by 1 to 2 $bits/s/Hz/cell$. The result we have is an expected result as stated in the paper [7]. The paper states that the loss in SE incurred by using the LS estimator under Rician fading can be quite large depending on the dominance of LoS paths. The performance difference could be even large because the estimator improves the one link only but when the links between the BS and UE became many the performance is multiplied by the number of links.

Another important point we note is that the improvement in the performance of our system compared to the previous systems was achieved both for LS channel estimation algorithm and the MMSE channel estimation algorithm. We can also understand from this that our massive MIMO system could always be improved by studying and controlling different parameters.

The curves are generated using the expressions from Section 4.5. As expected, the highest UL SE is obtained when the MMSE estimator is employed, since the LoS component and

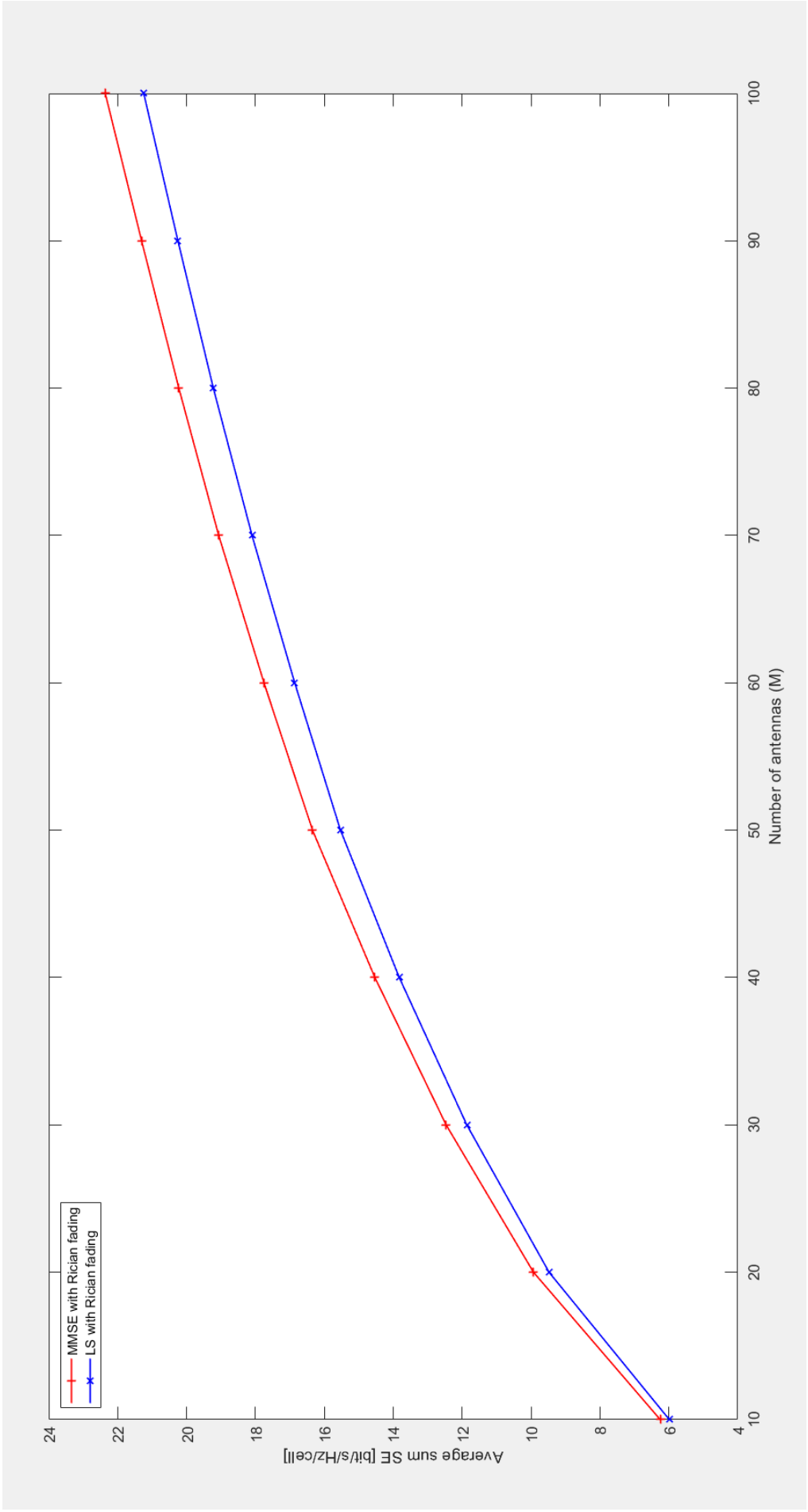

FIGURE 5.3: Average UL sum SE for K = 10 as a function of the number of BS antennas for different channel estimators.

spatial correlation are known and utilized. For Rician fading, the performance of MMSE is better than LS since it utilizes knowledge of the channels' mean values.

5.2.3 The Second Result

Here in this section, we will see the effect of the increase in the number of users in the LS and MMSE estimators (i.e. when the number of users increases, which one of the estimators is affected more ?).

Now, the graph below is produced from MATLAB by changing the value of the number of users and keeping other parameters the same. Table 5.2 is produced by varying the number of users a couple of times and averaging the received values.

Here, what we want is to see the effect of the increase in the number of users on LS and MMSE channel estimators. specifically, which channel estimator is affected more the LS or the MMSE estimator when the number of users change? Figures 5.4, 5.4 and 5.4 shows the effect of the change in users in LS and MMSE estimators.

As we can see from Figures 5.4, 5.4 and 5.4, the difference between the LS and MMSE estimators diminishes. This shows that the MMSE and the LS estimators become almost the same when the number of users increases beyond 60 to 100. This shows that the difference in performance between the two estimators approaches to zero when the number of users increases. One can conclude from this that the performance of the LS and the MMSE channel estimators is near to each other when the number of users is large.

The other observation from Figures 5.4, 5.4 and 5.4 is that when the number of users increases, the SE of the system increases to certain limit until the system reaches its full capacity. When the system reaches its full capacity the system (which is 60 to 100 users in our case with $M = 100$.), SE starts to decline. If we keep increasing the number of users until the number of users equals with the length of the coherence block, $K = Length\ of\ the\ Coherence\ Block = T_c * B_c = 400\ samples$, the system performance decreases to zero.

one of our system limitation, as discussed earlier, is the length of the coherence block. Our length of coherence block is 400 (as it was calculated earlier). So, the maximum number of user ,K, we can have for our system is $2K < 400 => K < 200$. We can see from Figure 5.4 that the LS and MMSE estimators have almost the same performance when the users are between 100 and 200. So, we can also that it is better to use the LS estimator when the number of users grow because the two estimators have the same performance and the MMSE estimator requires a lot of computations.

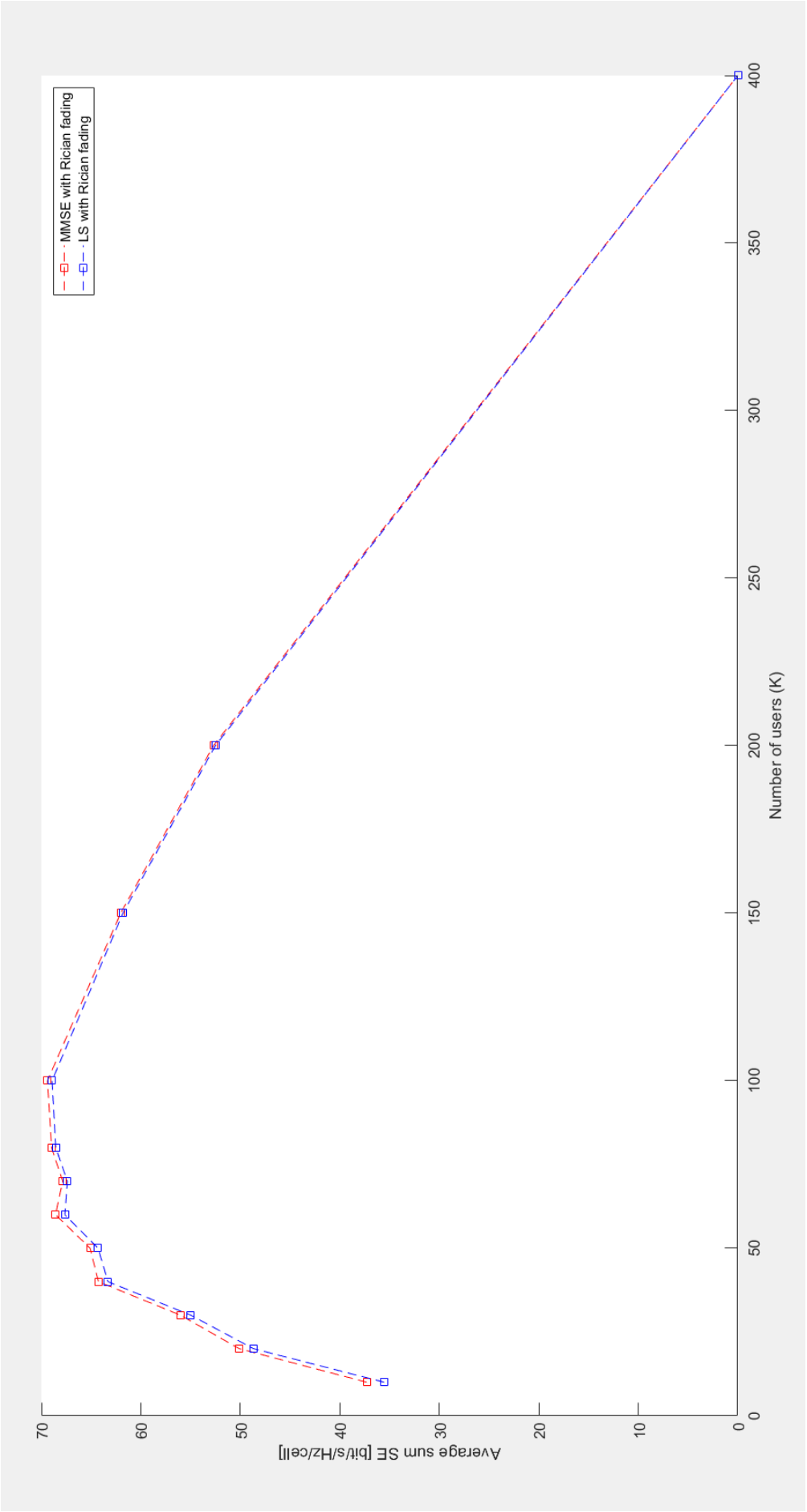

FIGURE 5.4: Comparing the effect of the number of users on the MMSE and LS estimators.

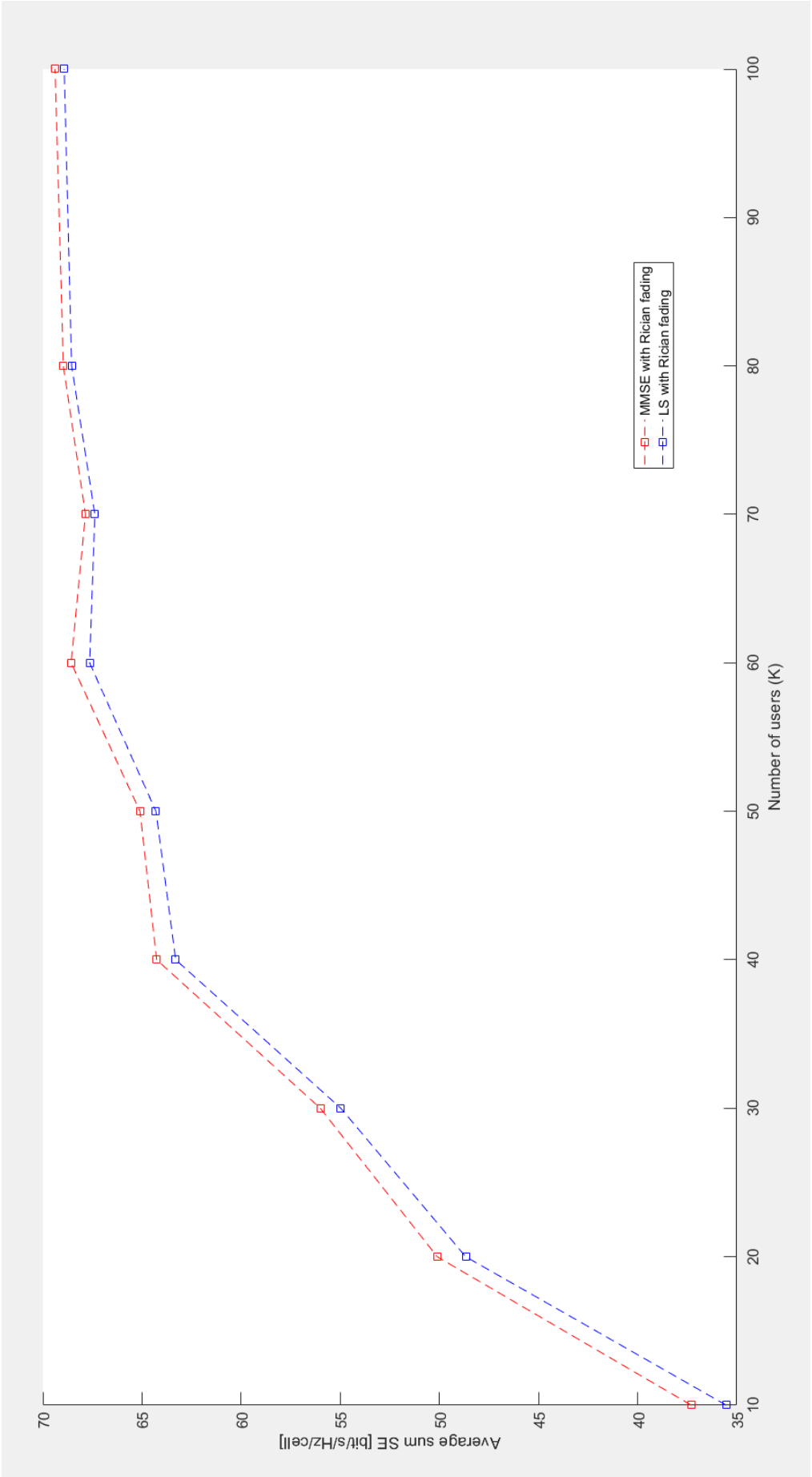

FIGURE 5.5: Comparing the effect of the number of users on the MMSE and LS estimators when Figure 5.4 magnified from 10 <K< 100.

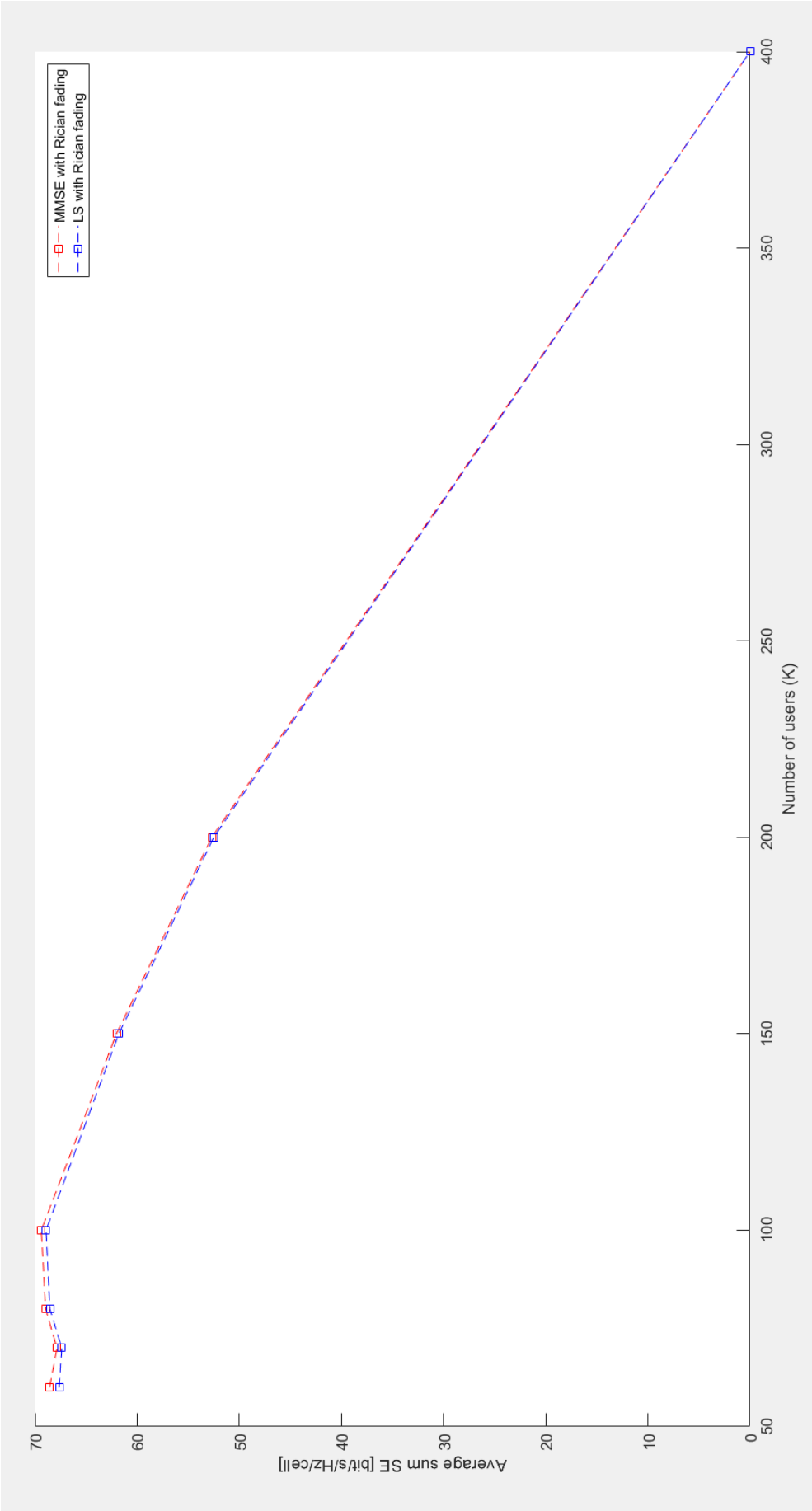

FIGURE 5.6: Comparing the effect of the number of users on the MMSE and LS estimators when Figure 5.4 magnified from 50 <K< 400.

5.2.4 The Third Result

Here in this section, we will see the effect of the increase in the number of antennas in the LS and MMSE estimators (i.e. when the number of antennas increases, which one of the estimators is affected more ?).

Now, the graph below is produced from MATLAB by changing the value of the number of antennas by keeping other parameters the same. Figures 5.7, 5.8, 5.9 and 5.10 show the effect of the change in the number of antennas in LS and MMSE estimators. As we can see from the figures, the SE of both estimators (the LS and MMSE) increases with out bound when the number of antennas increases. The difference in SE between the LS and MMSE estimators continues as it is when the number of antennas increase.

Here, what we want is to see the effect of the number of antennas on LS and MMSE channel estimators. specifically, which channel estimator is affected more, the LS or the MMSE estimator, when the number of antennas change? As we can see from Figures 5.7, 5.8, 5.9 and 5.10, the difference between the LS and MMSE estimators continues as it is. This shows that the difference in performance between the two estimators continues to be almost the same when we keep the number of antennas increasing.

One can conclude from this that the performance of the LS and the MMSE channel estimators continues with superiority of the MMSE channel estimator even when the number of antennas becomes very large.

We can also see from the figures that when the number of antennas increases, the SE of both estimators increases with out limit. We could also produce simulation results with $M > 1500$, but we have hardware limitations. This conclusion was also made by [60]. The paper stated that massive MIMO has unlimited capacity. The paper states that We proved that the capacity of Massive MIMO systems increases without bound as $M \to \infty$ in the presence of pilot contamination, despite the previous results that pointed toward the existence of a finite limit.

5.2.5 The Fourth Result

Now, in this section, we will try to compare the LS and the MMSE channel estimator values, H_{LS-UL} *and* $H_{MMSE-UL}$, based on their distance from the perfect channel Value H_{UL}. The comparison could be done based on instantaneous values and/or average values but here we will compare them based on the average value since it has the correct information to compare between different values.

Here, the comparison between the LS channel estimator and the MMSE channel estimator is easy. The one close to the perfect channel response, H_{UL} , has a good performance than

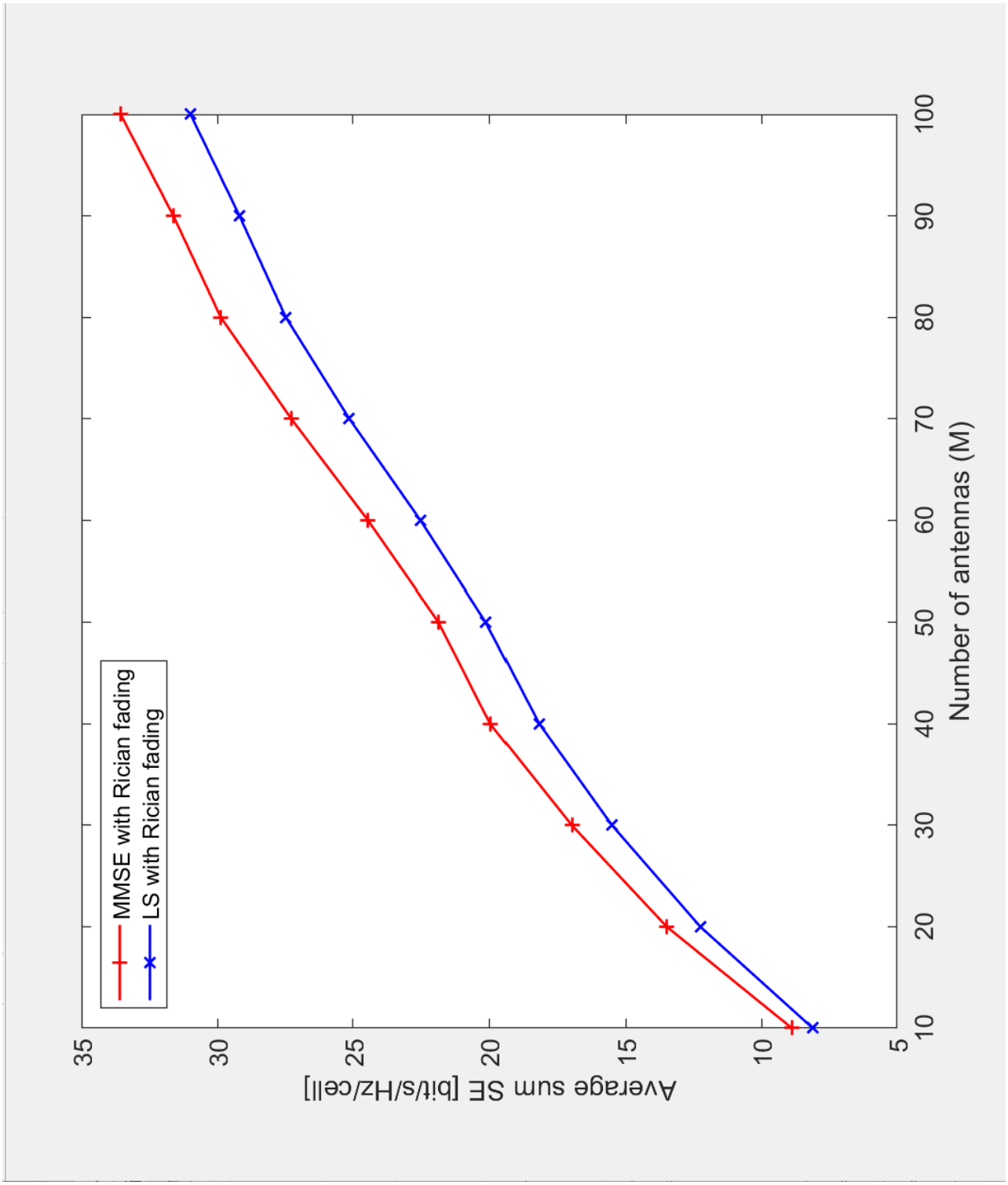

FIGURE 5.7: Comparing the effect of the number of antennas on the MMSE and LS estimators when $M = 100$.

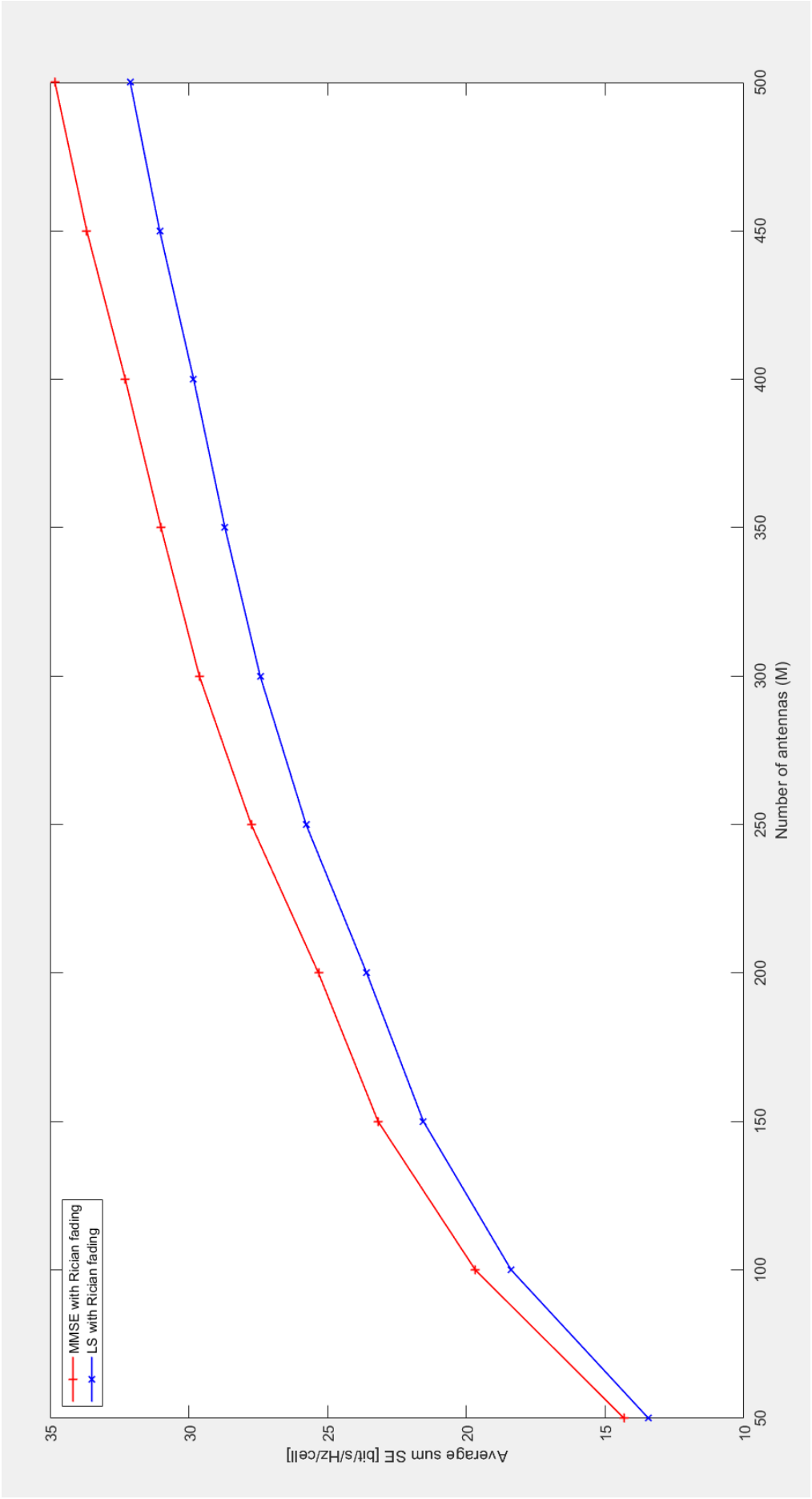

FIGURE 5.8: Comparing the effect of the number of antennas on the MMSE and LS estimators when $M = 500$.

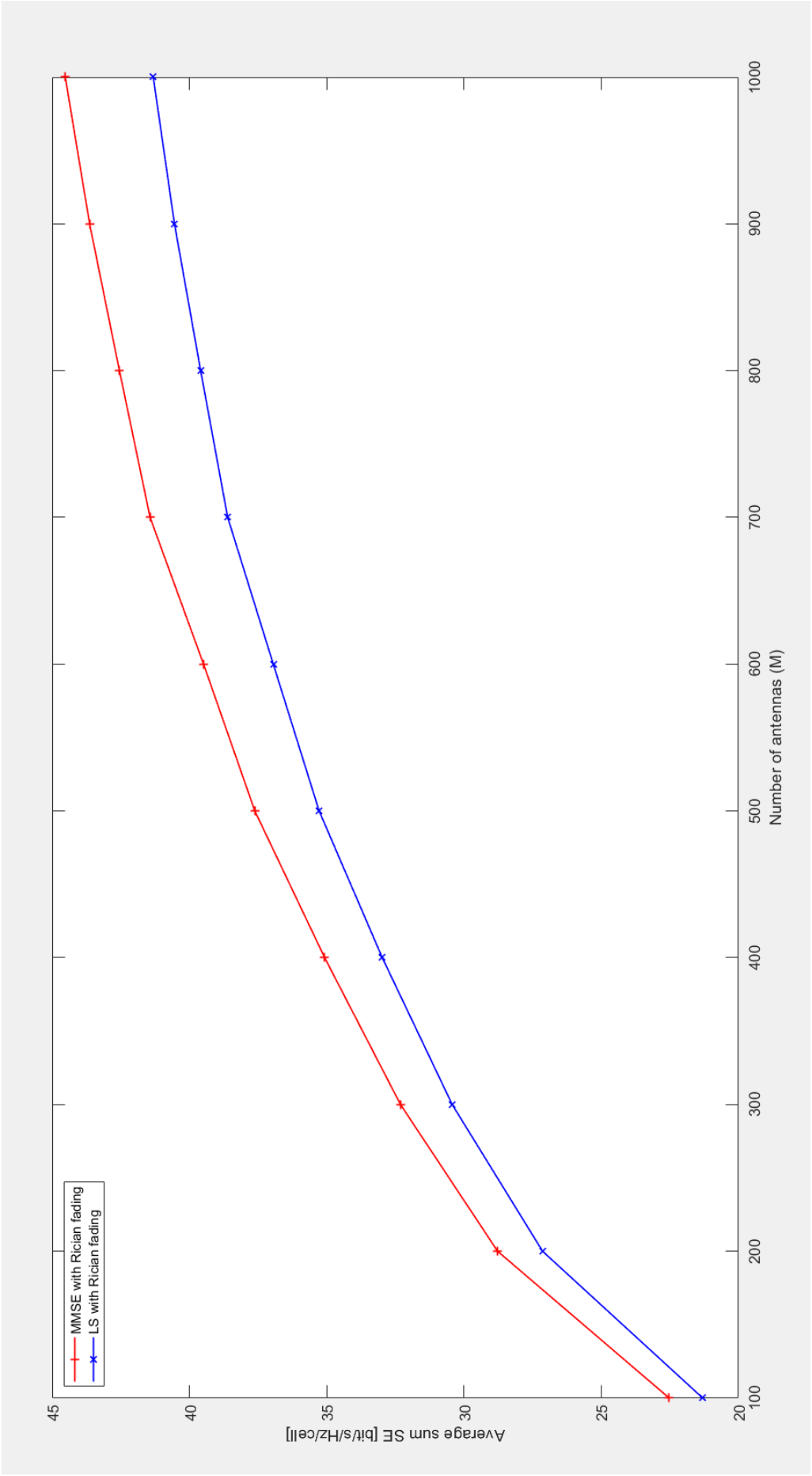

FIGURE 5.9: Comparing the effect of the number of antennas on the MMSE and LS estimators when $M = 1000$.

the one far from the perfect channel response, H_{UL}. Figure 5.11 was achieved for this analysis (i.e to compare between H_{LS-UL}, $H_{MMSE-UL}$ *and* H_{UL}).

Figure 5.11 shows the comparison between H_{LS} and H_{MMSE} with the respect of their distance from the perfect channel response, H_{UL}. The figure is plotted from the magnitude of each channel value or channel estimate. Particularly this figure is plotted for averaged results.

As we can see from the Figure 5.11, The H_{MMSE} has the least distance from the perfect channel response, H_{UL}. So, this shows that the MMSE channel estimator has better performance than the LS channel estimator. This further justifies the results we have achieved in the previous simulations. The other thing we see from this result is that the channel estimation value for each channel estimation technique remains the same even when the number of antenna increases. This is because we have ignored interferences in the system.

K	10	20	30	40	50	60	70	80	100	150	200	400
MMSE	37.296	50.112	56.006	64.26	65.102	68.576	69.686	68.968	69.384	62.026	52.698	0
LS	35.532	48.674	54.972	63.3	64.296	67.642	69.17	68.55	68.924	61.798	52.504	0

TABLE 5.2: Data collected from different MATLAB plots showing the effect of the number of users in a cell on the LS and MMSE estimators (the values are averaged from different values).

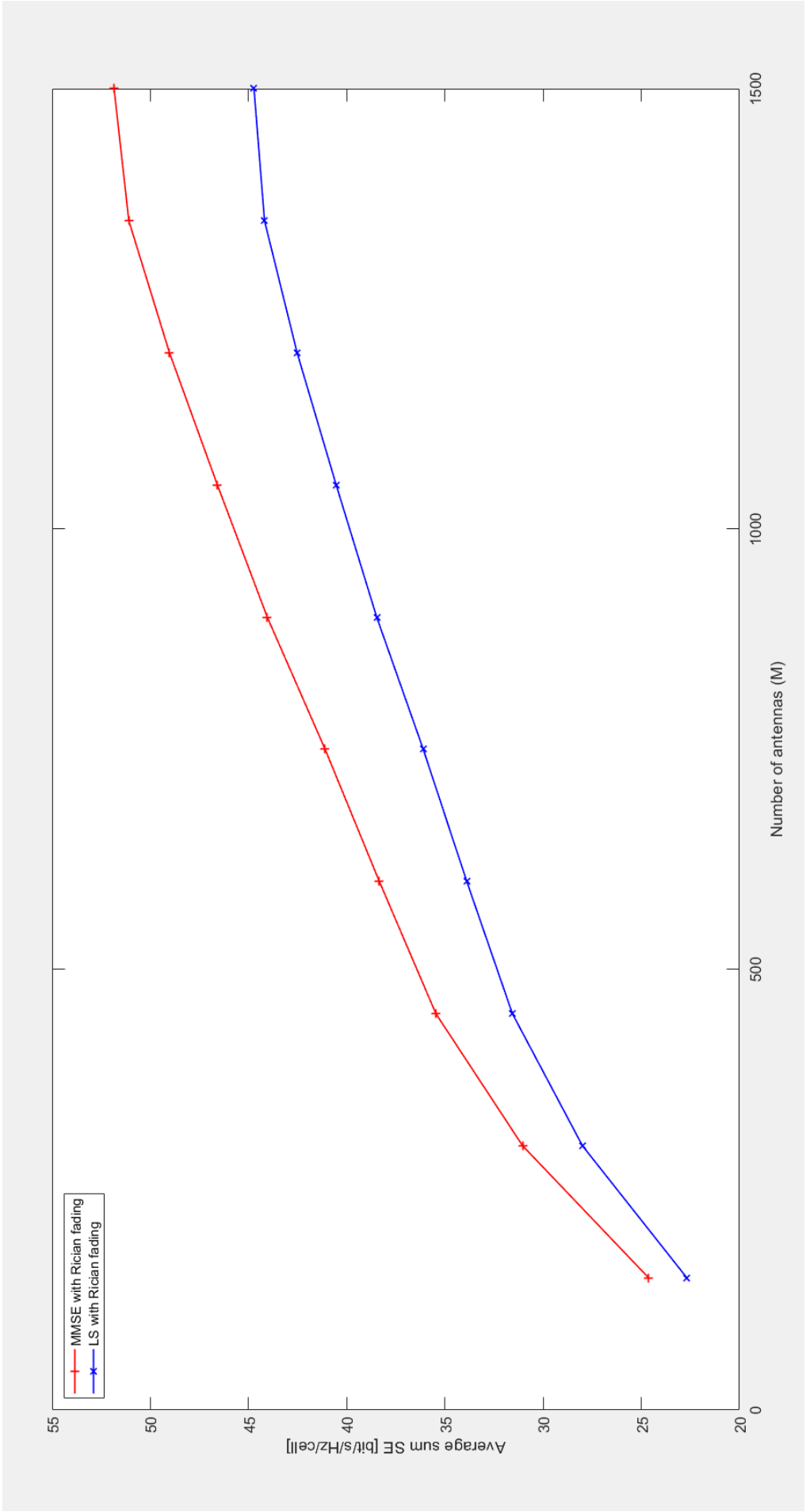

FIGURE 5.10: Comparing the effect of the number of antennas on the MMSE and LS estimators when $M = 1500$.

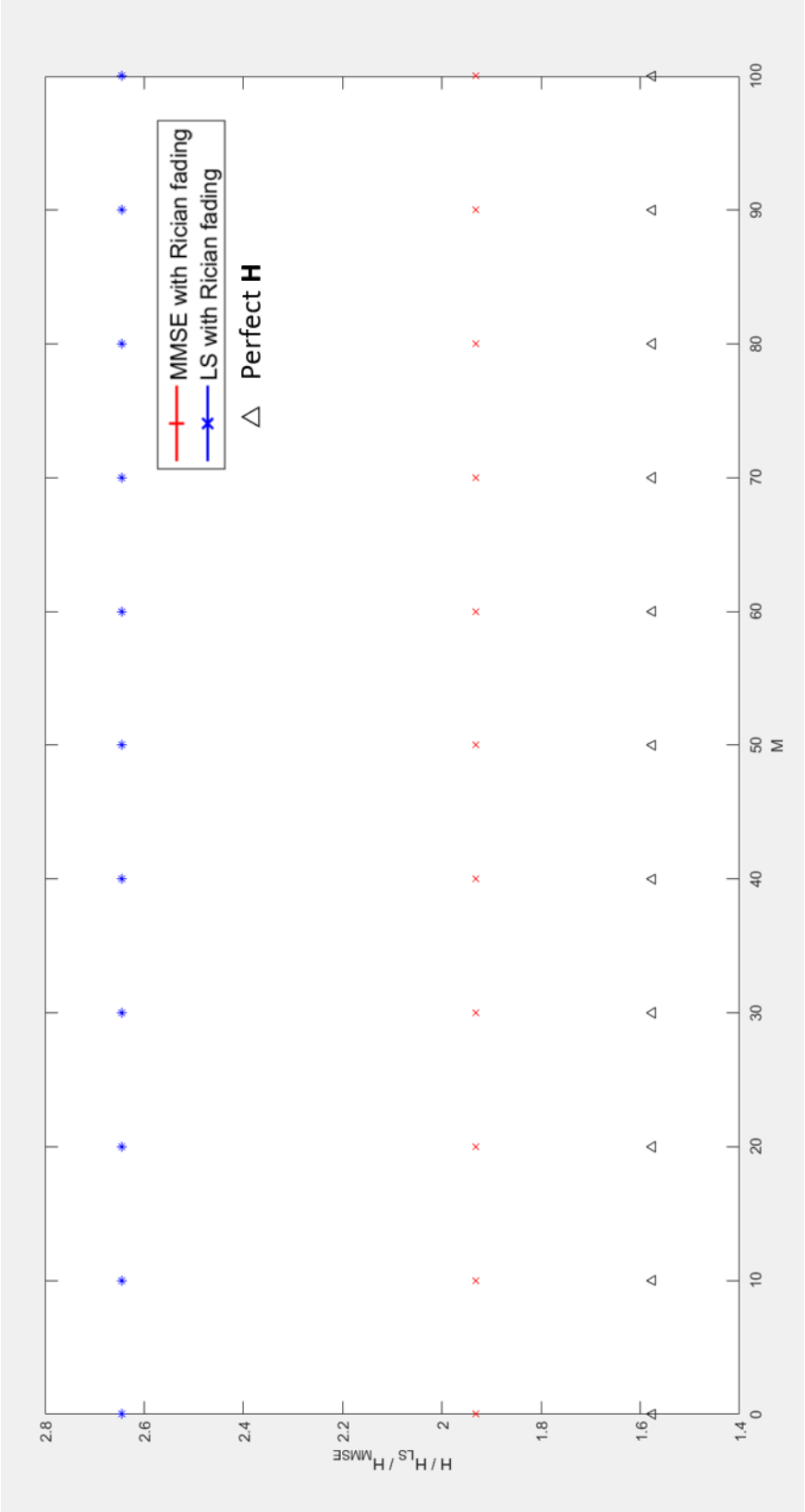

FIGURE 5.11: Comparing the LS and the MMSE channel estimator based on their distance $H_{LS-UL} and H_{MMSE-UL}$ from the perfect channel Value H_{UL}.

Chapter 6

Conclusion and Future Works

6.1 Conclusion

This thesis studied the UL performance of a single-cell massive MIMO system in terms of its SE and other metrics with Rician fading channels when the LS or the MMSE estimators are used. We derived SE expressions for both the MMSE and LS estimation when using the MR combining algorithm. Then, based on this mathematical expressions we produced simulations to compare between these estimations.

We observed that the existence of a LoS component improves the achievable SE in Massive MIMO. In addition, the MMSE estimator performs better than the LS estimator for Rician fading channels. The covariance matrices and the mean vectors were assumed to be known in the MMSE estimator. But, in practice, they might not be known perfectly.

As we can see from Figure 5.3, the SE of the massive MIMO system we have considered has improved with a considerable amount. This is because of the different we run the system and our choice of different antenna spacing value recommended by research papers written by antenna manufacturers. The other thing we have done is that we changed the choice of the standard deviation of shadow fading for NLoS component and LoS component according to the recommendations give by research papers.

The second thing we notice is from Figures 5.4, 5.5 and 5.6. We can see that, the difference in SE between the LS and MMSE estimators diminishes. This shows that the MMSE and the LS estimators become almost the same when the number of users increases beyond certain levels. This shows that the difference in performance between the two estimators approaches to zero when the number of users increases.

The third thing we learn is from Figures 5.7, 5.8, 5.9 and 5.10. We can see that, the difference between the LS and MMSE estimators continues as it is when the number of antennas increases. This shows that the difference in performance between the two estimators continues to be almost the same when the number of antennas increases. We can also

see from these results that the performance of massive MIMO systems increases as the number of antennas increases with out bound.

Figure 5.11 compares the perfect channel value with the LS and MMSE channel estimators. As we can see from this figure, the MMSE channel estimator is near to the perfect channel estimator than the LS channel estimator. This strengths the results we have achieved in the previous simulation results that the MMSE estimator has a better performance than the LS estimator.

6.2 Future Works

There are a lot of possible research areas related to this topic. One possible research idea is to see the per cell performance when the system is a single cell system and when it is multicell system. Specifically speaking, the the idea is to see the effect of increase the number of cells in the performance of each cell.

Another possible future research related to this paper is to see the effect of increasing the number of users on the difference between the LS and MMSE estimation techniques in the presence of pilot contamination. The same research could be done on the effect of increase in the number of antennas on the difference between the LS and MMSE estimation techniques in the presence of pilot contamination.

All the work in this paper is done assuming TDD operation of the massive MIMO systems. From this, we can see that doing all this experiments and simulations done on this thesis for FDD massive MIMO systems could be another possible field of research.

References

[1] T. V. Chien and E. Björnson, *5G Mobile Communications*, ser. Springer. Linkoing University Electronic Press, 2017, ISBN: 978-3-319-34206-1.

[2] M. Faran and P. Mor, "Comparison of Different Channel Estimation Techniques in OFDM Systems," *International Journal of Innovative Technology and Exploring Engineering (IJITEE)*, vol. 3, no. 2278-3075, p. 1, 2013.

[3] X. Gao, "Massive mimo in real propagation environments," PhD thesis, Department of Electrical and Information Technology, Lund University, Jan. 2016.

[4] G. S. Cin, "Can healthcare it infrastructure support internet of things growth?" *Low VoltageSolutions, Inc.*, no. 9, Nov. 2018.

[5] D. Neumann, M. Joham, and W. Utschick, "Channel estimation in massive mimo systems," Master's thesis, Department for Electrical and Computer Engineering, 80290 Munich, Germany, Mar. 2015.

[6] E. Björnson, J. Hoydis, and L. Sanguinetti, *Massive MIMO Networks: Spectral, Energy, and Hardware Efficiency*, 3rd ed., ser. 10. Sweden: authors' version of the manuscript, Jan. 2019, vol. 10.

[7] Özgecan Özdogan, E. Björnson, and E. Larsson, "Massive mimo with spatially correlated rician fading channels," Master's thesis, Department of Electrical Engineering, Linköping University, Linköping, Sweden, May 2018.

[8] Q. Cheng, "Novel channel estimation methods under pilot contamination in massive mimo," Master's thesis, Department of Engineering, Sydney, Australia, Mar. 2016.

[9] G. Gaspar, "Channel estimation in massive mimo systems," Master's thesis, Licenciado em Engenharia Electrotécnica e de Computadores, Nova University, Sep. 2016.

[10] A. A. Kwabena, "Multiple input multiple output (mimo) operation principles," Master's thesis, Information Technology, Helsinki Metropolia University of Applied Sciences, Jun. 2013.

[11] Nokia, "Massive mimo," Nokia, Texas, USA, Tech. Rep. 2, May 2019.

[12] Ericsson, "Massive mimo increasing capacity and spectral efficiency," Ericsson, Stockholm, Sweden, Tech. Rep. 2, Jun. 2019.

[13] E. Larsson, D. Danev, M. Olofsson, and S. Sörman, "Teaching the principles of massive mimo," *IEEE*, no. 4, pp. 1–13, Oct. 2016.

[14] H. Q. Ngo, "Massive mimo: Fundamentals and system designs," PhD thesis, Department of Electrical Engineering, Linköping University, SE-581 83 Linköping, Sweden, Jul. 2015.

[15] E. G. Larsson, F. Tufvesson, and T. L. Marzetta, "Massive mimo for next generation wireless systems," *IEEE*, no. 2, pp. 201–213, Jan. 2014.

[16] J. Mundy and K. Thomas, "What is massive mimo technology?" *5G.co.uk*, no. 6, Apr. 2019.

[17] M. Wang, "The role of massive mimo in 5g," *Rohde and Schwarz electronics group*, no. 6, pp. 1–11, Oct. 2018.

[18] Huawei, "Massive mimo: Key to simplified 5g networks," Mobile World Live, Tech. Rep. 2, Mar. 2019.

[19] J. Flordelis, F. Rusek, F. Tufvesson, E. G. Larsson, and O. Edfors, "Massive mimo performance—tdd versus fdd: What do measurements say?" *IEEE*, vol. 4, no. 2, pp. 1–12, Apr. 2017.

[20] C. Masterson, "Massive mimo and beamforming: The signal processing behind the 5g buzzwords," *Analogue Dialogue*, no. 6, pp. 1–5, Jun. 2017.

[21] rohde schwarz, "Massive mimo eight things to consider when testing antenna arrays," *Rohde and Schwarz electronics group*, no. 6, pp. 1–11, Aug. 2018.

[22] E. Björnson, L. Sanguinetti, H. Wymeersch, J. Hoydis, and T. Marzetta, "Massive mimo is a reality—what is next? five promising research directions for antenna arrays," no. 6, pp. 1–20, Jun. 2019.

[23] M. Passoja, "5g nr: Massive mimo and beamforming – what does it mean and how can i measure it in the field?" *RCR Wireless News*, no. 6, pp. 1–5, Sep. 2019.

[24] S. Wu, "Massive mimo channel modelling for 5g wireless communication systems," PhD thesis, School of Engineering and Physical Sciences, Heriot-Watt University, Oct. 2015.

[25] D. Mi, M. Dianati, L. Zhang, S. Muhaidat, and R. Tafazolli, "Massive mimo performance with imperfect channel reciprocity and channel estimation error," *IEEE TRANSACTIONS ON COMMUNICATIONS*, vol. 65, no. 9, pp. 3734–3745, Sep. 2017.

[26] M. BORTAS and S. GUNNARSSON, "Signal processing in massive mimo systems realized with low complexity hardware," An optional note, Master's thesis, DEPARTMENT OF ELECTRICAL and INFORMATION TECHNOLOGY, LTH, LUND UNIVERSITY, Feb. 2017.

[27] P. ORTEN and A. SVENSSON, "Sequential decoding of convolutional codes for rayleigh fading channels," *Wireless Personal Communications*, 61–74, Mar. 2002.

[28] Z. Alam, C. Patra, C. Patra, and A. Sobhan, "A novel technique for transmission of m-ary signal through wireless fading channel using wavelet denoising," *EEE Department, ADUST*, 1–11, Aug. 2011.

[29] Y. Liao, X. Shen, G. Sun, X. Dai, and S. Wan, "Ekf/ukf-based channel estimation for robust and reliable communications in v2v and iiot," *EURASIP Journal on Wireless Communications and Networking*, pp. 1–13, Jun. 2019.

[30] K. Parmar1 and S. Patel, "A survey on channel estimation algorithms for lte downlink systems," *International Journal of Innovative Research in Computer and Communication Engineering*, vol. 4, no. 4, pp. 13–22, Feb. 2016.

[31] A. Zaier and R. Bouallègue, "Blind channel estimation enhancement for mimo-ofdm systems under high mobility conditions," *International Journal of Innovative Research in Computer and Communication Engineering*, vol. 4, no. 4, pp. 207–212, Feb. 2012.

[32] A. Devasia and R. Reddy, "Semi blind channel estimation: An efficient channel estimation scheme for mimoofdm system," *Australian Journal of Basic and Applied Sciences*, vol. 7, no. 7, pp. 531–538, Jul. 2013.

[33] R.S.Ganesh and D. J. Kumari, "A survey on channel estimation techniques in mimo-ofdm mobile communication systems," *International Journal of Scientific and Engineering Research*, vol. 4, no. 5, pp. 1851–1855, May 2013.

[34] R. Govil, "Different types of channel estimation techniques used in mimo-ofdm for effective communication systems," *International Journal of Engineering Research and Technology (IJERT)*, vol. 7, no. 07, pp. 271–275, Jul. 2018.

[35] E. Bjornson, L. Sanguinetti, J. Hoydis, and M. Debbah, "Optimal design of energy-effcient multi-user mimo systems: Is massive mimo the answer?" *IEEE Transactions on Wire-less Communications*, vol. 16, no. 4, pp. 3059–3075, Jun. 2015.

[36] F. Wang, "Pilot-based channel estimation in ofdm system," PhD thesis, The University of Toledo, Electrical Engineering, Toledo, OH, USA, May 2011.

[37] S. Coleri, M. Ergen, A. Puri, and A. Baha, "Channel estimation techniques based on pilot arrangement in ofdm systems," *IEEE TRANSACTIONS ON BROADCASTING*, vol. 48, no. 3, pp. 223–229, Sep. 2002.

[38] S. B. Devamane, T. Rao, and R. K.P, "Training based channel estimation in ofdm systems," *International Journal of Technical Research and Science*, vol. 3, no. 1, pp. 5–8, Feb. 2018.

[39] Kumar and Santhosh, "Super resolution sparse mimo-ofdm channel estimation and cfo correction based on optimal lmmse," PhD thesis, Mar. 2015, pp. 1–36.

[40] A. A. AGARWAL, "Pilot based channel estimation for 3gpp lte downlink," Master's thesis, ELECTRICAL ENGINEERING, The University of Texas at Arlington, USA, Dec. 2011.

[41] A. Khlifi1 and R. Bouallegue, "Comparison between performances of channel estimation techniques for cp-lte and zp-lte downlink systems," *International Journal of Computer Networks and Communications (IJCNC)*, vol. 4, no. 4, pp. 3059–3075, Jul. 2012.

[42] M. MOQBEL, Wangdong, and A. marhabi Ali, "Mimo channel estimation using the ls and mmse algorithm," *IOSR Journal of Electronics and Communication Engineering (IOSR-JECE)*, vol. 12, no. 4, pp. 13–22, Jan. 2017.

[43] L. Panchal, M. Upadhyay, N. Shah, and A. Amin, "Significant implementation of ls and mmse channel estimation for ofdm technique," *Lokesh Panchal Int. Journal of Engineering Research and Applications*, vol. 4, no. 3, pp. 38–41, Mar. 2014.

[44] H. Permuter, "Mimo detection," Lecture Note, Dec. 2018.

[45] R. Tiwari and A. Mishra, "Mmse algorithm based mimo transmission scheme," *SSRG International Journal of Electronics and Communication Engineering (SSRG-IJECE)*, vol. 1, no. 6, pp. 41–45, Aug. 2014.

[46] X. Wang, J. Zhao, F. Meng, X. Yu, and Z. Zhang, "Mmse detection method in uplink massive mimo systems based on quantum computing," *National Mobile Communications Research Lab, Southeast University*, pp. 1–6, Jan. 2019.

[47] D. Malik and D. Batra, "Comparison of various detection algorithms in a mimo wireless communication receiver," *International Journal of Electronics and Computer Science Engineering*, pp. 1–8, Jun. 2012.

[48] ——, "Comparison of various detection algorithms in a mimo wireless communication receiver," *International Journal of Electronics and Computer Science Engineering*, pp. 1–8, Jun. 2012.

[49] A. Dowler and A. Nix, "Performance evaluation of channel estimation techniques in a multiple antenna ofdm system," *Centre for Communications Research, University of Bristol*, no. 2, pp. 1214–1218, 2003.

[50] S. Chapman, *MATLAB Programming for Engineers*, 3rd ed., ser. 10. 3 Apple Hill Drive, Natick, USA: Thomson Learning, part of the Thomson Corporation, Jul. 2008, vol. 4, ISBN: 978-0-495-24449-3.

[51] U. Berkeley, "Cellular telephone networks," *JPL's Wireless Communication Reference Website*, p. 1, Jan. 1995.

[52] GSMA, "5g spectrum gsma public policy position," *GSMA*, pp. 1–12, Jul. 2019.

[53] S. M, M. C, and L. C, "Association between walking speed and age in healthy, free-living individuals using mobile accelerometry–a cross-sectional study," *PLOS ONE*, p. 1, Aug. 2011.

[54] Healthline, "What is the average walking speed of an adult?" *Healthline*, p. 1, Mar. 2019.

[55] S. Farahani, "Rf propagation, antennas, and regulatory requirements," *ZigBee Wireless Networks and Transceivers*, p. 1, Jul. 2008.

[56] J.-A. Fabien, "Channel model implementation and application for new radio (nr) 3gpp rel-15," *Institute for Telecommunication Sciences*, p. 1, Aug. 2018.

[57] Kathrein, "Spacing out ... getting the most out of mimo with proper antenna spacing," *Kathrein USA*, p. 1, Sep. 2017.

[58] E. Bjornson, E. G. Larsson, and T. L. Marzetta, "Massive mimo: Ten myths and one critical question," *IEEE*, no. 9, pp. 1–10, Jul. 2015.

[59] S. Sun, T. Thomas, T. Rappaport, H. Nguyen, I. Kovacs, and I. Rodriguez, "Path loss, shadow fading, and line-of-sight probability models for 5g urban macro-cellular scenarios," *IEEE Global Communications Conference Workshop (Globecom Workshop)*, no. 7, pp. 1–7, Dec. 2015.

[60] E. Bjornson, J. Hoydis, and L. Sanguinetti, "Massive mimo has unlimited capacity," *IEEE*, pp. 1–17, Nov. 2017.